REGULATION AND FUNCTIONAL SIGNALING OF DECORIN IN THE TESTIS IN HEALTH AND DISEASE

Marion Adam

Dissertation der Fakultät für Biologie
der Ludwig-Maximilians-Universität München

München 2011

Institut für Anatomie und Zellbiologie der Ludwig-Maximilians-Universität München

REGULATION AND FUNCTIONAL SIGNALING OF DECORIN IN THE TESTIS IN HEALTH AND DISEASE

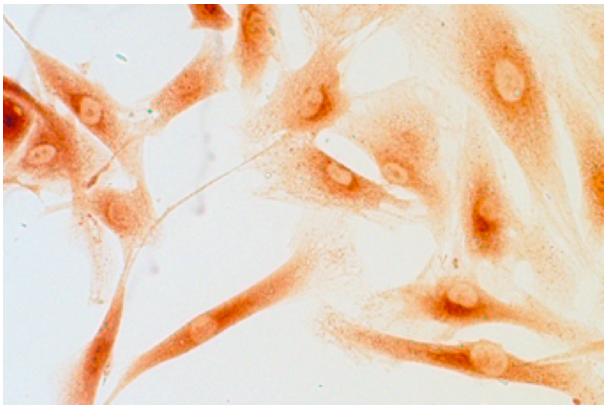

Marion Adam

Diese Dissertation wurde angefertigt
unter der Leitung von Prof. Dr. Artur Mayerhofer
am Institut für Anatomie und Zellbiologie
an der Ludwig-Maximilians-Universität München

Erstgutachter: PD Dr. Lars Kunz
Zweitgutachter: Prof. Dr. Michael Schleicher

Tag der Abgabe: 08.08.2011
Tag der mündlichen Prüfung: 15.11.2011

ERKLÄRUNG

Hiermit versichere ich ehrenwörtlich, dass meine Dissertation selbständig und ohne unerlaubte Hilfsmittel angefertigt worden ist.

Die vorliegende Dissertation wurde weder ganz, noch teilweise bei einer anderen Prüfungskommission vorgelegt.

Ich habe noch zu keinem früheren Zeitpunkt versucht eine Dissertation einzureichen oder an einer Doktorprüfung teilzunehmen.

München, den 15.11.2011

TABLE OF CONTENTS

LIST OF FIGURES

LIST OF TABLES

LIST OF ABBREVIATIONS

AR	Androgen receptor
a.u.	Arbitrary units
AROM+	Transgenic mouse expressing human P450 aromatase
ATP	Adenosine triphosphate
bp	Base pairs
BSA	Bovine serum albumin
°C	Celsius
Ca^{2+}	Calcium
cAMP	Cyclic adenosine monophosphate
cDNA	Complementary deoxyribonucleic acid
CO_2	Carbon dioxide
DAB	Diaminobezidin
DAPI	4′, 6′-diamidino-2′-phenylindole
d	Day(s)
DCN	Decorin
ddH_2O	Double-distilled water
DEPC	Diethylpyrocarbonate
15dPGJ2	15-deoxy-Δ^{12-14}-Prostagladin-J2
DMEM	Dublecco`s modified Eagle`s medium
DMSO	Dimethylsulfidoxide
dNTPs	Deoxynucleoside triphosphates
DTT	Dithiothreitol
ECM	Extracellular matrix
EDTA	Ethylenediaminetetraacetic acid
EGF	Epidermal growth factor
EGFR	Epidermal growth factor receptor
ELISA	Enzyme-Linked Immunosorbent Assay
ER	Estrogen receptor
ErbB2	V-erb-b2 erythroblastic leukemia viral oncogene homolog 2
ErbB3	V-erb-b2 erythroblastic leukemia viral oncogene homolog 3
ErbB4	V-erb-a erythroblastic leukemia viral oncogene homolog 4
Erk	Extracellular regulated kinase
FCS	Fetal calf serum

FGF	Fibroblast growth factor
FITC	Fluorescein isothiocyanate
Fluo-4-AM	Fluo-4, acetoxy-methylester
FSH	Follicle-stimulating hormone
g	Gram
GA	Germ cell arrest
GAG	Glycosaminoglycan
GDNF	Glial cell line derived neurotrophic factor
GnRH	Gonadotropin-releasing hormone
h	Hour(s)
HEPES	4-(2-hydroxyethyl)-1-piperazineethanesulfonic acid
HGF	Hepatocyte growth factor
HGFR	Hepatocyte growth factor receptor
HRP	Horseradish peroxidase
HTPC	Human testicular peritubular cell
HTPC-F	Human testicular peritubular cell from fibrotic testes
IGF-1	Insulin-like growth factor 1
IGF-1R	Insulin-like growth factor 1 receptor
IL	Interleukin
LH	Luteinizing hormone
M	Molar
mA	Milliampere
MA	Mixed atrophy
MAPK	Mitogen-activated protein kinase
MCP-1	Monocyte chemoattractant protein 1
mg	Milligram
min	Minute(s)
ml	Milliliter
mm	Millimeter
mM	Millimolar
MYH	Myosin heavy chain
mRNA	Messenger ribonucleic acid
ng	Nanogram
NGF	Nerve growth factor
NIH	National Institutes of Health
nm	Nanometer

nM	Nanomolar
NPE	Sodiumchloride/Pipes/EDTA
ONPRC	Oregon National Primate Center
PAR	Protease-activated receptor
PBS	Phosphate buffered saline
PCR	Polymerase chain reaction
PDGF	Platelet-derived growth factor
PDGFR	Platelet-derived growth factor receptor
PFA	Paraformaldehyde
pg	Picogram
PModS	Peritubular cell factor that modulates Sertoli cell activity
QRT-PCR	Quantitative real-time polymerase chain reaction
RLU	Relative luminescence units
RNA	Ribonucleic acid
RPL19	Ribosomal protein L19
rpm	Revolutions per minute
RPMI	Roswell Park Memorial Institute
RTK	Receptor tyrosine kinase
RT-PCR	Real-time polymerase chain reaction
SCO	Sertoli cell-only
sec	Second(s)
SEM	Standard error of the mean
SLRP	Small leucine-rich protein
SMA	Smooth muscle actin
SDS-PAGE	Sodium dodecyl sulfate polyacrylamide gel electrophoresis
TBE	Tris base/boric acid/EDTA
TBS	Tris buffered saline
TGF-α/-β	Transforming growth factor-alpha/beta
TNF-α	Tumor necrosis factor alpha
TNFR	Tumor necrosis factor receptor
V	Volt
VEGF	Vascular endothelial growth factor
VEGFR	Vascular endothelial growth factor receptor
WT	Wild type
y	Year(s)
µg, µl, µm	Microgram, -liter, -meter

1. INTRODUCTION

1.1 Male infertility

Human infertility is an emotionally charged problem affecting an estimated 15 % of all couples. It is defined as the inability to conceive within 12 months or longer (1). The man should be evaluated concurrently with the woman, since the male factor is the primary or contributing cause in approximately 40 % to 50 % of cases (1, 2). Thus, half of all cases of infertility can be attributed in part or completely to the male factor.

Fertility in men requires normal spermatogenesis, sperm transport, and accessory gland function. Hence, the causes for male infertility are diverse and are linked to e.g. hormonal imbalance, congenital abnormalities such as cryptorchidism, infections, antispermatogenic agents and sexual dysfunction (3). A general decrease of male fertility during the last decades has been reported and might be due to harmful environmental influences, stress and pollutants (4). Commonly, when it comes to diagnose male infertility, the analysis of the semen is the most obvious way to evaluate the man (2). A semen analysis allows determining sperm concentration, motility and morphology (World Health Organization 2003 (204)). Nevertheless, it is only a surrogate marker to assess male fertility because approximately 15 % of patients with male factor infertility have normal semen (5). In these cases other tests, such as hormone assessment, genetic studies and testicular biopsies, are necessary. The latter is needed to evaluate spermatogenesis in patients with potential genital tract obstructions. A high proportion of men with genital tract obstructions suffer from severe spermatogenic disorders (6). These cases of spermatogenesis failures reach from moderate to severe hypospermatogenesis. For instance, testes of men with germ cell arrest (GA) possess cellular components for functional spermatogenesis, but at a certain stage the process is interrupted and no functional spermatozoa are produced (3, 7). A further important testicular disease diagnosed in infertile men is the Sertoli cell-only (SCO) syndrome, where tubules contain Sertoli cells but no germ cells (3). Sub- or infertile men can also be diagnosed with mixed atrophy (MA), which is characterized by tubules with various degrees of degeneration of the germinal epithelium within the same biopsy. Seminiferous tubules, in which all germ and Sertoli cells have disappeared and only thickened walls are left, can occur in close proximity to normal tubules (8).

Although infertility in men can result from several reasons, it is an important fact, that in approximately 40 % to 50 % of all cases no specific etiologic cause can be defined and a full understanding of male infertility in these cases remains elusive (3).

1.2 Testicular morphology

The testis is a complex organ of the male reproductive system. Healthy male mammals possess two ellipsoid shaped testes. In healthy adult men average testicular volume is 15 – 30 ml and normal testis size is approximately 3.5 – 5.5 cm in length and 2.0 – 3.0 cm in width (9).

The two major functions of the testis are the production of hormones and spermatozoa. The testicular capsule, the tunica albuginea, consists of tight connective tissue and represents the outermost layer of the testis. Fibrous septa originate from the tunica albuginea and divide the organ into about 250 compartments, the so-called lobuli testes. Each lobuli testes contains 1 – 4 strongly coiled tubuli seminiferi, in which developing germ cells and Sertoli cells are located. The seminiferous tubules are surrounded by loose connective tissue containing Leydig cells, peritubular myoid cells, blood and lymphatic vessels, immune cells and neurons. The average diameter of the seminiferous tubule in sexual mature human testis is 150 – 250 μm. Seminiferous tubules are 30 – 70 cm in length and at the end of each tubule, the lumen narrows and continues in tubil recti, that connect the seminiferous tubules to the rete testis. Via ductuli efferentes the rete testis is connected to the epididymis (10). The seminiferous tubular compartment of the human testis occupies about 90 % of the organ volume (11).

1.3 Testicular cytoarchitecture and function

In adult mammals the testis comprises two structurally distinct but functionally connected compartments: the tubular seminiferous epithelium and the interstitial compartment between the seminiferous tubules (Figure 1-1). These two compartments fulfill the main functions of the testis: interstitial cells secrete testicular androgens, while seminiferous tubules produce male germ cells.

Seminiferous epithelium

The seminiferous epithelium contains Sertoli and germ cells. The latter occur at different developmental stages within the seminiferous epithelium. Ultrastructural examination of the human seminiferous epithelium has shown that the arrangement of germ cells is highly organized into a helical patterns based upon the geometry of concentric spirals (12). Spermatogonia, which represent a primitive stage of germ cell, are located in the basal compartment (Figure 1-1). After the onset of sexual maturity spermatogonia develop, during a complex process called spermatogenesis, to mature spermatozoa. Spermatogenesis begins with a series of mitoses in the spermatogonium and the newly formed cells can continue as stem cells for the spermatogenic lineage, type A spermatogonia, or as progenitor cells, type B spermatogonia. The latter differentiates into primary spermatocytes which undergo the first meiotic division, a process that results in secondary spermatocytes. Secondary spermatocytes occupy positions closer to the lumen of the tubule and quickly enter into the second

meiotic division that results in spermatides. During spermiogenesis, spermatides differentiate to spermatozoa. Finally, mature spermatozoa are released to the lumen of the seminiferous tubule, which ends in the rete testis and leads to the epididymis. The whole process of spermatogenesis lasts approximately 70 days (3, 10).

Sertoli cells provide structural and functional support to developing germ cells and extend from the basal lamina to the lumen of the seminiferous tubule and partially envelop germ cells (Figure 1-1) (9). They are characterized by their polar, elongated shape and their elongated, folded or indented nucleus (10, 12, 13). In adult human testis Sertoli cells continuously produce and secrete a fluid into the lumen of the seminiferous tubule, a process that is androgen-dependent. This fluid contains various factors to nourish germ cells, as well as, to support spermatogenesis and is responsible for the transport of sperm within the seminiferous tubule (3, 10).

In the basal part of the seminiferous tubule, adjacent Sertoli cells form tight junctions and constitute the so-called blood-testis barrier, which divides the seminiferous tubule into basal and adluminal compartements. The blood-testis barrier prevents large molecules, steroids and ions to pass from the blood into the lumen of the seminiferous tubule and thus creates a protected environment within the tubule to support spermatogenesis. In this way, the more advanced stages of spermatogenesis are protected against toxic agents transported by blood to the testis and furthermore against an auto-immune reaction caused by arising sperm proteins during puberty (10). During the reproductive period human Sertoli cells do not divide. Therefore they are extremely resistant to infections, malnutrition, and x-ray irraditation.

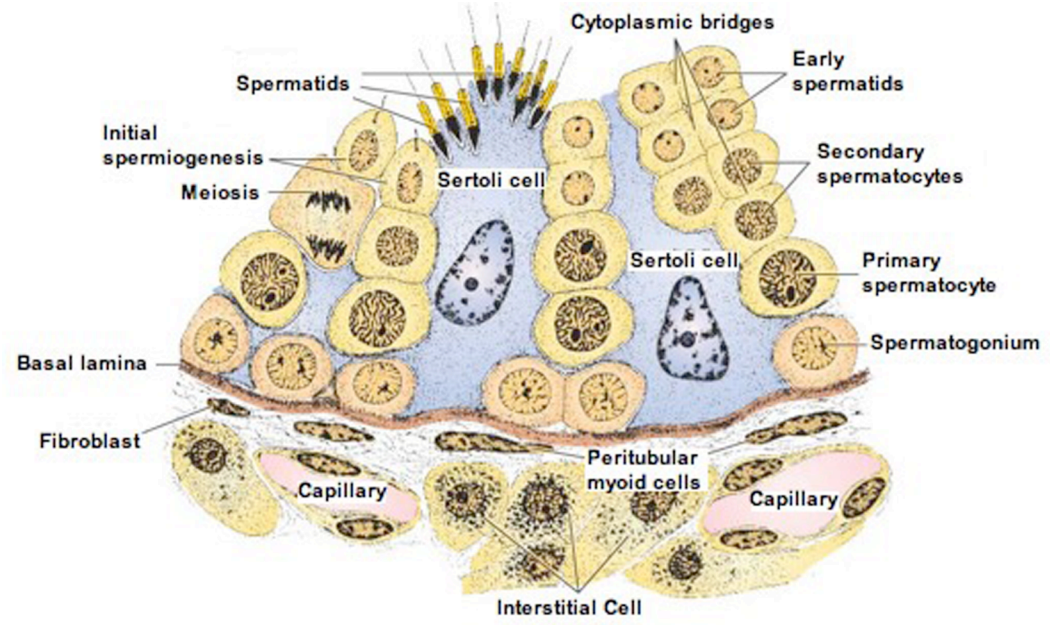

Figure 1-1: Diagram of the testicular compartments. A part of a seminiferous tubule and surrounding interstitial is shown. This figure was modified after Juniqueira *et al*., 2005 (10).

Interstitial tissue

The interstitial compartment in human testes is located between the seminiferous tubules and contains connective tissue, neurons, blood and lymphatic vessels, immune cells, peritubular myoid cells and Leydig cells. Adult Leydig cells are characterized by their round or polygonal shape and their ovoid nucleus with a prominent nucleolus. In a process called steroidogenesis, Leydig cells produce steroids, primarily testosterone, which are important for an efficient spermatogenesis and furthermore are responsible for developing secondary male sex characteristics (10, 12, 13).

As Leydig cells and interstitial fibroblasts, peritubular myoid cells are derived from mesenchymal cells. In the interstitial compartment they surround the seminiferous epithelium and are in contact with the basal surface of Sertoli cells (Figure 1-1). Because of their contractile phenotype, peritubular myoid cells are essentially involved in the transport of spermatozoa and testicular fluid through the seminiferous tubules (14).

A further interstitial component of the testis is the extensive extracellular matrix (ECM), which provides structural integrity of the testis. Numerous ECM components, including fibronectin, laminin, collagens type I and IV and proteoglycans, are produced and secreted by Sertoli cells, peritubular myoid cells and Leydig cells. Sertoli cells and peritubular myoid cells cooperate to form the basal lamina of the seminiferous tubules. The ECM is able to affect peritubular myoid and Sertoli cell functions and therefore plays an important role in male reproductive health (13, 14).

1.4 Regulation of testicular function

Spermatogenesis is a complex process, depending on hormones secreted by the hypothalamus, hormone gonadotropin-releasing hormone (GnRH), and hormones secreted by the pituitary gland, namely luteinizing hormone (LH) and follicle-stimulating hormone (FSH). The appropriate regulation of androgen activity via this hypothalamic-pituitary-testicular axis is necessary for developing male phenotype characteristics, as well as for the initiation and maintenance of spermatogenesis (10).

LH stimulates Leydig cell steroidogenesis, a process in which androgens, especially testosterone, are synthesized. Stimulation of the androgen pathways occurs mainly through cyclic adenosine monophosphate (cAMP) mediated mechanisms, including LH induced guanyl nucleotide binding, membrane phosphorylation and adenylat cyclase activation. Activation of cAMP dependent kinase likely leads to phosphorylation of proteins of the steroidogenic pathway and subsequently testosterone production is increased (15).

FSH acts on the seminiferous epithelium, in particular on Sertoli cells. Under FSH/testosterone control Sertoli cells secrete androgen-binding protein that serves to concentrate testosterone in the seminiferous tubule. Testosterone is essential for the initiation and maintenance of spermatogenesis

and therefore fertility, but how it exerts this effect is not completely clear (16, 17). Receptors for testosterone, androgen receptors (ARs), are expressed in Sertoli cells, germ cells and peritubular myoid cells. Continuing uncertainty exists over which cell type mediates testosterone control over spermatogenesis, but it has been shown in mouse testis that germ cells lacking the AR mature normally (18). Therefore testosterone is believed to regulate spermatogenesis via somatic cells in the testis. In mouse studies the importance of androgen action on peritubular myoid cells for normal spermatogenesis has been shown (19).

The factors produced by testicular cells do not only influence the testis itself but also affect some extratesticular functions. Testosterone, for example, can affect secondary sex characteristics. It influences hair growth, skin, muscle and male accessory sex organs (10).

Estrogens are required for a normal testicular function, as well. Reports of testicular anomalies in men with naturally occurring mutations in the aromatase gene and of rodents lacking a functional estrogen receptor alpha (ER-α) support the view that estrogens are essential in human male differentiation, spermatogenesis and steroidogenesis (20-22).

Testicular functions are known to be primarily regulated by endocrine mechanisms via LH and FSH. However, the proximity of different cell types in the testis, as well as a number of regulatory factors produced intratesticularly, strongly suggest a role of paracrine regulation in testicular function (23-25). For example, intratesticular produced growth factors have been shown to influence proliferation and biological function of various human testicular cells (26). Among these growth factors, epidermal growth factor (EGF), a cytokine that promotes cell proliferation, regulates tissue differentiation, and modulates organogenesis in several species (27, 28), has been described. In the human testis the receptor for EGF (EGFR) has been detected in Leydig and peritubular myoid cells, but not in Sertoli and germ cells (26). Very few studies have dealt with EGF/EGFR signaling in the human testis, but in rat it was reported to be involved in testis development and spermatogenesis (28).

A further important growth factor system has been identified in the testis, namely platelet-derived growth factor (PDGF) and its receptors PDGFR-α and -β. In rodents, PDGF was reported to play important roles in testis development and the regulation of spermatogenesis (29, 30). Furthermore, it has been shown, that PDGF enhances testosterone production by adult rat Leydig cells (31) and stimulates proliferation of peritubular myoid cells (32). PDGF and PDGFRs have been reported to be expressed in the human testis possibly could affect testis developmental processes, spermatogenesis and male infertility (33).

1.5 Peritubular myoid cells

Peritubular cells, which are of particular interest in the present study, have been described for the first time in 1901 by Regaud (34) who observed a single layer of flattened cells surrounding the seminiferous tubule in the rat testis. Electron microscopic studies of the peritubular connective tissue in human testis by Ross and Long in 1966 (35) revealed the presence of "contractile-type" cells. Similar to smooth muscle cells, cytoplasmic filaments, cell surface invaginations and centrally located organelles were found in peritubular cells. These cytological resemblances to smooth muscle cells finally lead to the name "peritubular myoid cells" (36). Because of their contractility, peritubular myoid cells play an important role in the transport of the spermatozoa within the lumen of the seminiferous tubule. It has been shown that several substances, e.g. prostaglandins, Tumor growth factor beta (TGF-β) and endothelin, can affect the contractions of the seminiferous tubules (14).

Ultrastructural analysis showed that cytoplasmatic filaments within the peritubular myoid cells are expressed and distributed in a species-specific manner (14, 37). Among actin isoforms, alpha-smooth muscle actin (α-SMA) occurs only in myoid and vascular smooth muscle cells and in no other rat cell type (38). In the monkey α-SMA is used as specific marker for testicular peritubular myoid cells (39). In addition to actin, peritubular myoid cells of several species, including the human, were shown to also contain myosin and intermediate filaments (40).

The number of cell layers surrounding the seminiferous tubule varies from species to species (41). While in rodents (rat, mouse, hamster) peritubular myoid cells form a single flat layer, multiple (five till seven) layers exist in humans. In the human testis each layer is separated by laminae of extracellular connective tissue. Species-specific differences also exist in the degree of differentiation from fibroblasts to smooth muscle cells in the myoid cell population. In humans the one or two outermost layers of peritubular cells are regarded to be fibroblasts and the inner layers are thought to be smooth muscle cells (42).

In addition to their role in contraction of the seminiferous tubules, peritubular myoid cells are able to synthesize numerous substances. Among those are components of the ECM, including fibronectin, type I and IV collagens and proteoglycans. In cooperation with Sertoli cells, that produce laminin, type IV collagen and proteoglycans, peritubular myoid cells form the basal lamina of the seminiferous tubules (14, 43).

Previous studies indicated that peritubular myoid cells in rodents via their secreted products can contribute directly or indirectly to spermatogenesis and testicular development. They possess the ability to secrete factors such as PModS (peritubular cell factor that modulates Sertoli cell activity in rodents (44)), or growth factors like TGF-α (45), TGF-β (46), insulin-like growth factor 1 (IGF-1) (47), activin-A (48) and fibroblast growth factor (FGF) (49). Thus, human peritubular myoid cells may as well affect adjacent testicular cell types via secreted factors and thus have regulatory functions in spermatogenesis and testis development.

1.6 Testicular fibrosis, mast cells and macrophages

Fibrosis is a pathological event that occurs in many organs of the body, e.g. the lung, liver, kidney, heart and skin, and is characterized by increased fibroblast numbers and accumulation of ECM proteins (50-52).

In the human testis, various forms of hypospermatogensis are accompanied by fibrotic thickening of the wall of the seminiferous tubules (53). As mentioned above, increased levels of ECM components are produced under these pathological conditions and lead to fibrotic remodeling of the tubular wall which is a typical event associated with male infertility (3). While the average thickness of the peritubular wall in normal testis is 7 – 9 µm, in patients with disturbed spermatogenesis it is increased to 12 – 20 µm (42, 54). However, regardless of the varying thickness of the ECM, the number of cellular layers surrounding the seminiferous tubule remains constant (42). The reasons for the fibrotic changes in the testis and their consequences for male infertility are not clear, but it has been speculated that the thickened testicular peritubular wall could disturb the exchange of fluid between the tubular compartment and the interstitial compartment (55).

Interestingly, several studies showed that fibrotic changes in the testis and testicular dysfunction correlate with increased numbers of testicular immune cells (54, 56-62). In the healthy human testis, mast cells, macrophages and leukocytes occur, and are located mainly to the interstitial compartment (63, 64). Normally, testicular mast cells are characterized by their round phenotype and besides their occurrence in the interstitial compartment, about 13 % of total mast cells can be detected in the peritubular region (54). In infertile men, suffering from GA or SCO syndrome, a two respectively three times higher testicular mast cell number than in normal testis was found. Another striking difference to normal testis was reported: more mast cells are located in the peritubular wall of infertile men. In testes of GA and SCO patients, 19 % respectively 26 % of total testicular mast cells were located in the peritubular region. The phenotype of mast cells in the testis of infertile men is altered as well. Mast cells of men with impaired spermatogenesis are heterogeneous, with an irregular, round or elongated shape and show signs of activation and degranulation. Interestingly, the thickness of the fibrotic remodeled tubular wall in infertile men coincides with the number of activated mast cells (54). This important finding raised the question how increased numbers of activated testicular mast cells can be linked to sub-/infertility. Several studies showed that mast cells, in general, are able to secrete various products, including histamine, serotonin, growth factors, prostaglandins, cytokines and proteases (62, 65-67). In rodents, testicular mast cell products (e.g serotonin or histamin) that could be involved in regulation of testicular steroidogenesis have been identified (68, 69). Human testicular mast cells secrete mainly histamine, chymase and tryptase (54, 57, 70). The serine protease tryptase has been shown to activate the protease-activated receptor (PAR)-2 (59, 71), a process that leads to fibroblast proliferation (66, 72, 73). Furthermore, PAR-2 activation by tryptase can stimulate synthesis of type I collagen (74, 75) and enhance fibroblast chemotaxis (59).

The observation that mast cell numbers are increased in testis of men with spermatogenesis defects, especially in the peritubular region, led to the suggestion that mast cells via tryptase could be directly responsible for the development of testicular fibrosis in infertility patients (54, 57).

Morphological studies revealed that testicular macrophages are located in the interstitial compartment and occasionally in the peritubular region and inside the lumen of seminiferous tubules of the normal human testis (58, 64, 76). Because of their ability to produce and secrete some inflammatory cytokines, e.g. interleukin 1 alpha (IL-1α), interleukin 1 beta (IL-1β) and tumor necrosis factor alpha (TNF-α) (77, 78), testicular macrophages play a potential role in paracrine interactions with other testicular cell types (58, 79).
Surprisingly, in the testis of men suffering from infertility the total number of macrophages is increased in comparison to normal testis (58). A two times higher macrophage number has been detected in GA and SCO syndrome patients. In MA patients the number of total macrophages is not altered, but the number of peritubular and intratubular macrophages is higher than in fertile men. In all pathologic states, a shift of macrophages from the interstitial compartment to the lumen of the tubules has been observed (58). These increased macrophage numbers in the testes with hypospermatogonism or complete absence of germ cells led to the suggestion that macrophages via their secretory products could contribute to the formation of male infertility.
It has been shown that mast cells and macrophages can interact with each other. This interaction leads to proliferation of fibroblasts and formation of collagen in some tissues (80, 81). The close anatomic proximity between macrophages and mast cells in the testicular interstitial area and in the wall of seminiferous tubules has been described and therefore an interaction between testicular mast cell and macrophages, that causes fibroblast proliferation and collagen formation and leads to testicular fibrosis, could be assumed (72). It remains unknown, what induces the fibrotic remodeling, called a hallmark of human male infertility (3), but mast cells and macrophages via their direct and indirect products may be involved.

1.7 The proteoglycan decorin

The components of the ECM of the human testis and their specific functions are not well known, but different collagen types, fibronectin, laminin (42, 82-88) and the proteoglycans, decorin (DCN) and biglycan (89) have been identified.
The first time that DCN, originally called PG40, appears in the literature is in 1986, when Krusius and Ruoslahti (90) described a small chondroitin/dermatan sulfate proteoglycan with a molecular weight of 40 kDa, which was expressed by human fibroblasts. DCN, whose name has derived from its

morphological nature to decorate collagen fibers *in vivo* (91), turned out to be a widely distributed component of the ECM. Besides its structural functions to regulate collagen fibrillogenesis, DCN might play an important regulatory role because of its ability to bind other ECM proteins, growth factors and growth factor receptors (92-94).

DCN is the prototype member of an expanding gene family of secreted proteoglycans called the small leucine-rich proteoglycans (SLRPs). The SLRPs share the unique structural motif of leucine-rich tandem repeats that are responsible for most of their biological functions (95). The family of SLRPs contains at least nine different members, including DCN, biglycan, lumican, proline-arginine-rich and leucine-rich repeat protein, keratocan, fibromodulin, lumican, epiphycan, and osteglycin, which are encoded by separate genes (96). The distribution of SLRPs among species and throughout evolution reflects a diversity of biological functions. Initially thought to act exclusively as structural constitutes and regulators of collagen fibrillogenesis, SLRPs are nowadays recognized as key players in cell signaling. They are able to influence cell proliferation, differentiation, survival, adhesion, migration and inflammatory responses (97-99).

The best-known and most studied members of the SLRP family are DCN and biglycan. Despite their structural similarity (55 % amino acid identity), DCN and biglycan show distinct patterns of temporal and spatial expression, indicating their different biological functions (100).

With regard to structural characteristics, DCN originally was divided into four distinct domains (Figure 1-2) (96). Domain I contains a signal peptide and a propeptide. The biological role of the propeptid is still unclear, but it may function as a recognition signal for the first enzyme, xylosyltransferase, involved in the synthesis of glycosaminoglycan (GAG) chains (101). The second structural domain of DCN is a negatively charged region, which contains four cysteine residues and one GAG chain. The central structural region, domain III, contains ten tandem leucine-rich repeats and is responsible for binding collagen type I (102, 103). It has been reported that besides collagen type I, DCN can also bind collagen type II (104), type III (105), and type VI (106). The fourth domain of the DCN molecule, the carboxyl end, contains a relatively large loop with two cysteine residues.

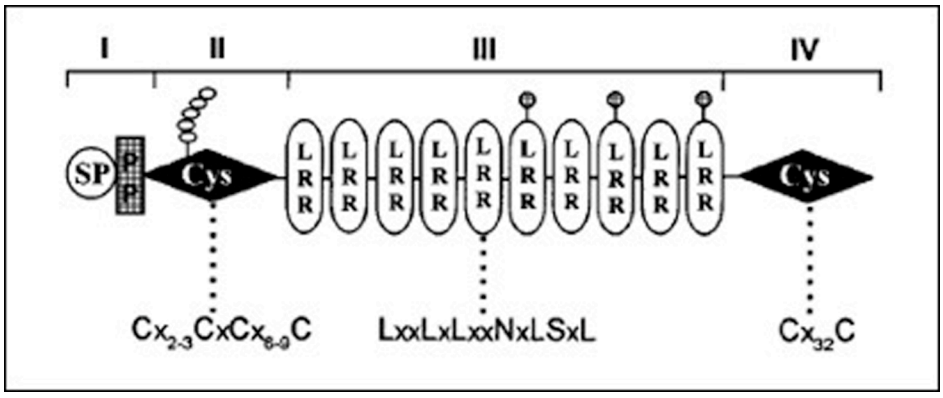

Figure 1-2: Diagram of the structural characteristics of DCN. The structure of the prototype member of the small leucine-rich proteoglycans can be diveided in four distinct domains (I-IV). SP: signal peptide, PP: propeptide, Cys: cysteine-rich region, LRR: leucine-rich repeat. This figure was modified after Iozzo, 1998 (96).

The *DCN* gene maps to the chromosome 12 (12q23) in humans (107), and to chromosome 10 in mice (108). The human *DCN* gene is encoded by eight distinct exons. The intron/exon junctions are highly conserved with nearly identical exon organization in the human and murine *DCN*. The human *DCN* gene harbors two leader exons (Ia and Ib) that are alternatively spliced to exon II (107), whereas the murine gene does not contain exon Ib (108). The promoter region of *DCN* is functional active (109) and contains two functional TNF-α-responsive elements that mediate a TNF-α-induced transcriptional repression of the *DCN* gene (110). It has been shown that *DCN* expression can be induced by IL-1 (111) or by IL-4 (112). In contrast, DCN is downregulated by TGF-β (109).

Computer modeling suggested that the human DCN core protein is arch shaped with a single GAG chain and three N-linked oligosaccharides located on the same side of the molecule. The leucine-rich repeats form a central cavity with the β-sheet on the inner concave surface and the α-helices on the outer convex surface (113). In the past it was assumed that the inner concave surface is able to bind one collagen molecule (113), but recent studies suggest that the protein core of one DCN molecule interacts with four to six collagen molecules (114).

The binding of DCN to fibrillar collagen (Figure 1-3) has important biological consequences *in vivo*, as has been shown by the DCN knock out mouse model. The disruption of the DCN gene in these mice lead to skin fragility with markedly reduced tensile strength and abnormal collagen morphology, characterized by uncontrolled lateral fusion of collagen fibrils (115).

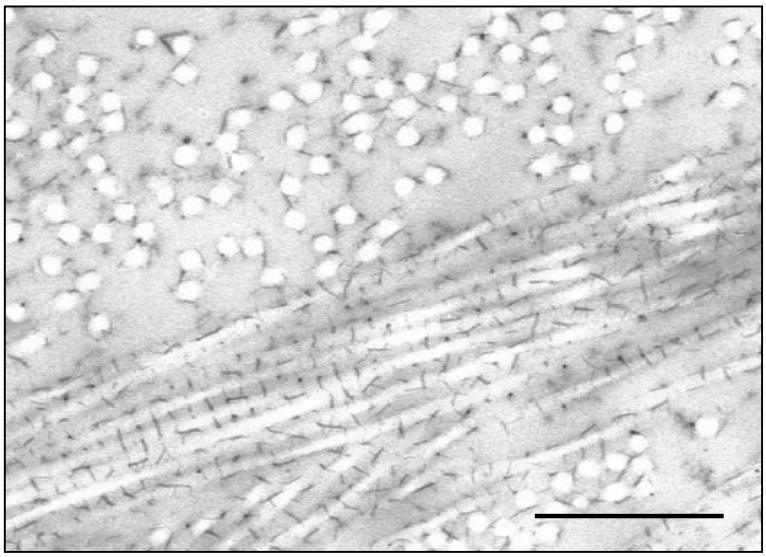

Figure 1-3: Electron micrographic view of DCN precipitates in the peritubular wall of human testis. Fine and distinct Cupromeronic blue precipitates (small black needles), representing DCN, interconnect adjacent collagen fibrils. Longitudinal and cross sections through collagen fibrils are shown. The length of the bar is approximately 0.1 µm. Electron micrographic picture was done by Prof. Dr. Dr. U. Welsch.

In addition to collagen fibrillogenesis, two other actions of DCN have been recognized, linking DCN to fundamental biological processes, including cell migration, adhesion and proliferation (116, 117). First, within the interstitial ECM, DCN binds a variety of soluble and insoluble ligands, thus regulating their availability and activity. This is well documented for TGF-β (118, 119) and PDGF (117). Second, DCN itself can act as a non-selective ligand for several growth factor receptors, including EGFR (120, 121), insulin-like growth factor 1 receptor (IGF-1R) (120-122), vascular endothelial growth factor receptor (VEGFR) (123) and hepatocyte growth factor receptor (HGFR) (124). It appears that DCN may cause initial activation of the respective signaling pathway, followed by its inactivation, as shown for example for EGFR (125). In tumor cells the binding of DCN to the EGFR leads to growth suppression by activation of the mitogen-activated protein kinase (MAPK)-pathway, calcium (Ca^{2+}) influx, induction of the cyclin-dependent kinase inhibitor p21, and subsequently down-regulation of the receptor (125-130).

In 1995 DCN was described for the first time in the healthy human testis (89). It has been reported that DCN gene expression is located to single, dispersed fibroblastic cells in the interstitial compartment, as well as to the adventitious layer of ateries and to cells of the peritubular wall. The possible role of DCN in the testis has not been investigated.

1.8 The cellular model

In the past very few studies dealt with human peritubular cell cultures (37, 131). Testicular tissue was obtained from prepubertal patients and enzymatic digestion methods have been used to isolate peritubular cells and investigate their temporarily steroidogenic potential (37). Another study showed the expression pattern of intergrins in human peritubular myoid cells as well as their role of the inhibition of contractility in rat and human pertitubular myoid cells (131).

A few years ago the successful isolation and cultivation of human testicular peritubular cells (HTPCs) (55) opened the door to the investigation of this unexplored testicular cell type and its involvement in paracrine mechanisms in the adult human testis *in vitro*. Peritubular cells were cultured from explants from testicular biopsies obtained from men undergoing reconstructive surgery for obstructive azoospermia but displaying normal spermatogenesis (for details see 2.1 and 3.1.1). Morphologically, HTPCs are characterized by their elongated, myofibroblast-like appearance. As they have been shown to be immunonegative for FSH and LH receptors, contaminations with Sertoli or Leydig cells can be excluded (55, 132).

The origin of isolated HTPCs from the peritubular region was proven *in vivo* and *in vitro* by immunostaining with fibroblast markers (CD90/THY1) and the smooth muscle cell marker, α-SMA (55). Furthermore the expression of ECM genes and genes coding for basement membrane components, such as collagen type I, IV and XVIII, fibronectin and laminin, by HTPCs was shown (55). Cultivated HTPCs express functional receptors for the immune cell products histamine (H1), tryptase (PAR-2) and the cytokine TNF-α (TNFR1 and -2) (55, 132, 133). The secretory character of these cells was identified and secreted products such as nerve growth factor (NGF), monocyte chemoattractant protein (MCP-1), prostaglandins, IL-6 and glial cell line derived growth factor (GDNF) were detected (132, 133).

Recently the isolation of HTPC-Fs, the corresponding cells from testes of men with existing fibrotic changes and spermatogenesis defects, was described (132). The reported loss of contractility markers and hypertrophy in cultured peritubular cells of men with impaired spermatogenesis indicates a switch of the phenotype of peritubular cells from a contractile to a synthesizing cell type (134).

1.9 The AROM+ mouse

Aromatization of androgens is a key step in estrogen production in the gonads (135). The enzyme aromatase is responsible for this process. With regard to male reproductive functions, the estrogen/androgen ratio in the testis is of particular interest (21). To study the important regulation of the balance between estrogen/androgen in the testis, transgenic mice expressing human P450 aromatase under the human ubiquitin C promoter were generated (AROM+) (135). While AROM+ females are unaffected, AROM+ males are characterized by an imbalance in intratesticular sex hormone metabolism, resulting in elevated serum estradiol and prolactin concentrations, combined with significantly reduced testosterone and FSH levels. The mice suffer from structural and functional alterations in the reproductive organs, including cryptorchidism, Leydig cell hyperplasia, and impaired spermatogenesis. Furthermore, the AROM+ males develop rhabdosphincter atrophy and rudimentary sex glands (136).

Old male AROM+ mice (15 months) develop Leydig cell hypertrophy and adenoma (137). Chronic inflammation, characterized by an increased number of activated, TNF-α producing, macrophages in the testicular interstitial region of aging AROM+ mice, has been reported. The increased activity of the macrophages is associated with Leydig cell depletion and an increased number of mast cells and fibroblasts in the interstitial compartment. Interestingly, similar findings have been made in testes of infertile men (54).

1.10 Aims of the study

Impaired spermatogenesis in men is frequently accompanied by accumulation of testicular immune cells and by fibrotic remodeling of the walls of the seminiferous tubules. Surprisingly little is known about this remodeling process that is associated with male infertility, but striking alterations of the cellular components of the testicular peritubular wall and of the ECM are evident. The expression and the role of ECM proteoglycans, such as DCN, in the testis has not been studied yet. Because studies in other organs have shown that DCN acts as a ligand of growth factor receptors or can store growth factors, similar interactions with growth factor signaling might play a role in the testis in health and disease.

In order to examine this hypothesis, the present study investigates DCN expression sites in the human, non-human primate (rhesus monkey) and mouse testes. To gain further insights in DCN expression in pathologically altered testis, human samples of MA, GA and SCO syndrome patients and samples of a transgenic mouse model (AROM+) were investigated. AROM+ males are characterized by infertility and a high amount of activated macrophages, infiltrating mast cells and interstitial fibrosis in the testis and thus are an appropriate model for the study of inflammation-associated male infertility. Finally,

expression of DCN during testicular development was studied in the non-human primate, using testicular samples of rhesus monkeys of different ages.

Having established strong expression of DCN in the human testicular peritubular compartment, cells of this region were further examined with respect to regulation and action of DCN. DCN regulation and function in the human testis in health and disease were examined using primary HTPCs, which stem from testes with normal spermatogenesis and from men suffering from spermatogenic failure and fibrotically altered tubular walls (HTPC-Fs). Testicular factors known to play important roles in male reproductive health, were investigated for their ability to regulate DCN. The expression of growth factor receptors in HTPCs and HTPC-Fs was examined and the ability of DCN to interact with growth factor signaling, especially with EGF and PDGF, was studied.

Since strong DCN expression was found in testes of AROM+ males, primary mouse testicular fibroblasts were isolated to further examine DCN regulation in this cell type.

In additional experiments, the action of the cancer drug imatinib mesylate, an exogenous ligand to growth factor receptors, on viability of HTPCs and its interaction with PDGF signaling in these cells were studied.

2. MATERIAL

2.1 Human biopsies

Human testicular tissue used in this study was obtained by open biopsy carried out by Prof. Dr. J. U. Schwarzer (Praxis Urology-Andrology, Freising, Germany) or Prof. Dr. F. M. Köhn (Andrologicum, Munich, Germany). Testicular biopsies were isolated from vasectomized men with obstructive azoospermia undergoing reconstructive surgery but displaying normal spermatogenesis. Furthermore, biopsies were obtained from patients with spermatogenesis defects and fibrosis in the wall of the seminiferous tubules. In these cases of sub-/infertility, men are suffering from different testicular disorders, including MA, GA or SCO syndrome. The ages of the patients in this study range between 27 and 53 years. All participants granted written informed consent. The ethics committee of the Technical University in Munich approved the study.

2.2 Transgenic mice expressing human P450 aromatase

In this study the AROM+ mouse model was used (135-137). Generation of transgenic male mice expressing human aromatase complementary deoxyribonucleic acid (cDNA) under the control of ubiquitin C promotor (AROM+ mice) was carried out by Dr. Leena Strauss (Department of Physiology and Turku Center for Disease Modeling, Institute of Biomedicine, University of Turku, Finland). The mice were fed with Soya free diet, and they were maintained in a specific pathogen-free stage at Central Animal Laboratory at the University of Turku, complying with international guidelines on the care and use of laboratory animals. All animal experiments were approved by the Finnish Animal Ethics Committee.

The AROM+ mice were generated in FVB/N genetic background (135). For genotyping of the mice, polymerase chain reaction (PCR) analyses were performed using DNA extracted from tail biopsies. Genotyping was carried out by Dr. Leena Strauss as described by Li *et al.* in 2001 (135).

Testicular samples from at least three young (3 – 5 months of age) and old adult (9 – 10 months of age) AROM+ and age-matched wild type (WT) males were fixed in Bouin's solution, embedded in paraffin and 5 µm-thick sections for immunohistochemistry were prepared (137). Freshly isolated testes of AROM+ and wild type mice of different ages (2 weeks till 9 months) were used for cell culture experiments. In addition, testes from at least three young and three old wild type and AROM+ mice were frozen and kept until isolation of ribonucleic acid (RNA).

2.3 Rhesus monkey testicular samples

Testes from rhesus monkeys (*Macaca mulatta*) that were primarily involved in other unrelated studies (138) were obtained through the Oregon National Primate Research Center (ONPRC) Tissue Distribution Program by Prof. Dr. Henryk F. Urbanski and Vasilios T. Garyfallou. The animals were cared for by the ONPRC in accordance with the National Research Council's Guide for the Care and Use of Laboratory Animals. They were classified as: infantile (0 - 1 year; n = 4), juvenile (1 - 2 years; n = 1), peripubertal (3 - 4 years; n = 2), young adult (5 - 6 years; n = 3) and old adult (24 - 30 years; n = 5).

For the purpose of this study, the testes were isolated and were fixed for at least 48 h in Bouin's solution, followed by 70 % ethanol, and then embedded in paraffin. Sections (5 µm) were prepared for immunohistochemistry experiments.

2.4 Other materials

All chemicals, kits and assays, antibodies, machines and laboratory materials, used in this study, are listened in the APPENDIX (table 10-1 till 10-6). An overview about composition of all buffers and solutions employed is given in the APPENDIX (table 10-7).

3. METHODS

3.1 Cell culture

3.1.1 Isolation and cultivation of HTPC/-Fs

HTPC and HTPC-Fs were isolated as described by Albrecht *et al*. in 2006 (55). Immediately after removal, the testis tissue was transferred to Dublecco`s modified Eagle`s medium (DMEM)/Ham´s F12 medium containing 20 mM 4-(2-hydroxyethyl)-1-piperazineethanesulfonic acid (HEPES), 0.5 g/l sodium bicarbonate, 15 % fetal calf serum (FCS), 100 U/ml penicillin, and 100 µg/ml streptomycin. Under sterile conditions the testicular tissue covered with medium was dissected into small pieces (1 – 2 mm^3) using forceps and scalpel. Drops (approximately 10 µl) of human plasma supplemented with calcium chloride (1 mM) were placed on a 60-mm plastic culture dish and the tissue samples were placed in these drops to adhere the testicular explants to the surface of the culture dish. Small drops of medium were placed between the tissue samples to assure sufficient humidity. The explants were incubated over night at 37 °C, 5 % CO_2 and 95 % humidity, and subsequently checked for adherence. The adherent explants were cultured in medium composed as described above. After about one week the cell outgrowth started and tissue pieces were carefully removed. When the cells have grown to confluence they were trypsinized and subcultured adding 1.5 ml trypsin-ethylene-diaminetetraacetic acid (EDTA) for 4 min. The reaction was stopped adding 3 ml DMEM supplemented with 10 % FCS and centrifuging the cell suspension at 1,000 revolutions per minute (rpm). HTPCs and HTPC-Fs were cultured in DMEM supplemented with 10 % FCS unless indicated otherwise.

Before the cells were used for further investigations, every sample was tested for mycoplasma contamination using a commercial mycoplasma detecting kit for conventional PCR according to the manufacturer`s protocol. Cells from passages 2 – 15 were used freshly or cryopreserved for all experiments. Cyropreservation in 1.6 ml cryocups was performed using DMEM (high Glucose 4.5 g/L; with L-Glutamine and Phenol Red) containing 10 % FCS and 5 % dimethylsulfidoxide (DMSO).

3.1.2 Isolation of mouse testicular fibroblasts

At first, mouse testicular peritubular cells were isolated and cultivated using the explant method described for HTPCs above. Three different media were used for this approach. Immediately after removal, one group of mouse testicular samples was transferred to the medium as used for cultivating HTPCs (DMEM/Ham`s F12 medium containing 20 mM HEPES, 0.5 g/l sodium bicarbonate, 15 % FCS, 100 U/ml penicillin, and 100 µg/ml streptomycin), another group into Roswell Park Memorial

Institute (RPMI) 1640 medium (Ready mix with L-Glutamine, Phenol Red and 10 % FCS) and a third group of testicular samples was transferred into a smooth muscle cell-specific growth medium. Under sterile conditions the testes covered with medium were decapsulated and dissected into small pieces (1 – 2 mm^3). Afterwards the samples were processed as described for human samples.

In about 70 % of cultures with fibroblast growth medium and about 40 % of cultures with RPMI cell outgrowth started from few explants after about five days. The cells grew very slowly to confluence and when they were trypsinized for subculturing, a high death rate could be observed. No cell growth could be observed in samples cultured with DMEM/Ham´s F12. Mice of different ages, from two weeks till five months, were used for cell isolation experiments, but cell growth could not be improved.

Since mouse peritubular cells, using the explant method did not grow well, mouse testicular fibroblasts from the interstitial region were isolated by collagenase digestion. Testes were removed from 4 – 10 months old animals and collected in DMEM supplemented with 10 % FCS, 100 U/ml penicillin, and 100 µg/ml streptomycin. The tunica albuginea and as much of the vascular tissue as possible were removed. The tissue was transferred into fresh medium and was minced in a petri dish under sterile conditions. The tissue fragments were treated with a solution of collagenase I (200 U/ml) in DMEM with 10 % FCS. During incubation in a water bath at 37 °C for 1 h 30 min, the samples were gently vortexed every 10 min. After this digestion procedure the epithelial cell fraction was allowed to sediment for 2 min. The supernatant, containing the fibroblasts, was transferred to a new tube and centrifuged at 800 rpm for 3 min. Afterwards it was washed twice with phosphate buffered saline (PBS). The cell pellet was resolved in DMEM (supplemented with 10 % FCS, 100 U/ml penicillin and 100 µg/ml) and seeded on 60 mm plastic culture dishes. The number of culture dishes depended on the size of the cell pellet. Usually six dishes per animal were obtained. The cells were incubated over night at 37 °C, 5 % CO_2 and 95 % humidity, subsequently checked for adherence and washed twice with DMEM.

3.1.3 NIH/3T3 cells

NIH/3T3 (3-day transfer, inoculum 3 x 10^5) cells, standard mouse fibroblasts, were used for initial studies in mice. Originally, this cell line was established from primary mouse embryonic cells (139). The cells were cultured in DMEM supplemented with 10 % FCS and were incubated in a 5 % CO_2 atmosphere at 37 °C and 95 % humidity.

3.1.4 Cell treatment

It was assumed that substances, which are known to play important regulatory roles in the testis, might affect DCN gene expression in the peritubular wall. The regulation of DCN expression in the nearly unexplored cellular models HTPC and HTPC-Fs was investigated performing an initial screening by challenging respectively both cell types with several substances as stated below.

Testosterone is the main regulating androgen produced by the testis. Therefore, HTPC/-Fs which possess AR (unpublished data), were challenged with testosterone. A concentration of 100 nM for a time period of 24 h was used. Testosterone was dissolved in 100 % ethanol and used at a 1:1000 dilution. Since the estrogen/androgen level plays a significant role in male reproductive health (135), peritubular cells of healthy testis and cells of testis of infertile men were treated with 17β-estradiol (concentrations: 100 nM and 1 µM; dissolved in 100 % ethanol and diluted 1:1000 and 1:100) for 6 h and 24 h. While in these first experiments steroid hormones, which are important regulators of testicular functions under normal physiological conditions, were used, additionally substances known to play a role in pathologically altered testis were tested on DCN regulation. For instance the prostaglandin D2 system is of special relevance in testis of infertile men (134, 140). Thus HTPC/-F, that express receptors for protsglandin D2, were treated with 15-deoxy-$\Delta^{12\text{-}14}$-Prostagladin-J2 (15dPGJ2; 10 µM) for 7 days. 15dPGJ2 was dissolved in 100 % ethanol and used at a 1:1000 dilution.

Forskolin is a diterpene commonly used to raise cAMP levels. Since stimulation of the androgen pathways occurs mainly through cAMP mediated mechanisms, e.g. adenylate cyclase activation (15), forskolin was also used in this study for cell stimulation. HTPCs and HTPC-Fs were treated with 50 nM forskolin for 4 h. Forkolin was dissolved in 100 % ethanol and used at a 1:200 dilution.

Mast cells and macrophages are present in increased numbers in fibrotic remodeled testis (54, 58). Their main secreted products, besides histamin, TNF-α and tryptase were used to challenge HTPCs as well as HTPC-Fs. Cell treatment was performed with human recombinant TNF-α (dissolved in H_2O and diluted 1:1000 to a final concentration of 5 ng/ml), human recombinant rhSkin β tryptase (dissolved in H_2O and diluted 1:1000 to a final concentration of 100 ng/ml) and PAR-2 agonist peptide SLIGKV (dissolved in H_2O and diluted 1:1000 to a final concentration of 10 µM) for two different time points, 24 and 72 h.

Solvents for all substances were included as controls. Reagents and solvents are summarized in table 3-1. The respective reagent or solvent was added to the culture medium (DMEM supplemented with 10 % FCS) and cells were incubated at 37 °C, 5 % CO_2 and 95 % humidity. Cell treatment was followed by isolation of RNA or protein. Supernatants were collected for enzyme-linked immunosorbent assay (ELISA) experiments.

NIH/3T3 cells were treated with mouse TNF-α (dissolved in H_2O and diluted 1:1000 to a final concentration of 5 ng/ml) for 24 and 72 h. TNF-α was added to the culture medium (DMEM

supplemented with 10 % FCS) and cells were incubated at 37 °C, 5 % CO_2 and 95 % humidity. Solvents were included as controls for each time period. Cell treatment was followed by RNA and protein isolation.

In addition to DCN regulation, the actions of DCN in HTPCs and HTPC-Fs were investigated. In initial experiments, cells were cultivated in presence of different concentrations of human recombinant or bovine articular cartilage DCN (1, 10 and 20 µg/ml) and acute Ca^{2+} signals or levels of adenosine triphosphate (ATP) levels after 24 h were measured. As 10 µg/ml of DCN proved to be effective, this concentration was used for further investigations. DCN was dissolved in H_2O and diluted 1:200 to a final concentration of 10 µg/ml. No difference in the ability of the DCN preparation to mobilize intracellular Ca^{2+} or to change cell viability was observed. Subsequently, unless indicated otherwise, bovine DCN was generally used, but for each experiment human recombinant DCN was tested, as well.

As DCN is known to be able to interact with growth factor signaling, this possibility was investigated by treating HTPC/-Fs with different concentrations of human recombinant EGF and human recombinant PDGF-BB for different time points and ATP measurements, measurements with an automated cell counting device (CASY) and 4′, 6′-diamidino-2′-phenylindole (DAPI) experiments were performed after cell stimulation. EGF was dissolved in H_2O and diluted 1:1000 to a final concentration of 50 ng/ml. PDGF-BB isoform was used because it is known to bind all PDGFR isoforms and dimerizes α- and β-receptors into different configurations (PDGFR-αα, -αβ, -ββ) (29). PDGF-BB was dissolved in 4mM HCl containing 0.1 % BSA and was used at a 1:1000 dilution (5 ng/ml). Details of cell treatment are described for every single experiment below.

In addition to DCN actions, the influence of the cancer drug imatinib mesylate on growth factor signaling in HTPCs was investigated in this study. Imatinib mesylate (originally called STI571; Glivec or Gleevec, Novartis Pharma, Basel, Switzerland) is a chemotherapeutic agent employed to treat patients with chronic myeloid leukemia (141). Imatinib specifically inhibits Abelson tyrosine kinase, an abnormal tyrosine kinase resulting from the Philadelphia chromosome, which is constitutively expressed in chronic myeloid leukemia (141). The imatinib concentrations required for inhibition of the Abelson tyrosine kinase also inhibit other receptor tyrosine kinases (RTKs), including c-kit and PDGFR (142-144). In the developing rat testis, c-kit and PDGF/PDGFR signaling pathways play essential roles in the development and migration of Leydig cells and peritubular myoid cells, and proliferation and survival of spermatogonia (145). Cells of both groups were treated with different concentrations (10, 20, 50 or 100 µM) for 1 or 4 days of imatinib mesylate and/or 5 ng/ml PDGF-BB. Subsequent experiments, such as measuring of ATP levels and DAPI experiments, were performed as detailed below. Cells, treated with solvents, were included as controls. Reagents and their solvents used for cell treatment are summarized in table 3-1 and cell stimulation details are described for each single experiment below.

Table 3-1: Summary of reagents and their solvents.

Substance	Solvents (stock)
DCN	PBS
15dPGJ2	100 % Ethanol
17β-Estradiol	100 % Ethanol
EGF	H_2O
Forskolin	100 % Ethanol
Imatinib mesylate	H_2O
PDGF-AA	H_2O
PDGF-BB	4 mM HCl + 0.1 % BSA
Testosterone	100 % Ethanol
Human recombinant TNF-α	H_2O
Mouse recombinant TNF-α	H_2O
Human recombinant tryptase	H_2O
SLIGKV	H_2O

3.2 Molecular biology

3.2.1 RNA-Isolation

The cells were grown to subconfluence and incubated with/without stimulant in DMEM containing 10 % FCS for different time points. Subsequently, the cells were washed twice with DMEM without FCS and suspended in 600 µl RLT-buffer containing 1 % β-mercaptoethanol. Tissue of human testicular biopsies was homogenized in 600 µl RLT-buffer containing 1 % β-mercaptoethanol using an Ultrathurax. RNA-isolation was performed at room temperature using a QIAGEN RNeasy minikit. Each cell/tissue lysate was passed five times through a cannula and transferred directly into a spin column placed in a 2 ml collection tube. Samples were centrifuged at 10,000 rpm for 30 sec. The flow through was resuspended in 600 µl ethanol (70 %) and transferred to a RNeasy spin column placed in a 2 ml collection tube. Samples were centrifuged at 10,000 rpm for 15 sec. The flow-through was discarded and several washing steps were performed (700 µl RW1 buffer, 2 x 500 µl RPE buffer). The RNA was eluted using 30 µl RNase-free water and RNA content and quality were determined by measuring the absorbance of an 1:30 RNA:RNase-free water solution at 260 nm in a biophotometer. The RNA samples were stored at -80 °C until reverse transcription was performed.

RNA of frozen or freshly removed WT/AROM+ mouse testis was isolated using a different method. Samples were homogenized in 1 ml TRIsure reagent using an Ultrathurax and subsequently incubated

for 5 min at room temperature. 200 µl chloroform were added and samples were shaken by hand for 15 sec. After incubation for 3 min at room temperature, samples were centrifuged at 10,000 rpm for 15 min at 2-8 °C. The colorless upper aqueous phase was transferred into a fresh tube and the RNA was precipitated by mixing with 500 µl isopropyl alcohol. Samples were incubated for 10 min at room temperature, followed by centrifugation at 10,000 rpm for 10 min at 2-8 °C. The pellet was washed with 1 ml ethanol (75 %), vortexed, centrifuged at 7,000 rpm for 5 min at 2-8 °C and air-dried for 10 min. Finally the RNA pellet was dissolved in diethylpyrocarbonate- (DEPC-) treated water by incubating for 10 min at 60 °C in a thermomixer.

The RNA concentration was determined measuring 1 µl RNA sample in a NanoDrop. To check RNA quality gel electrophoresis using a 1 % tris base/boric acid/EDTA- (TBE-) buffered agarose gel and 1 µg of each sample was performed. Agarose gel electrophoresis is described in detail below.

To eliminate contaminating DNA during RNA purification a Deoxyribonuclease I Amplification Grade Kit was used. Duplicate RNase-free, 0.5 ml microcentrifuge tubes for positive and negative reverse transcriptase samples were prepared. The experiment was performed on ice. The reagents for the amplification reaction are listed in table 3-2. After incubation for 15 min at room temperature, 1 µl of 25 mM EDTA solution was added to the samples to inactivate DNase I. After an incubation step at 65 °C for 10 min, the samples were ready for reverse transcription.

Table 3-2: Summary of reagents and their volumes used for amplification.

Reagent	Volume
RNA sample (1 µg)	0-8 µl
10 x DNase I Reaction Buffer	1 µl
DNase I, Amp Grade 1 U/µl	1 µl
DEPC-treated water	0-8 µl
Total volume	10 µl

3.2.2 Reverse transcription polymerase chain reaction

Reverse transcription polymerase chain reaction (PCR) was used to transcribe single-stranded RNA into double-stranded DNA. Concerning HTPC/-Fs and mouse testicular fibroblasts, the cDNA template was produced using 1.6 µl of random 15-mer primer and 400 ng of total RNA. DEPC-treated water was added to a total volume of 23 µl. All working steps were performed on ice. Samples were incubated in a thermocycler for 10 min at 70 °C and afterwards 5 min at 25 °C. Subsequently 15 µl of master mix, containing 5 x first strand buffer, 0.1 M dithiothreitol (DTT), deoxynucleoside

triphosphates (dNTPs) and RNasin (40 U/µl; RNase Block Ribonuclease Inhibitor), was added. Details for master mix reagents see table 3-3. Samples were incubated for 10 min at 25 °C and subsequently for 2 min at 42 °C, before 2 µl Superscript II 200 U/µl) were added. The total volume of the RT-PCR was 40 µl. The program for reverse transcription see table 3-4.

Table 3-3: Mastermix composition for reverse transcription PCR with 15-mer primers.

Reagent	Volume
5 x first strand buffer	8 µl
DTT 0.1 M	4 µl
dNTP mix 10 mM	2 µl
RNasin 40 U/µl	1 µl

Table 3-4: Temperatures and time periods for reverse transcription.

Temperature (°C)	Time (min)
42	50
70	15
4	10

At the Institute of Biomedicine, University of Turku, a different RT-PCR method than described above was used. The RNA template was produced using 1.0 µl random hexamer primers (300 ng/µl), 10 µl 2 x buffer, 2 µl M-Mul VRT RNase and 0.5 µg of total RNA. DEPC-treated water was added to a total volume of 20 µl (details for mastermix see table 3-5). All working steps were performed on ice. The program for reverse transcription see table 3-6.

Table 3-5: Mastermix compostition for reverse transcription PCR with hexamer primers.

Reagent	Volume
Buffer	10 µl
Hexamer Primer	1 µl
RNase	2 µl
RNA template (0.5 µg)	0 – 7 µl
DEPC-treated water	0 – 7 µl
Total volume	20 µl

Table 3-6: Summary of temperatures and time periods for reverse transcription.

Temperature (°C)	Time (min)
25	10
37	30
85	5

3.2.3 Semi-quantitative real-time PCR

Real-time (RT-) PCR was used to amplify specific genes (146) and was performed using 1 µl of cDNA in a total reaction volume of 50 µl. Mastermix ingredients and volumes are summarized in table 3-7. To exclude contamination by genomic DNA, negative controls using 1 µl RNA of each sample were performed. All pipetting steps were performed on ice. PCR conditions are listed in table 3-8.

Table 3-7: Mixture for one PCR reaction.

Reagent	Volume
5x GoTaq-Buffer	10 µl
dNTPs (2 mM)	5 µl
Primer forward (50 pmol/µl)	1 µl
Primer reverse (50 pmol/µl)	1 µl
GoTaq-Polymerase	0.25 µl
DEPC-treated water	31.75 µl
cDNA template	1 µl
Total volume	50 µl

Table 3-8: Real-time PCR program.

Step	Temperature (°C)	Time
Initialization	95	2 min
Denaturation	95	1 min
Annealing	Primer-specific annealing temperature	30 sec
Elongation	72	1 min
Final elongation	72	5 min
Final hold	4	

All PCR primers used were designed using the open source program Primer 3 (version 0.4.0; http://frodo.wi.mit.edu/primer3/). Purified and lyophilized primers were purchased at metabion international AG, Martinsried, Germany. Information about primer sequences, annealing temperatures and product sizes are summarized in table 10-1 (see APPENDIX 10.1).

Amplified PCR products were visualized and identified by agarose gel electrophoresis, described below. To verify their identity, PCR products were purified using the QIAGEN MinElute® PCR Purification Kit and sequenced by GATC-biotech Konstanz, Germany. Results of sequencing were analysed using BLAST software (basic local alignment search tool; www.ncbi.nlm.nih.gov/projects/gemone/seq/BlastGen).

3.2.4 Quantitative real-time PCR (qRT-PCR)

QRT-PCR studies were carried out at the Department of Physiology and Turku Center for Disease Modeling, Institute of Biomedicine, University of Turku, Finland. Synthesis of cDNAs for qRT-PCR was performed employing a DyNAmo two-step SYBR Green qRT-PCR kit and an Engine Opticon system for continuous fluorescent detection. For each set of conditions samples were analyzed in triplicates. A mastermix of 10 µl SYBR Green and 1 µl forward and 1 µl reverse primer (10 pmol/µl) per sample was prepared. 8 µl of cDNA (diluted 1:50) were used. In initial experiments annealing temperatures were determined by running gradient PCRs, analyzing the expression levels at different annealing temperatures from 55-61 °C. DEPC-treated water was used as negative control in each experiment. Table 3-9 shows the detailed program used for qRT-PCR.

The expression levels in human cDNA samples were determined in proportion to the human ribosomal protein L19 (RLP19) housekeeping gene. For mouse samples the mouse RPL19 was used as housekeeping gene. Primer sequences and specific annealing temperatures are summarized in table 10-1 (see APPENDIX 10.1)

Table 3-9: Summary of qRT-PCR conditions.

Temperature (°C)	Time
95	15 min
94	10 sec
Primer-specific annealing temperature	30 sec
72	30 sec
78	1 sec
Read Plate, go to step 2	
72	10 min
Melting curve from 72-95	Read every 0.5 °C, hold 1 sec
72	5 min

3.2.5 Agarose gel electrophoresis

PCR products were visualized by ethidium bromide staining in TBE-buffered agarose gels (2 %). To detect the size of the DNA fragment a 100 bp DNA ladder was used. Electrophoresis was performed at 90 V for 30 min. PCR fragments were visualized by ultraviolet light and evaluated densitometrically using ImageJ Software (version 1.40g; National Institutes of Health, Bethesda, MD, USA). The intensity of each sample was normalized to values obtained for cyclophilin housekeeping gene within the respective sample.

3.3 Protein biochemistry

3.3.1 Protein extraction and measurement of protein content

Protein was extracted either from human testicular biopsies or from cultured cells (HTPC/-Fs and NIH/3T3 cells) grown to confluence on 60-mm dishes. The whole preparation was performed on ice to avoid protein denaturation. Testis tissue was homogenized in 1.5 ml Sodiumchloride/ Pipes/EDTA-(NPE-) buffer using an Ultrathurax. HTPC/-Fs and NIH/3T3 cells were initially washed twice with DMEM without additives to remove FCS. Subsequently, 1.5 ml NPE-buffer were added and cells were scraped off the plate and transferred to a 1.5 ml Eppendorf cup. The samples, homogenized in NPE-buffer, were centrifuged at 4 °C and 10,000 rpm for 3 min and afterwards the buffer was removed. The cell/tissue pellet was resuspended in 1.5 ml PBS and centrifuged again. Subsequently, 50 or 100 µl inhibitor cocktail, depending on the size of the pellet, were added to each sample and cells were treated with ultrasonic sound for about 10 sec.

To determine the concentration of the solubilized protein in each sample, a colorimetric DC Protein Assay based on the method of Lowry (147), was performed. A working reagent was prepared by adding 20 µl of reagent S to each ml of reagent A used. 5 µl of standards (0 – 2.0 µg/µl) and samples were pipetted in duplicates a clear 96-well microplate. 25 µl working solution and 200 µl of reagent B were added to each well and the plate was incubated for 15 min at room temperature. The absorption of standards and samples was measured at 750 nm in a microplate reader. Values were compared to a standard curve to determine the protein content. Finally 10 % β-mercaptoethanol and 10 % bromphenol blue were added to each sample. Samples were incubated for 5 min at 95 °C in a thermomixer before they were directly used in Western blot experiments or frozen at -20 °C.

3.3.2 Sodium dodecyl sulfate polyacrylamide gel electrophoresis

Sodium dodecyl sulfate polyacrylamide gel electrophoresis (SDS-PAGE) was performed to separate proteins according to their molecular weight. Two gels of different acrylamide contents, a loading and a separating gel, were used. A loading gel of 4 % acrylamide has been used for all experiments. The acrylamide content of the separating gel varied depending on the molecular weight of the investigated protein. For example, for detecting DCN protein with a molecular weight of approximately 40 kDa a 12.5 % acrylamide gel was used, whereas phospho-EGFR and phospho-PDGFR with molecular weights of approximately 180 and 150 kDa were analysed on a 7.5 % acrylamide gel.

First the separating gel (7.5 % or 12.5 % acrylamide) was poured, covered with a thin layer of isopropyl alcohol and allowed to polymerize for about 30 min. Thereafter isopropyl alcohol was removed and the loading gel (4 % acrylamide) was poured. Details for acrylamide gel ingredients are listed in table 3-10.

Table 3-10: Summary of acrylamide gel contents.

Ingredients	Separating gel		Loading gel
	7.5 %	12.5 %	4 %
Acrylamide (30 %)	2.4 ml	3.9 ml	0.48 ml
Separating gel buffer pH 8.8	2.5 ml	2.5 ml	-
Loading gel buffer pH 6.8	-	-	1.25 ml
H_2O bidest.	7.0 ml	5.5 ml	3.17 ml
SDS (10 %)	100 µl	100 µl	100 µl
Ammonium persulfate (10 %)	75 µl	75 µl	38 µl
TEMED (100 %)	7.5 µl	7.5 µl	3.8 µl

The gel was loaded with equal amounts of protein (6 µg) for each sample. To define the molecular weight of the proteins, a Full Range Molecular Weight Marker Rainbow and a Precission Plus Protein Kaleidoscope Standard were added on the gel. Proteins were separated using 1 x electrophoresis buffer (Laemmli) and 190 V and 400 mA for about 1 h.

3.3.3 Western blot

The proteins were blotted from the gel onto a nitrocellulose membrane employing a Wet-Blot-System in a Mini Trans-Blot® chamber. Transferblotting was carried out at 100 V and 400 mA for 1 h. Afterwards the proteins on the membrane were visualized by staining them with 1 x Ponceau S. Blocking of non-specific binding was achieved by incubating the membrane in 5 % non-fat dry milk in Tris buffered saline (TBS)-Tween 20 or 5 % BSA in TBS-Tween 20 for 30-60 min. BSA blocking solution was only used in cases where phospho-extracellular regulated kinase (Erk) 1/2 should be detected, for all remaining antibodies non-fat dry milk blocking solution was used. Membranes were incubated with the following antibodies over night: monoclonal goat anti-human DCN antibody (1:1,000), monoclonal mouse anti-human α-SMA antibody (1:500), polyclonal rabbit anti-human Erk 1/2 antibody (1:1,000), monoclonal mouse anti-human phospho-Erk1/2 antibody (1:1,000), rabbit anti-phospho-PDGFR-β antibody (1:100), anti-phospho-EGFR antibody (1:250), monoclonal rabbit anti-human EGFR antibody (1:100) and polyclonal rabbit anti-human PDGFR-β antibody (1:200). Antibody details are summarized in table 10-3 (see APPENDIX 10.3).

Proteins were detected in a Chemi smart 5000 chemiluminescence instrument using a chemiluminiscent reagent. Afterwards a β-actin antibody (1:5,000) was used to allow corrections for small differences in loading. Western blot bands were analyzed densitometrically with ImageJ Software and the results normalized to the ones obtained for β-actin.

3.3.4 Enzyme-linked immunosorbent assay

DCN was detected in conditioned media (3 days) using a commercial enzyme-linked immunosorbent assay (ELISA). Medium supernatants (total 2 ml per 60-mm dish) of the same tryptase/SLIGKV-treated and untreated control cells, which were used in the Western blot experiments, were examined in duplicates. Standards were contained in the ELISA kit. All working steps were performed at room temperature. A 96-well microplate was covered with 100 µl Capture Antibody (2.0 µg/ml) per well and incubated overnight. The plate was washed three times with buffer (0.05 % Tween 20 in PBS; pH 7.2 – 7.4) before blocking for 1 h in 300 µl of reagent diluent (1 % BSA in PBS; pH 7.2 – 7.4). The wash steps were repeated. 100 µl of each sample (conditioned media diluted in reagent diluent 1:1,000) and standards (0 – 1000 ng/ml) were added and the plate was incubated for 2 h. After repeating the wash steps, 100 µl Detection Antibody (250 ng/ml) were added to each well and incubated for 2 h. The wash steps were repeated, before 100 µl of Streptavidin-horseradish peroxidase (HRP; 1:200) were added. The plate was incubated for 20 min avoiding direct light and then washed again. 100 µl Substrate Solution (1:1 mixture of Color Reagent A and Color Reagent B) per well were added and the plate was incubated for 20 min avoiding direct light. To stop the reaction, 50 µl stop solution (1 M sulfuric acid) were added to each well and the optical density was detected immediately using a FLUOstar Optima reader (software: Optima version 2.20) at 450 nm and 540 nm wavelength. Readings at 540 nm were subtracted from readings at 450 nm to correct for optical imperfections in the plate. DCN amounts of each sample were calculated accordingly to the standards and results were expressed as secreted DCN per total cellular protein.

3.3.5 Phosphorylation experiments: Proteome Profiler and Western blot

To obtain a profile of RTKs phosphorylated by DCN, a commercial antibody-based array for 42 differnet human phospho-RTKs was performed. A total of 10^6 cells, HTPCs and HTPC-Fs respectively, were seeded on a 60-mm plastic culture dish and treated for 5 min with 10 µg/ml DCN, a concentration, which induced robust increases in intracellular Ca^{2+} (described below, see 3.8) PBS was added to the culture medium of control cells. Cellular protein was extracted using a Nonident P-40 (IGEPAL) lysis buffer. Lysates from DCN-treated and untreated cells were added to respectively one nitrocellulose membrane on which capture and control antibodies were spotted, and incubated overnight at 4 °C on a rocking platform shaker. After three wash steps with TBS containing 0.1 % Tween 20, membranes were incubated with an anti-phospho-tyrosine HPR detection antibody for 2 h at room temperature on a rocking platform shaker. The wash step was repeated. Chemiluminiscent reagent was added and images were captured. Results were evaluated with ImageJ Software. The experiment was repeated with cell lysates of two different patients (HTPCs).

The ability of DCN to phosphorylate EGFR and PDGFR, was further studied in Western blot experiments as described above. For each experiment cells were freshly trypsinized and grown over night on a 60-mm. Cells of three men with normal testis and two men with testicular fibrosis were treated each with 10 µg/ml BSA, 10 µg/ml DCN, 50 ng/ml EGF or 5 ng/ml PDGF-BB for 10 min. Control cells were incubated with PBS added to the culture medium. Cellular protein was isolated and immunoblots with anti-phospho-PDGFR-β and anti-phospho-EGFR antibodies were performed as described above. For control purposes, anti-EGFR and anti-PDGFR-β antibodies were used.

3.4 Immunohistochemistry

Testis tissue, stemming from humans, mice, rats, hamster or monkeys, was fixed in Bouin`s fixative, embedded in paraffin, and sections of a thickness of 5 µm were produced using a microtome. The slices were mounted on glass slides.

For immunohistochemistry the sections were deparaffinized by putting the sections in xylene and isopropyl alcohols (100 %, 90 %, 80 %, 70 %). Afterwards the sections were rehydrated with PBS. Subsequently, the sections were pretreated in 10 mM sodium citrate buffer in a microwave oven. Slides were allowed to cool and then rinsed with three times with PBS for 5 min before 3 % hydrogen peroxide in methanol for 20 min was added to block endogenous peroxidase activity. To reduce nonspecific antibody binding the sections were incubated with 5 % normal serum (donkey normal serum for DCN antibody and goat normal serum for all the rest of antibodies used) in a humid chamber for 30 min at room temperature. Afterwards the sections were incubated with the primary antibody against DCN (1:100 or 1:50) or SMA (1:2,000) in a humid chamber over night at 4 °C. The same antibodies as for Western blot experiments were used. Antibody details are summarized in table 10-3 (see APPENDIX 10.3). Incubation with normal non-immune serum instead of the specific antibody, or omission of the primary antibody served as controls. After primary antibody incubation, the sections were washed three times with PBS for 5 min and a biotinylated secondary anti-goat or anti-mouse antibody (1:500) was applied for 1 – 2 h. Thereafter the sections were treated with avidin-biotin peroxidase complex (ABC-method (148)) solution for 1 h, followed by two wash steps with PBS for 5 min. After incubation with Tris-hydrogen chloride buffer for 10 min, the antibody was localized by a color reaction with 3, 3`-diaminobenzedine (DAB) and hydrogen peroxide. The DAB reaction was stopped by placing the slides in double-distilled water (ddH_2O). Sections were dehydrated in isopropyl alcohols with ascending concentrations (70 %, 80 %, 90 %, 100 %) and xylene and finally coverslipped with entellan.

3.5 Immunocytochemistry

Cells were seeded on glass cover slips that were placed in a 24-well microplate. After wash the cells two times with 500 µl PBS, they were fixed with 250 µl paraformaldehyde solution (PFA; 4 % in 0.01 M PBS; pH 6.8) for 30 min. Fixation was followed by several wash steps (3 x PBS for 5 min, 3 x KPBS for 10 min) and cells were incubated in LKPBS for 10 min. Afterwards, cells were incubated in the presence of a primary antibody, diluted in LKPBS, over night at 4 °C. Monoclonal mouse antibodies against SMA (1:2,000), CD90 (1:100), collagen type I (1:200) and type IV (1:250) were employed. For controls, the primary antibody was omitted. Next day, the cells were washed three times with KPBS for respectively 5 min and once with LKPBS for 10 min. All following steps were performed avoiding direct light. Cells were incubated with a fluorescein isothiocyanate (FITC) labeled secondary antibody (1:200 in LKPBS) for 1 h at room temperature and afterwards washed three times with KPBS for 10 min. Finally, cells were washed once with ddH_2O for 5 min. The cover slips were covered with Prolong Antifade Kit and placed on glass slides. Fluorescence was detected with a fluorescence microscope using a stimulation wavelength of 488 nm and an emission wavelength of 530 nm.

3.6 Nuclear staining

To evaluate mitotic figures of cultured HTPC/-Fs, DAPI staining was employed. Cells were seeded on glass cover slips in a 24 well plate and different time periods (6 h, 18 h and 24 h) of treatments with DCN (10 µg/ml) or PDGF-BB (5 ng/ml) have been studied. Only at 24 h a significant increase of proliferative events in stimulated cells over controls could be observed and therefore a treatment time of 24 h was used for subsequent studies.

In detail, after incubation with DCN, imatinib (10 µM), EGF (10, 50, 250 ng/ml) or PDGF-BB for 24 h, cells were washed two times with PBS and subsequently fixed with PFA (4 % in 0.0.1 M PBS; pH 6.8) for 30 min. After washing cells again with PBS and ddH_2O, the cover slips were covered with DAPI reagent and mounted on glass slides. DAPI, when bound to DNA emits at wavelength of about 460 nm producing blue fluorescence, was detected using a fluorescence microscope and a stimulation wavelength of about 360 nm. At 20 x magnification pictures were taken. Nuclei (> 200/ slide) were counted and the percentage of metaphase, anaphase and telophase figures was determined.

3.7 Measurement of cell viability and apoptosis

3.7.1 ATP measurements

Viability of cells was determined by using the CellTiter-Glo® Luminescent Cell Viability Assay which is based on quantification of ATP. The amount of measured ATP is directly proportional to the number of metabolically active cells present in culture. After cell lysis and ATP release, the luciferase reactions starts and mono-oxygenation of luciferin is catalyzed by luciferase in the presence of magnesium, ATP and molecular oxygen to oxyluciferin.

Cells were seeded in quadruplicates on 24-well plates and cultured in DMEM without phenol red and FCS for 24 h in the presence or absence of DCN (10 µg/ml), EGF (250 ng/ml), PDGF-BB (5 ng/ml), imatinib (10, 20, 50 or 100 µM) or combinations. The assay was performed at room temperature, avoiding direct light. The kit reagent was mixed with an equal volume of medium. To induce cell lysis, 200 µl of this mixture were added directly to the cells, which were subsequently incubated on an orbital shaker for 2 min. To stabilize the luminescent signal, the plate was incubated without shaking for 10 min. The luminescence of luciferase reaction was measured in a FLUOstar Optima reader. Control cells consistent of incubation with the respective solvent of each substance. To obtain a value for background luminescence, control wells containing only medium without cells were included in the experiment. The mean of the background values was subtracted from the results.

3.7.2 Caspase assay

To confirm that DCN does not induce apoptosis in HTPC/-Fs, the activity of cysteine aspartic acid-specific protease (caspase)-3 and -7 in these cells was measured using the Caspase-Glo® 3/7 Assay. Within this assay cell lysis is followed by caspase cleavage of the substrat and generation of a luminescent signal, produced by luciferase. The luminescence is proportional to the amount of caspase activity.

Cells were seeded in a 96-well plate and allowed to adhere over night. Afterwards DCN (10 µg/ml) was added to the culture medium (DMEM without phenol red and FCS) for 24 h. Untreated control cells were included in the experiment, as well. The whole assay was performed at room temperature, avoiding direct light. The kit reagent was mixed with an equal amount of culture medium before a total of 200 µl was added to the cells. The plate was incubated for 1 h and the luminescence of each sample was measured in a FLUOstar Optima reader. Control wells containing only medium without cells were included in the experiment to detect background luminescence. The mean of the background values was subtracted from the results.

3.7.3 CASY - measurements with an automated cell counting device

Measurements of cells in an automated cell counting device (CASY) were performed to further examine the effect of DCN, growth factors (PDGF-BB, PDGF-AA, EGF) or imatinib, on cell proliferation or cell diameter. CASY technology assesses cell viability based on the integrity of the plasma membrane. Cells are exposed to a low voltage field and the electric current cannot go through the intact plasma membrane.

An equal number of cells was seeded on each 60-mm dish used. Cells were treated either with DCN (10 µg/ml), PDGF-BB (5 ng/ml), PDGF-AA (5 ng/ml), EGF (250 ng/ml) or imatinib (10 µM) for four days. To one of the treatments groups, DCN was added in combination with EGF/PDGF-BB. Control cells, treated with solvents of each substance, were included in each experiment. After the treatment, cells were trypsinized and resolved in 1 ml DMEM without FCS and a 1:100 dilution of the cell suspension in 10 ml CASYton was used in CASY measurements.

3.8 Measurements of intracellular Ca^{2+} levels

Cells were grown on a glass cover slip in DMEM supplemented with 10 % FCS for 24 h and subsequently loaded with 5 µM fluo-4 acetoxy-methylester (fluo-4AM) for 30 min at 37 °C and 5 % CO_2. After washing the cells with FCS-free DMEM, the cover slip was transferred into a recording chamber mounted on a TCS SP2 confocal microscope. Fluorescence was monitored at 500-540 nm (excitation wavelength: 488 nm) every 2 sec and the intensity was quantified over single cells. To assess whether HTPC/-Fs may possess functional PAR-2, changes of intracellular Ca^{2+} levels were recorded on-line during application of 100 ng/ml tryptase or 10 µM agonist peptide SLIGKV like it has been described (55, 132). To assess whether HTPCs and HTPC-Fs respond in a similar manner to tryptase or SLIGKV the number of responding cells was counted for each experiment and the percentage of HTPCs and HTPC-Fs (n = 3/group) responding to 100 ng/ml tryptase and 10 µM SLIGKV was determined.

In initial studies, actions of 10 µg/ml bovine articular cartilage DCN and human recombinant DCN on Ca^{2+} signaling were compared. As no difference in the ability of the DCN preparation to mobilize intracellular Ca^{2+} was observed, bovine DCN was generally used for subsequent studies, but for each experiment human recombinant DCN was tested, as well. Furthermore, experiments testing different concentrations of EGF (50 ng/ml, 250 ng/ml and 1 µg/ml) and PDGF-BB (5 ng/ml and 10 ng/ml) were conducted. 50 ng/ml EGF and 5 ng/ml PDGF-BB proved to be effective stimulators of Ca^{2+} release, therefore these concentrations were used for subsequent experiments. In additional studies, HTPCs as well as HTPC-Fs were pretreated with 10 µg/ml DCN for 24 h before measuring Ca^{2+} levels upon EGF, PDGF or DCN stimulation. Additionally, Ca^{2+} signals were recorded after addition of 100 µM

histamine which served as a positive control (55). Measurements with 10 µl/ml BSA (pH = 7.8) were performed to exclude non-specific protein effects.

3.9 Laser capture microdissection

Human biopsies embedded in paraffin wax were cut in 5 µm-thin sections and mounted onto a 1.35 µm-thin polyethylene naphthalene membrane pasted to a glass object slide. The sections were deparaffinized, lightly stained with haemalaune/eosin and subjected to laser capture microdissection. The peritubular compartment was cut out using the high photonic energy of a nitrogen laser. To isolate the microdissected area from the surrounding tissue, the laser was focused below the specific region and with a single laser shot the tissue was catapulted from the slide into the cap of a 0.5 ml microfuge tube. 50 µl of RNA stabilization reagent were added to each sample, before they were shortly centrifuged and frozen at -80 °C until RNA extraction was performed. RNA was extracted using a QIAGEN RNeasy FFPE kit. Reverse transcriptase PCR using oligo-dT primers was performed. RT-PCRs, using nested (for amplifying EGFR and PDGFR-α) or semi-nested (for amplifying PDGFR-β) primers, were performed as described above. In order to ensure that the sections contained suitable RNA for this procedure, a whole deparaffinized consecutive section was also scraped from the slide and processed as described. For informations on primers and annealing temperatures, please see table 10-1 (APPENDIX 10.1).

3.10 Data analysis

Results of PCR, Western blot and dot blot experiments were analyzed using the public domain image processing program, ImageJ (version 1.40g; NIH, MD, USA).

Results obtained were analyzed using PRISM 4.0 (GraphPad Software, Inc., San Diego, CA). Student *t*-tests or one-way ANOVAs were performed, as indicated. Differences between the groups were evaluated with the appropriate post hoc tests (e.g. Newman-Keuls Multiple Comparison). All data are expressed as mean ± SEM.

4. RESULTS

4.1 DCN expression in the mammalian testis

4.1.1 Testicular DCN expression in the human, non-human primate and the mouse

Initially, DCN mRNA expression was examined in the testes of three different mammalian species, namely human, rhesus monkey and mouse. RT-PCR experiments, using mouse-specific primer pairs for mouse samples, human DCN primer pairs for human and rhesus monkey samples (in case of rhesus monkey human nested DCN primers were used additionally) revealed DCN mRNA in the testes of all examined species (Figure 4-1). All amplified PCR products were verified after sequencing.

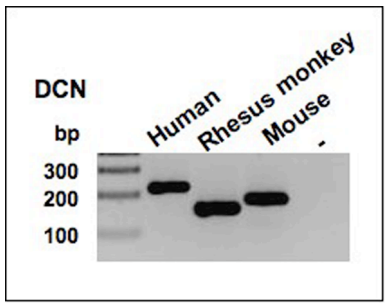

Figure 4-1: Testicular DCN mRNA expression in adult human, monkey and mouse.
Amplified RT-PCR products were visualized using an ethidium bromide stained gel. DCN mRNA is expressed in commercial testicular human cDNA, in whole testis tissue samples from monkeys and mice (human DCN: 221 bp; human nested DCN: 122 bp; mouse DCN: 181 bp; -: no input cDNA).

Testicular DCN was detected by immunohistochemistry. In the testes of adult humans and rhesus monkeys (Figure 4-2 A, C; n = 3 humans; n = 3 monkeys) DCN staining in the ECM of the interstitial and the peritubular compartment, as well as staining of peritubular cells became evident. As the cytoplasm of peritubular cells also stained, these cells are likely the producers of DCN. In contrast to the strong expression in human and rhesus monkey testis, in testes samples of adult rodents (mouse, rat, hamster), no or a very low DCN staining was found (Figure 4-2 D, E, F). Controls in which the primary antibody was omitted (Figure 4-2 B) or replaced by non-immune serum, were negative. Western blotting confirmed DCN expression in human testicular biopsies of men with normal spermatogenesis (data not shown).

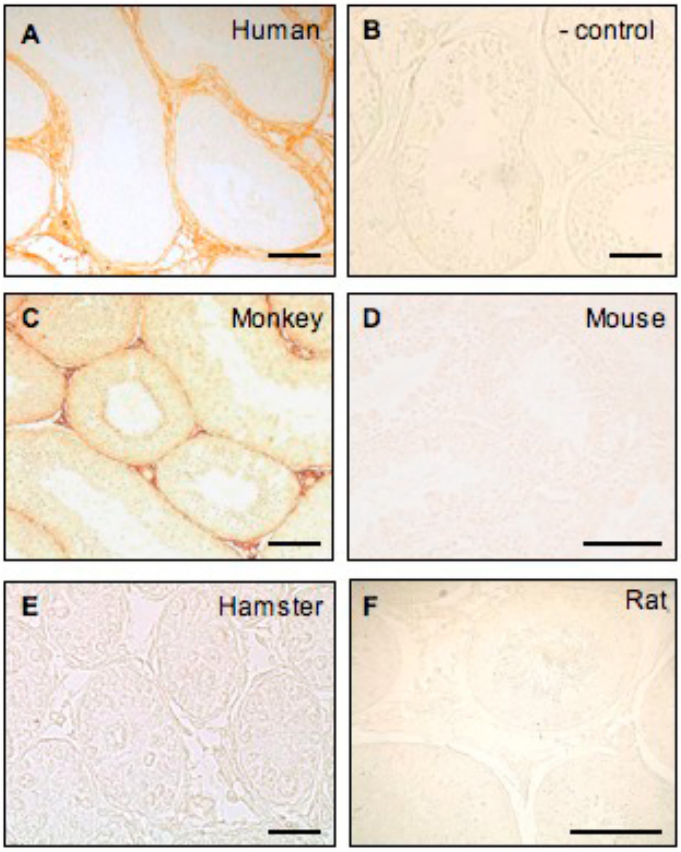

Figure 4-2: Sites of DCN expression in testes of adult man, non-human primate and rodents.
A, Immunohistochemical DCN staining is located to the peritubular wall and interstitial areas in normal human testis. **B,** Control (human biopsy), in which the antiserum was replaced by buffer, was immunonegative. **C,** In the testis of rhesus monkey DCN staining is located to peritubular areas. No or very low levels of DCN could be detected in the testis of **D,** mouse, **E,** hamster and **F,** rat. The length of the scale bars in each picture is approximately 100 µm.

4.1.2 Testicular DCN expression in human sub-/infertility

The distribution pattern of immuno-positive DCN in the testes of men with MA (n = 8), GA (n = 3) and SCO syndrome (n = 4) patients was similar to that observed in testis of fertile men. However, in these cases of impaired spermatogenesis and interstitial and tubular fibrosis, DCN staining of the affected peritubular region, both in the cytoplasm of peritubular cells and in the thickened ECM of the peritubular wall (Figure 4-3 A-C), was increased when compared to biopsy samples of healthy testis. As seen in sections of MA patients (Figure 4-3 A), the accumulation of DCN in the thickened ECM of completely fibrotically remodeled tubules strongly contrasted to only weakly stained ECM areas of adjacent walls of normal tubules with larger diameter and without fibrotic remodeling. In the massively fibrotically altered tubular walls of patients suffering from GA (Figure 4-3 C) DCN staining

was abundant, as well. DCN deposits in the thickened layers of the ECM were observed. Samples of SCO syndrome patients (Figure 4-3 B) showed clear DCN staining in the fibrotically thickened ECM of the peritubular walls and in cells of the interstitial compartment. The peritubular region in MA, GA and SCO syndrome patients was clearly shown by specifically staining of corresponding sections with an antibody against SMA (Figure 4-3 D-F). All of the controls, performed with non-immune serum (Figure 4-3 I) and omission of primary antibody (Figure 4-3 G, H), showed negative immuno-histochemical staining.

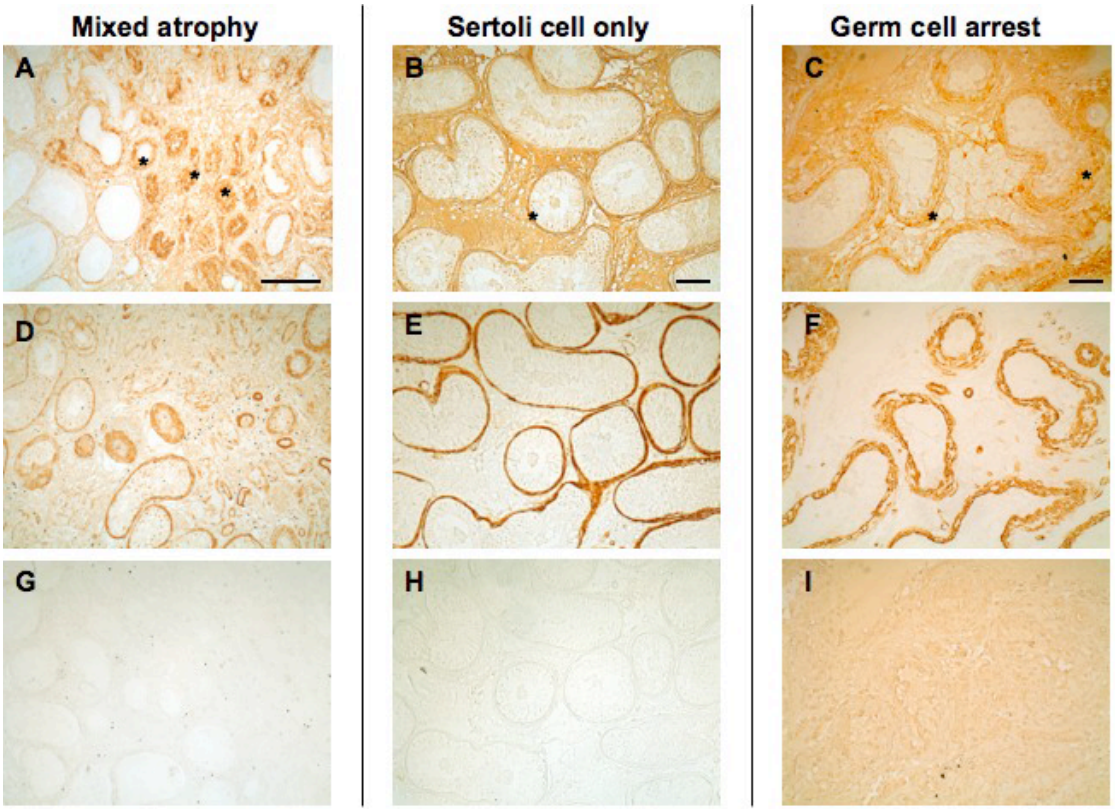

Figure 4-3: DCN in the testis of infertile men.
DCN deposits are observed in the interstitial region and several, massively remodeled tubules (asterisks) in biopsies of **A,** MA, **B,** SCO and **C,** GA patients. **D-F,** SMA staining to indicate the peritubular region in MA, GA and SCO patients. **G** and **H,** Controls in which the primary antibody was omitted were negative. **I,** Control staining in which the primary antibody was replaced by non-immune serum was negative as well. The length of the scale bar in **A** is approximately 200 µm and in **B** and **C** 100 µm.

4.1.3 DCN expression in the testis of infertile AROM+ mice

Results of qRT-PCR measurements showed low DCN mRNA levels in the testes of WT mice at the age of 5, respectively, 10 months (Figure 4-4 A). Compared to WT, significantly increased DCN mRNA expression levels in the testes of 5-month-old transgenic AROM+ mice ($P < 0.05$;

Figure 4-4 A) were observed. While DCN mRNA expression level is not significantly altered in testes of aged WT mice, it further increases in AROM+ mouse testes.

Below the age of 2 – 3 months, AROM+ mice have normal testicular morphology and function, but then develop progressive age-dependent testicular fibrosis, inflammatory reactions and disturbed spermatogenesis (135). Immunohistochemistry results of AROM+ mouse samples showed that these changes were correlated with high levels of testicular DCN (Figure 4-4 D). In 3-month-old AROM+ mice DCN staining is likewise low as in testicular samples of adult WT animals (Figure 4-2 D), but it can be already detected in the interstitial areas and the peritubular compartments (Figure 4-4 B). At the age of 9 – 10 months an enormous DCN expression in the peritubular region and the enlarged interstitial areas was apparent in testes of AROM+ animals (Figure 4-4 D). All controls performed with non-immune serum or omission of primary antibody showed negative immunohistochemical staining (Figure 4-4 C).

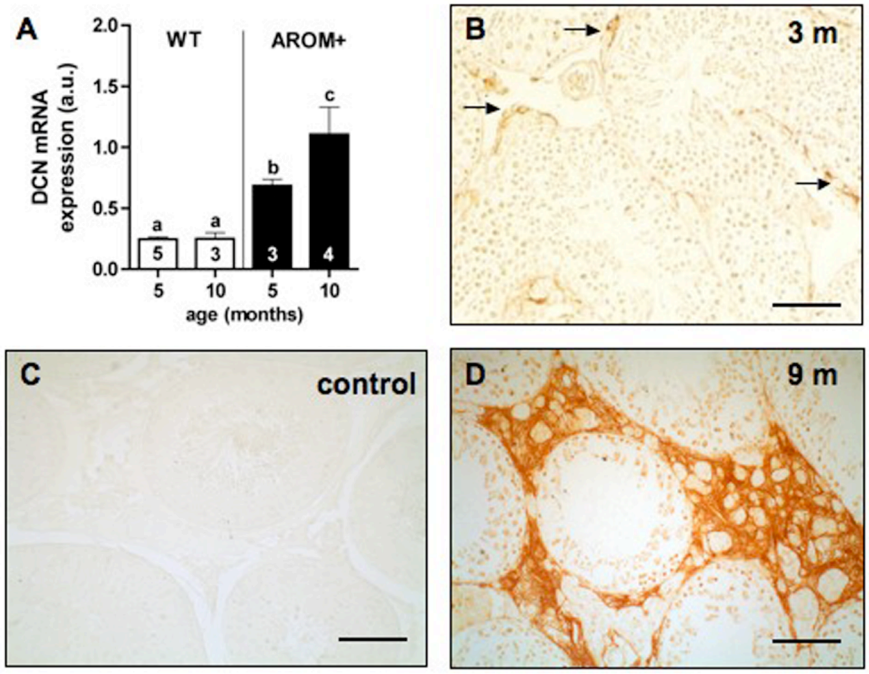

Figure 4-4: DCN accumulation in the testis of AROM+ mice.
A, QRT-PCR results of screening of whole testis samples of WT and AROM+ mice (5- and 10-month-old). Results (mean + SEM) were normalized to the housekeeping gene RPL19 and are given in arbitrary units (a.u.). Statistically significant differences ($P < 0.05$) are indicated by different letters above the columns. Numbers within the columns indicate the number of individuals per group. **B,** Immunhistochemical staining for DCN in the testis of an AROM+ mouse at 3 months of age is low, but it is already evident in some peritubular and in interstitial regions (arrows). The bar represents a length of approximately 100 µm. **C,** The control in which the antiserum was replaced by buffer is immuno-negative. The length of the bar is approximately 50 µm. **D,** DCN accumulates massively in testicular interstitial cells of a 9-month-old AROM+ mouse. The length of the bar is approximately 50 µm.

4.1.4 Testicular DCN expression during rhesus monkey development

Testicular DCN during ontogeny was studied in the non-human primate. In young, prepubertal rhesus monkeys, immunohistochemical staining showed strong DCN immunoreactive signals associated with connective tissue cells (Figure 4-5 A, B). DCN is massively expressed in the peritubular wall and within the interstitial compartment. In contrast, in adult monkeys, in which connective tissue is reduced, DCN levels decreased and distinctly marked the peritubular wall and interstitial areas (Figure 4-5 D-F), comparable to normal human testes (Figure 4-1 A).

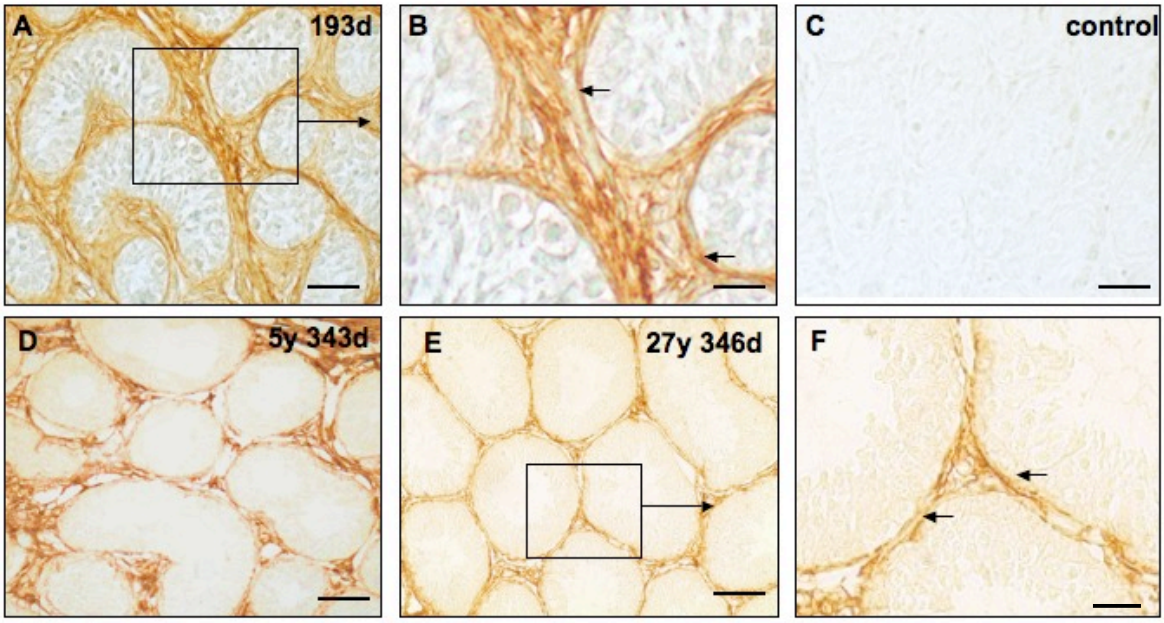

Figure 4-5: DCN during testicular development in the rhesus monkey
A, Immunohistochemical staining for DCN in the testis of a prepubertal rhesus monkey (193 days of age). DCN is strongly expressed in peritubular and interstitial regions. The length of the bar is approximately 50 µm. **B,** Magnified view of the boxed area in A. DCN staining of cells of the peritubular wall (arrows) and the interstitial area of a prepubertal monkey testis. The length of the bar is approximately 25 µm. **C,** Control (prepubertal animal) in which the antiserum was replaced by buffer (bar: approximately 50 µm). **D,** Testicular DCN can be detected in a rhesus monkey at the age of 5 years and 343 days. DCN staining is seen in peritubular and interstitial regions. The length of the bar is approximately 50 µm. **E,** In the testis of monkey of 27 years and 205 days of age a low DCN expression in the peritubular area can be detected. The bar is approximately 50 µm in length. **F,** Magnified view of the boxed area in E. DCN staining of cells of the peritubular wall (arrows) and the interstitial area is low in an adult monkey testis. The length of the bar is approximately 25 µm.

4.2 Cultured human testicular peritubular cells – a cellular model to study male infertility

4.2.1 Expression of smooth muscle cell and fibroblast markers

In the present study cultured human testicular peritubular cells derived from patients with normal spermatogenesis (HTPCs) and corresponding cells stemming from sub-/infertile patients (HTPC-Fs), were investigated. A couple of experiments have been performed to show that HTPC and HTPC-Fs are comparable cellular models, derived from the peritubular region in the testis.

RT-PCR results revealed that HTPCs, as well as HTPC-Fs, express several markers for fibroblasts (collagen type IV and CD90) and smooth muscle cells (SMA, MYH11 and calponin; Figure 4-6 A). Cells of three different individuals of each group, HTPC and HTPC-F, were tested in RT-PCR experiments. The identities of all amplified PCR products were verified by sequencing. Western blot studies with cells of at least eight different patients of each group, HTPC and HTPC-F, confirmed RT-PCR results for SMA at protein level and furthermore showed that both cell types express similar amounts of SMA (Figure 4-6 B).

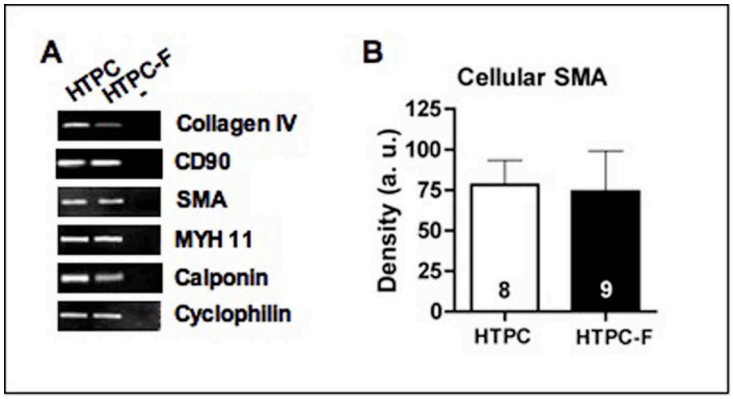

Figure 4-6: HTPCs and HTPC-Fs express several fibroblast and smooth muscle cell markers.
A, RT-PCR results show the expression of collagen type IV and CD90 (fibroblast markers) and SMA, MYH11 and calponin (smooth muscle cell markers) in HTPC/HTPC-Fs. Representatives of results obtained in three different patients/group are shown. Cyclophilin amplifications were used to evaluate differences in applied cDNA amounts. **B,** Summary of Western blot results (mean + SEM) indicate that HTPCs and HTPC-Fs do not differ in SMA expression levels. To account for possible small differences in applied protein amounts, SMA levels were normalized to β-actin levels and given in a.u. The numbers within the columns indicate the number of individual patients used for this experiment.

Smooth muscle cell and fibroblast characteristics of HTPCs as well as HTPC-Fs were further proven in immunocytochemical stainigs. Both cells types were positive for collagen type I and type IV, SMA and CD90 (Figure 4-7). Cells stemming from respectively three different men per group were used. No differences in expression patterns of these markers in HTPCs and HTPC-Fs have been observed. Results obtained for HTPCs have been published previously (55).

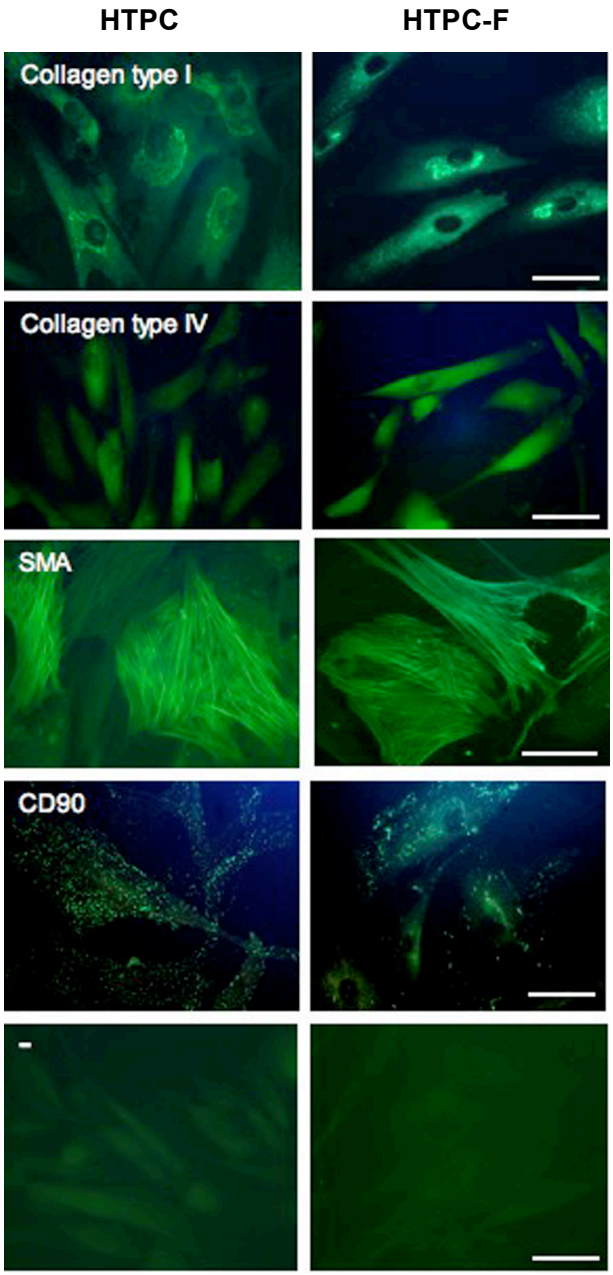

Figure 4-7: Equal expression patterns of collagen type I and IV, SMA and CD90 in HTPC/-Fs. Representative immunocytochemistry results of HTPCs (left) and HTPC-Fs (right) show expression of collagen type I and type IV, SMA and CD90. Cells of 3 patients/group (HTPC/-F) were stained. Negative controls were performed by omitting the primary antibody (-). The length of the bar is approximately 10 µm.

4.2.2 Expression of receptors in HTPCs and HTPC-Fs

HTPCs and HTPC-Fs express functional receptors for immune cell products

It has been already shown that mRNAs of receptors for tryptase (PAR-2) and TNF-α (TNFR-1/-2) are expressed in HTPCs and HTPC-Fs (55, 132, 133).

To investigate if HTPCs and HTPC-Fs respond in a similar way to PAR-2 activation, measurements of transient intracellular Ca^{2+} release, after addition of human recombinant tryptase (100 ng/ml) or a selective PAR-2 agonist peptide SLIGKV (10 µM), were performed. Tryptase and SLIGKV led to acute Ca^{2+} elevations in HTPCs and HTPC-Fs (Figure 4-8 A, B), indicating that functional PAR-2 is expressed in either cell type. The number of responding cells was counted for each experiment and the percentage of HTPCs and HTPC-Fs (n = 3/group) responding to 100 ng/ml tryptase and 10 µM SLIGKV was determined. Results indicate a similar response in both cell types (Figure 4-8 C). As 100 ng/ml tryptase and 10 µM SLIGKV proved to be effective concentrations to induce Ca^{2+} signals in HTPC/-Fs, these concentrations were used for subsequent studies.

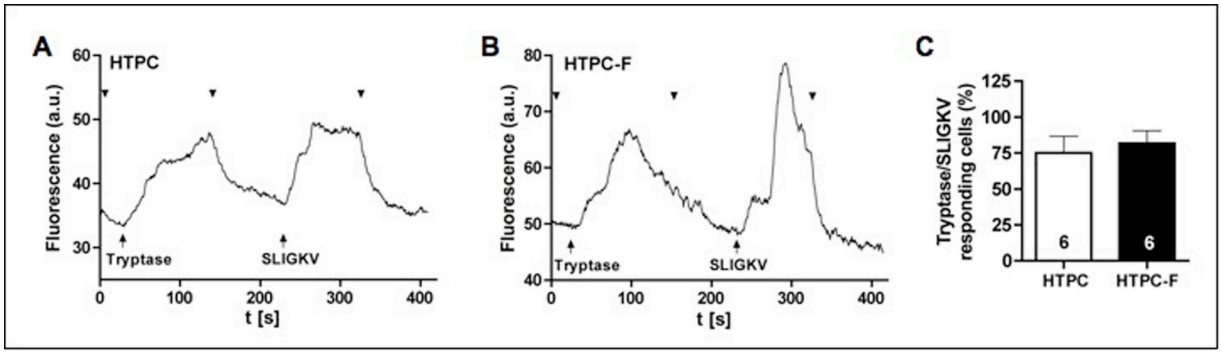

Figure 4-8: HTPCs and HTPC-Fs bear a functional receptor for tryptase, PAR-2.
A, Representative results of measurements of intracellular Ca^{2+} release after addition of tryptase (100 ng/ml) and agonist SLIGKV (10 µM) in single HTPCs and **B,** HTPC-Fs. The arrowheads indicate the addition of buffer (DMEM). **C,** The percentage of HTPCs and HTPC-Fs (n = 3 patients/group) responding to tryptase/SLIGKV with acute Ca^{2+} signals were not significantly different (mean + SEM).

Previous studies indicated that TNFR-1 and -2 are expressed in the human testis and in HTPCs and HTPC-Fs (132, 133). In the present study, functionality of these receptors in HTPC-Fs was investigated as has been described for HTPCs (133). TNF-α binding to TNFRs activates MAPK cascade and leads to phosphorylation of Erk1/2 (149). Western blot experiments with TNF-α (5 ng/ml) stimulated HTPC/HTPC-F samples were performed and phosphorylation of Erk1/2 in both cell types could be demonstrated after 10 and 20 min, but not after 60 min, of TNF-α stimulation (Figure 4-9). These results indicate the presence of functional TNFRs in HTPCs as well as in HTPC-Fs. Cells isolated of respectively three different patients per group were used for this experiment.

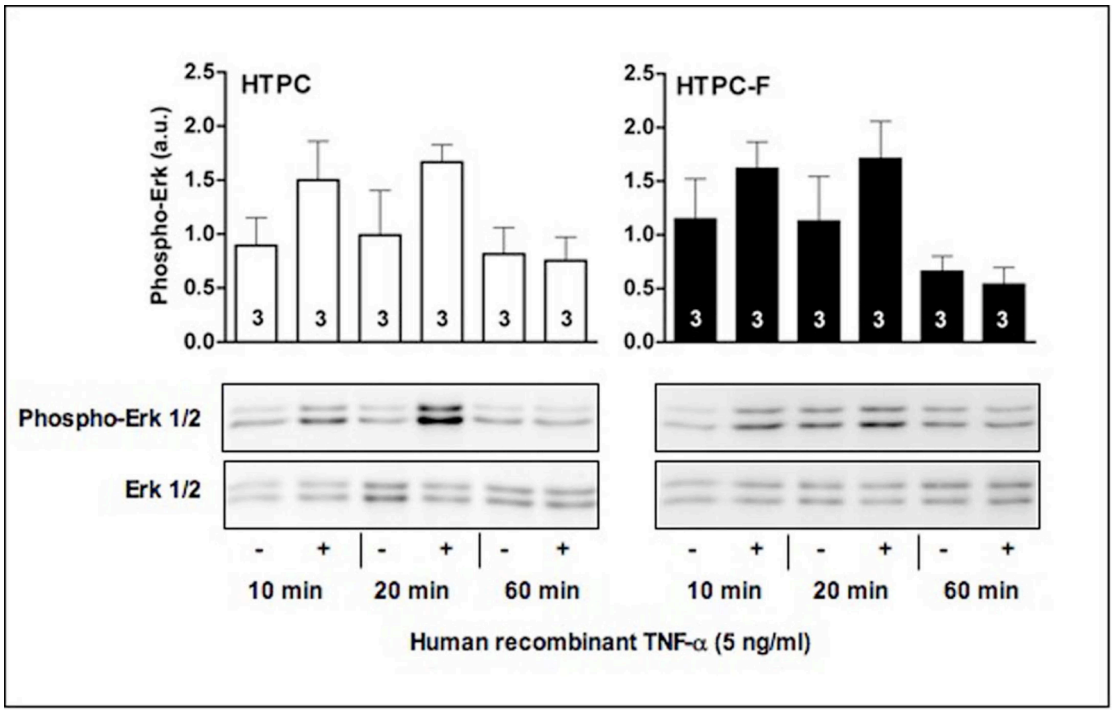

Figure 4-9: HTPCs and HTPC-Fs possess functional TNFRs.
Results of Western blot experiments performed at different time points revealed phosphorylation of Erk1/2 (Phospho-Erk1/2) after 10 and 20 min, but not after 60 min, of TNF-α treatment (5 ng/ml) of HTPCs (left) and HTPC-Fs (right). All results were normalized to levels of total Erk1/2 and are given as mean + SEM (a.u.). Numbers within the columns indicate the number of different patients. Examples of representative Western blots of HTPCs (left) and HTPC-Fs (right) are shown below.

HTPCs and HTPC-Fs express several growth factor receptors

Several growth factor receptors are known from other cellular systems to be partners of DCN signaling (121-124). RT-PCR screening followed by sequencing revealed that cultured HTPCs, as well as HTPC-Fs, express a number of those growth factor receptors. The data indicate mRNA expression of receptors of the EGFR family, namely EGFR, v-erb-b2 erythroblastic leukemia viral oncogene homolog 2 (ErbB2), v-erb-b2 erythroblastic leukemia viral oncogene homolog 3 (ErbB3) and v-erb-a erythroblastic leukemia viral oncogene homolog 4 (ErbB4), PDGF receptors (PDGFR-α and PDGFR-β), IGF-1R, HGFR and VEGR (Figure 4-10). For each PCR samples of three different patients per group were used.

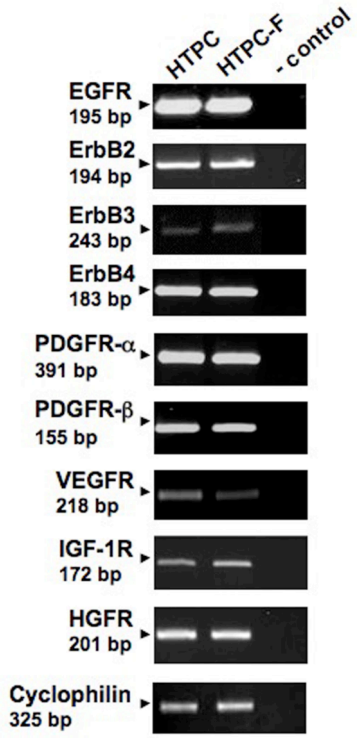

Figure 4-10: Growth factor receptor expression in HTPC and HTPC-Fs.
Results of RT-PCR analysis are shown using ethidium bromide-stained gels. HTPCs and HTPC-Fs express receptors of the EGFR family (EGFR, ErbB2, ErbB3 and ErbB4), PDGFRs (-α and -β), VEGFR, HGFR and IGF-1R. Negative controls were performed without cDNA input (- control).

In the present study, DCN interferences with the EGF/EGFR and PDGF/PDGFR signaling systems were examined. In order to determine whether EGFR and PDGFRs are expressed in the human peritubular wall *in vivo*, this compartment was isolated by laser capture microdissection and subsequently subjected to RT-PCR and sequencing. Sections of normal testis and testis of MA patients were used. The results revealed EGFR- and PDGFR (-α and -β)-expression in the peritubular wall of normal human testis as well as in testis with spermatogenic failure. Evidence for EGFR and PDGFR-α and -β mRNA expression was also found in sections of whole testes, which had been scraped from the slide and used as a positive control (Figure 4-11).

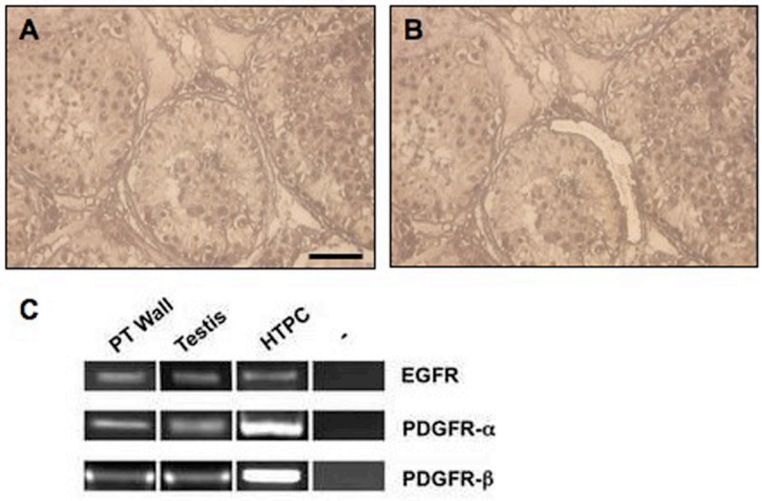

Figure 4-11: Expression of EGFR/PDGFR in the peritubular wall of human testis.
A and **B,** Micrographs showing a human testicular biopsy of an MA patient before and after laser microdissection. Areas of the peritubular wall were excised, RNA was extracted and subjected to RT-PCR. The length of the scale bars is approximately 50 µm. **C,** Ethidium bromide-stained gel, showing results of a RT-PCR experiment (EGFR: 195 bp, PDGFR-α nested: 158 bp, PDGFR-β semi-nested: 136 bp). EGFR and PDGFR-α and -β are expressed in human peritubular wall (PT). HTPCs and whole testes cDNAs were used as positive controls. The negative control was performed without cDNA input.

4.3 Human testicular peritubular cells express DCN *in vitro*: Higher basal DCN levels in HTPC-Fs than in HTPCs

RT-PCR/sequencing, Western blotting and ELISA measurements revealed that isolated HTPCs and HTPC-Fs (n = 3-7 patients/group) produce and secrete DCN (Figure 4-12). However, both cell types differ apparently in DCN expression quantity. QRT-PCR showed that within 24 h DCN mRNA expression levels are significantly elevated in HTPC-Fs as compared to HTPCs (Figure 4-12 A). All results were normalized to the human housekeeping gene RPL19.

A significant increase in cellular DCN protein in HTPC-Fs as compared to HTPCs could be found by Western blotting ($P < 0.01$). To account for possible small differences in applied protein amounts, DCN results were normalized to β-actin levels (Figure 4-12 B). Additionally, ELISA experiments revealed that within 24 h, HTPC-Fs released significantly greater quantities of DCN into the culture medium than HTPCs. Constitutive secretion occurred and the levels further increased up to 72 h (Figure 4-12 C). These data, showing higher expression and secretion of DCN in HTPC-Fs, correlate with immunohistochemistry results indicating massive DCN deposits in ECM in the testes of infertile men (Figure 4-3 A-C).

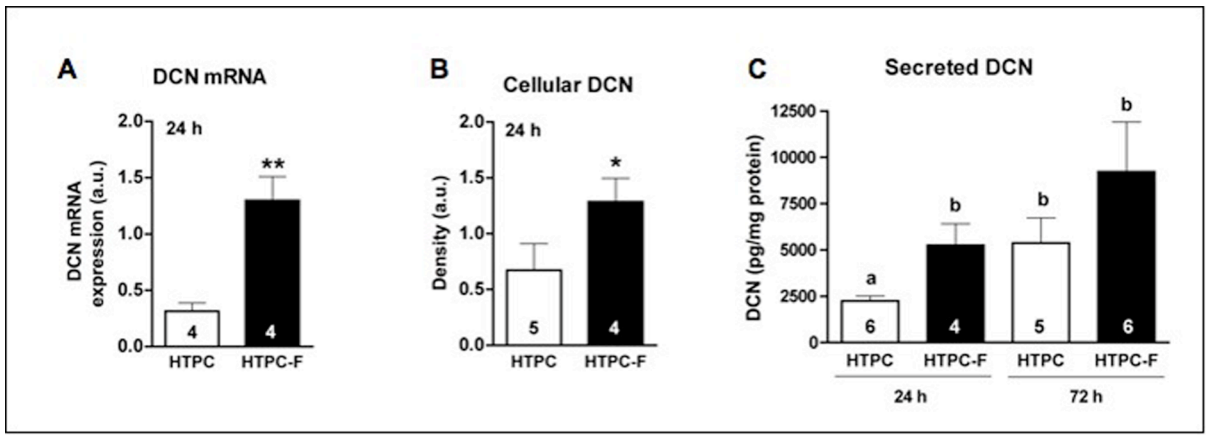

Figure 4-12: HTPCs and HTPC-Fs produce and secrete DCN: Quantitative differences.
A, QRT-PCR results show a significantly higher DCN mRNA expression in peritubular cells of patients with fibrotically altered testes and impaired spermatogenesis than in patients displaying normal spermatogenesis ($P < 0.01$). Results were normalized to the housekeeping gene RPL19. **B,** Summary of DCN Western blots reveal a significant increase in cellular DCN protein in HTPC-Fs as compared to HTPCs ($P < 0.01$). To account for possible small differences in applied protein amounts, DCN levels were normalized to β-actin levels. **C,** Results of ELISA measurements show an increased DCN protein release from HTPC-Fs into the culture media over a period of 24 h ($P < 0.05$). DCN secretion is further increased after 72 h. ELISA results were normalized to total cellular protein. Results were expressed as mean + SEM and given in a.u. or pg/mg protein. The numbers within columns show the number of different patients.

4.4 Regulation of DCN in human testicular peritubular cells

4.4.1 Testosterone and 17β-estradiol do not influence DCN expression in HTPC and HTPC-Fs

In order to find how DCN expression is regulated in the peritubular wall of normal and infertile testis, HTPCs and HTPC-Fs were treated with testosterone (100 nM) for 24 h and in separate experiments with two different concentrations of 17β-estradiol (100 nM and 1 µM) for 6 respectively 24 h. Control cells were incubated only with the solvents of stimulants. QRT-PCRs revealed that testosterone, when added to the cells for 24 h, is not able to alter DCN mRNA levels in HTPC/-Fs compared to controls (Figure 4-13 A). Both concentrations of 17β-estradiol, added for different time periods, do not influence DCN mRNA expression either (Figure 4-13 B, C).

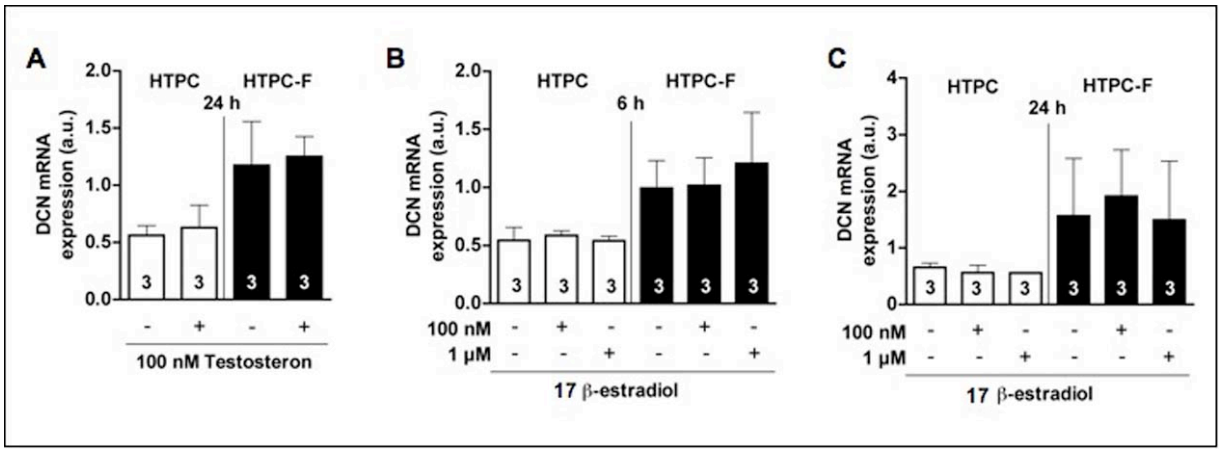

Figure 4-13: Testosterone and β-estradiol do not alter DCN mRNA expression in HTPC/-Fs.
QRT-PCR results of screening of respectively cells from three patients with normal spermatogenesis and three patients with fibrotic altered testes and impaired spermatogenesis show that neither **A,** testosterone (100 nM) after 24 h stimulation nor β-estradiol in different concentrations (100 nM and 1 µM) for **B,** 6 respectively **C,** 24 h can change DCN mRNA expression. All results (mean + SEM) were normalized to the housekeeping gene RPL19 and are given in arbitrary units (a.u.). The numbers within the columns indicate the number of patients.

4.4.2 Forskolin and prostaglandin 15dPGJ2 do not affect DCN expression

HTPCs and HTPC-Fs were treated with forskolin (50 nM) for 4 h and in a separate experiment with 15dPGJ2 (10 µM) for 7 days. Control cells were incubated only with the solvents of stimulants. QRT-PCRs revealed that both treatments do not alter DCN mRNA levels in HTPC/-Fs compared to controls (Figure 4-14).

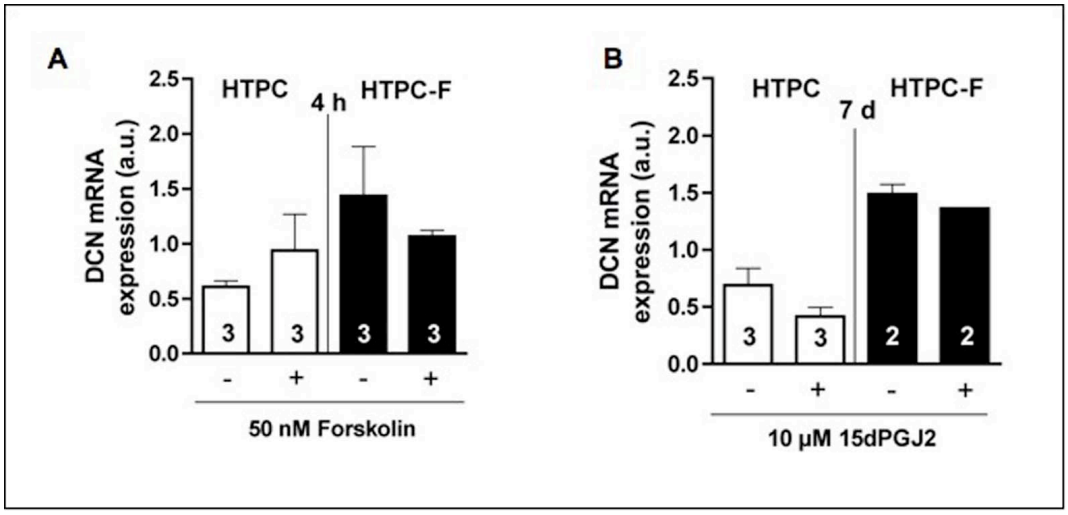

Figure 4-14: Forskolin and 15dPGJ2 do not affect DCN mRNA expression in HTPC/-Fs.
A, Forskolin (50 nM) after 4 h stimulation and **B,** 15dPGJ2 (10 µM) after 7 days do not change DCN mRNA expression. All results (mean + SEM) were normalized to the housekeeping gene RPL19 and are given in arbitrary units (a.u.). The numbers within the columns indicate the number of different patients.

4.4.3 Tryptase stimulates DCN production and secretion via PAR-2 after 72 h in HTPC-Fs, but not in HTPCs

The number of tryptase producing mast cells is increased in the testes of sub-/infertile men (54, 150). As mentioned above HTPCs, as well as HTPC-Fs, express functional receptors for tryptase, PAR-2. QRT-PCR analysis showed that tryptase (100 ng/ml) does not influence DCN mRNA regulation in HTPC/-Fs after a stimulation period of 24 h (Figure 4-15 A). ELISA experiments confirmed these results at protein level (Figure 4-15 B).

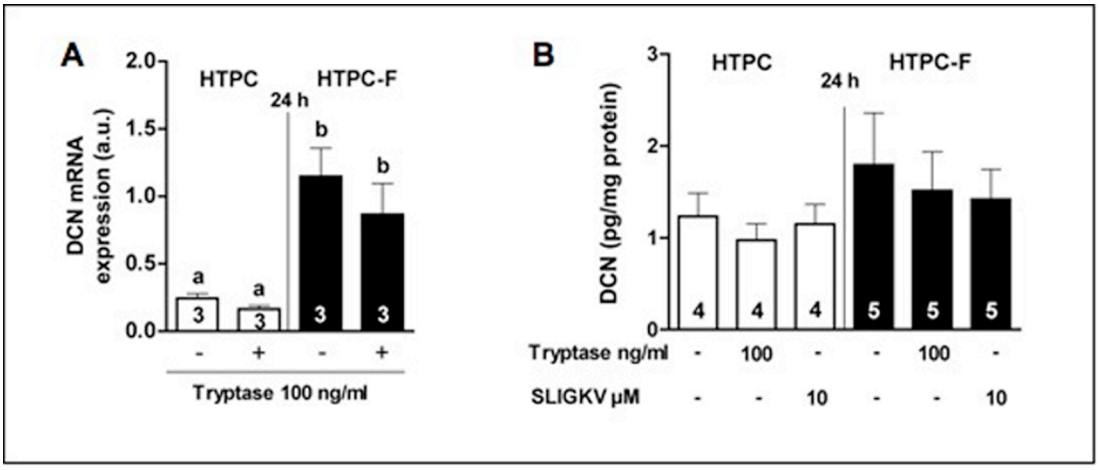

Figure 4-15: DCN expression in HTPC/-Fs is not altered by tryptase after 24 h.
A, QRT-PCR data show that tryptase treatment for 24 h (100 ng/ml) does not alter DCN mRNA expression levels in HTPC and HTPC-Fs. Results (a.u.) were normalized to the housekeeping gene RPL19. **B,** Results of ELISA experiments show that neither tryptase, nor SLIGKV (10 µM) after 24 h, alter DCN protein secretion amounts of HTPC/-Fs. Levels of secreted DCN were normalized to the total amount of protein of each sample. Numbers within columns show the number of patients.

When cells were stimulated for 72 h with tryptase (100 ng/ml) or SLIGKV (10 µM), a regulation of DCN expression in HTPC-Fs, but not in HTPC, could be observed. Tryptase and SLIGKV increased not only DCN mRNA expression, but also cellular and secreted protein levels. Compared to the corresponding control cells, DCN mRNA and protein levels in stimulated HTPC-Fs, but not HTPCs, are significant higher (Figure 4-16).

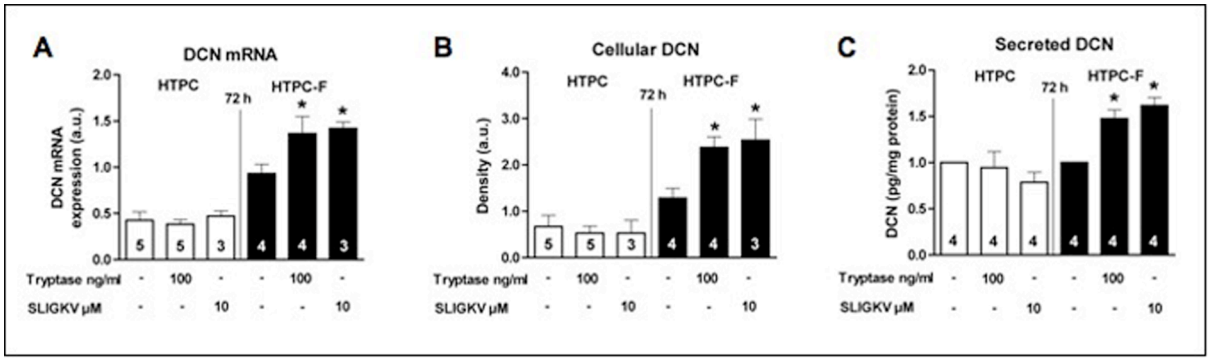

Figure 4-16: Tryptase treatment for 72 h stimulates DCN production and secretion in HTPC-Fs.
A, QRT-PCR results show DCN mRNA expression levels in HTPCs and HTPC-Fs, after 72 h exposed to 100 ng/ml tryptase or 10 µM SLIGKV. DCN mRNA levels in stimulated HTPC-Fs are significantly increased compared to controls ($P < 0.05$; mean + SEM). DCN mRNA levels in HTPCs are not changed upon stimulation. Results (a.u.)were normalized to the housekeeping gene RPL19. **B,** The summary of Western blot data reveals that DCN protein levels in HTPC-Fs are significantly increased by tryptase (100 ng/ml)/SLIGKV (10 µM) after 72 h ($P < 0.05$), while they are not altered in HTPCs. Results (a.u.) were normalized to β-actin and given as mean + SEM. **C,** Results of ELISA measurements show a significant increase in secreted DCN amounts in tryptase/SLIGKV-treated HTPC-F samples compared to HTPCs and control cells (n = 4/group). Values were normalized to total protein amounts. Because of high varation among results of different patients, results were normalized to their controls. Numbers within the columns indicate the number of different cell donators.

4.4.4 TNF-α stimulates DCN production and secretion via TNFRs after 72 h in HTPC-Fs, but not in HTPCs

Testicular mast cells and macrophages produce and secrete the cytokine TNF-α (54, 58, 133, 150). Recent studies showed, that HTPCs and HTPC-Fs possess TNFR-1 and TNFR-2 (132, 133). Functionality of these receptors was proven by detecting phosphorylation of Erk1/2 in HTPC/-Fs after 10 or 20 min TNF-α (5 ng/ml) treatment (Figure 4-9). DCN expression in HTPC/-Fs was investigated after 24 h respectively 72 h treatment with TNF-α (5 ng/ml). No significant changes in DCN mRNA expression in HTPC/-Fs after 24 h TNF-α stimulation could be detected (data not shown). However, after 72 h HTPC-Fs responded to TNF-α by increasing DCN production (Figure 4-17). DCN mRNA levels in HTPC-Fs are significantly elevated upon TNF-α stimulation compared to untreated control cells (Figure 4-17 A). No DCN regulation by TNF-α could be observed in cells of fertile patients. The qRT-PCR results could be confirmed at protein level by Western blot and ELISA experiments. Thus, cellular and secreted DCN amounts of HTPC-Fs are increased by TNF-α after 72 h (Figure 4-17 B, C).

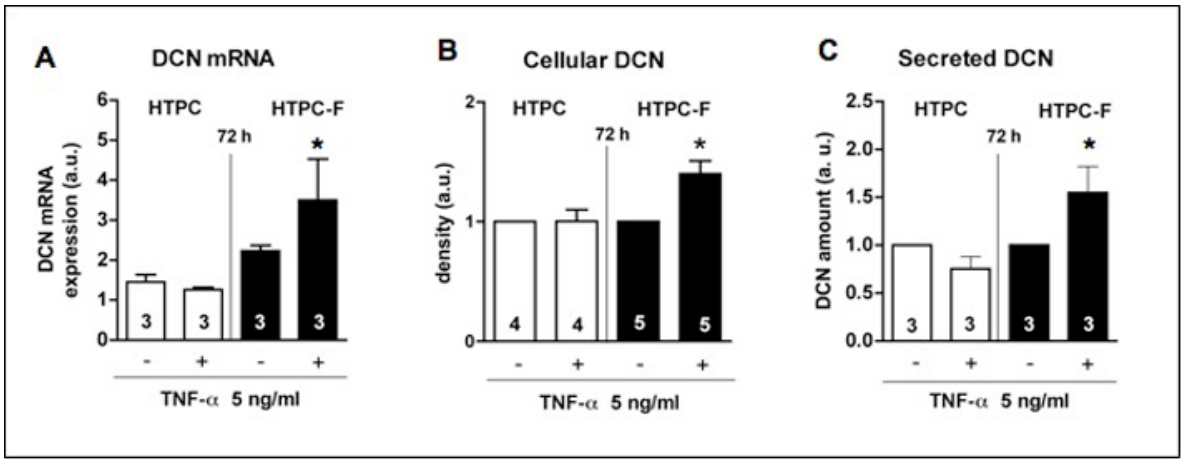

Figure 4-17: The cytokine TNF-α stimulates DCN production and secretion in HTPC-Fs.
A, Results of qRT-PCR: DCN mRNA expression in TNF-α (5 ng/ml) stimulated HTPC-Fs, but not HTPCs, is significant higher than in untreated control cells ($P < 0.05$; mean + SEM). Results (a.u.) were normalized to the housekeeping gene RPL19. Numbers within columns show the number of patients. **B,** Western blot results: TNF-α significantly increases DCN protein levels in HTPC-Fs after 72 h ($P < 0.05$). All results were normalized to β-actin protein levels and given in a.u. Results of TNF-α stimulated cells were normalized to values of untreated control cells, because of high variation between different patients. Data shown are mean + SEM of blots performed with 3 – 5 patients/group. **C,** ELISA results: Compared to HTPCs and control cells, a significant increase in secreted DCN became evident in HTPC-F samples after 72 h TNF-α treatment ($P < 0.05$; n = 4/group). All values were normalized to total protein amounts and given in a.u. Results of TNF-α stimulated cells were normalized to values of untreated control cells, because of high variation between different patients. Data of cells of four patients/group are shown.

4.5 Mouse fibroblasts

4.5.1 TNF-α increases DCN expression in NIH/3T3 cells

NIH/3T3 cells, standard mouse fibroblasts were used for initial mouse studies by treating them with mouse TNF-α for 24 h and 72 h. QRT-PCRs revealed that DCN mRNA is expressed in NIH/3T3 cells and that levels of DCN mRNA are increased by TNF-α treatment for both time periods (Figure 4-18 A). DCN protein could hardly be detected in NIH/3T3 cells, but when cells were grown in the presence of TNF-α for 24 h or 72 h, DCN protein levels were increased (Figure 4-18 B).

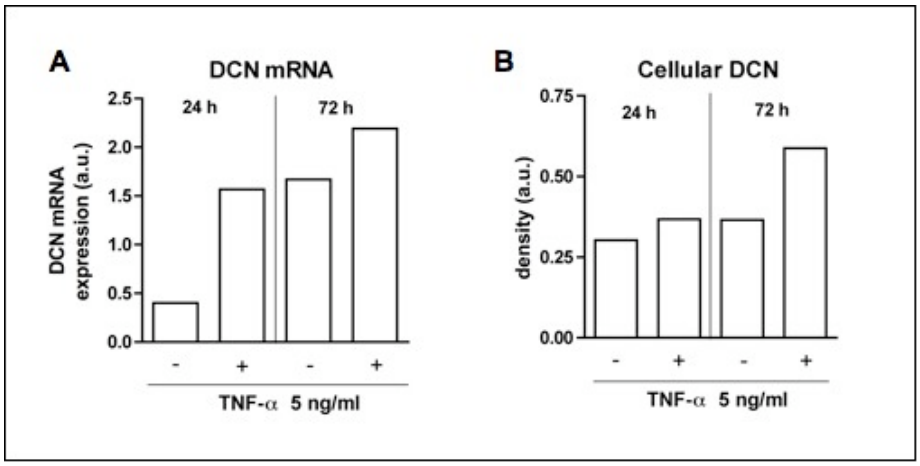

Figure 4-18: TNF-α stimulates DCN expression in NIH/3T3 cells.
A, Results of qRT-PCR indicate an increased DCN mRNA expression after treatment with TNF-α (5 ng/ml) for 24 h respectively 72 h. Results were normalized to the housekeeping gene RPL19 and are given in a.u. **B,** Results of Western blotting reveal that TNF-α increases DCN protein levels after 24 h/72 h. Results were normalized to β-actin protein levels and given in a.u.

4.5.2 Mouse testis cell culture

Explants of mouse testicular tissue of WT and AROM+ were cultured to gain mouse testicular peritubular cells. After approximately five days elongated cells extended from the explants (Figure 4-19 A) which were stained positive with SMA (data not shown). As cell growth was observed only in few explant pieces and cells grow slowly, mouse testicular fibroblasts of the interstitial compartment were isolated using collagenase. Growing cells showed a morphology that was characterized by mainly elongated cells with fibroblast appearance (Figure 4-19 B). As cells have to be used freshly for each experiment, because subcultivation was not possible with the methods used, it was not possible to gain sufficient cell yields for further experiments within the present study.

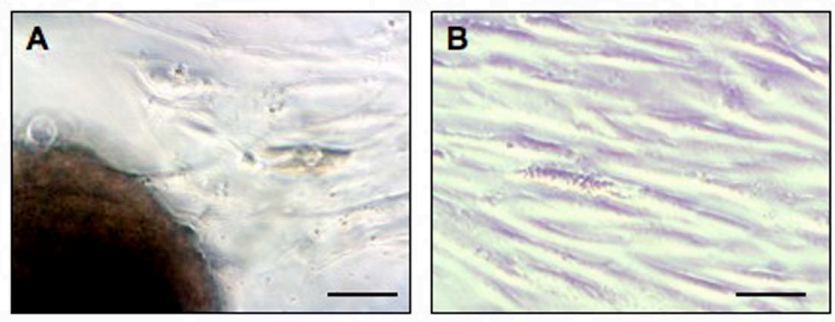

Figure 4-19: Cultures of mouse testicular cells.
A, Small pieces of testicular biopsies were seeded onto culture dishes and after five days, cells start growing out of the explants. **B,** Cells of mouse testis isolated using collagenase display an elongated phenotype. The length of the bar is approximately 20 µm.

4.6 DCN effects on HTPCs and HTPC-Fs

4.6.1 DCN acutely increases intracellular Ca^{2+} levels in HTPC/-Fs

DCN is known to be a potential signaling molecule that interacts with several growth factor systems in various tissues. The present study indicated that a number of growth factor receptors are expressed by peritubular cells of the human testis (Figure 4-10). When HTPCs or HTPC-Fs were incubated with DCN (10 µg/ml), cells generate an immediate and reversible increase in intracellular Ca^{2+} (Figure 4-20). Apparently, DCN can act as a ligand to some receptor linked to signal transduction events involving Ca^{2+} release in HTPC/-Fs. Since the existence of a special DCN receptor is not known, these findings suggest DCN interaction with one or more growth factor receptors in HTPC/-Fs. Cells of at least three different patients per group, HTPC and HTPC-F, were tested and approximately 80 – 100 % of the cells measured respond to DCN stimulation with transient elevations of Ca^{2+}. To exclude, that Ca^{2+} signals are only a non-specific protein effect, experiments with BSA (10 µg/ml)

were conducted as well. When BSA was added, intracellular Ca^{2+} levels in HTPC/-Fs were not altered (Figure 4-20 C).

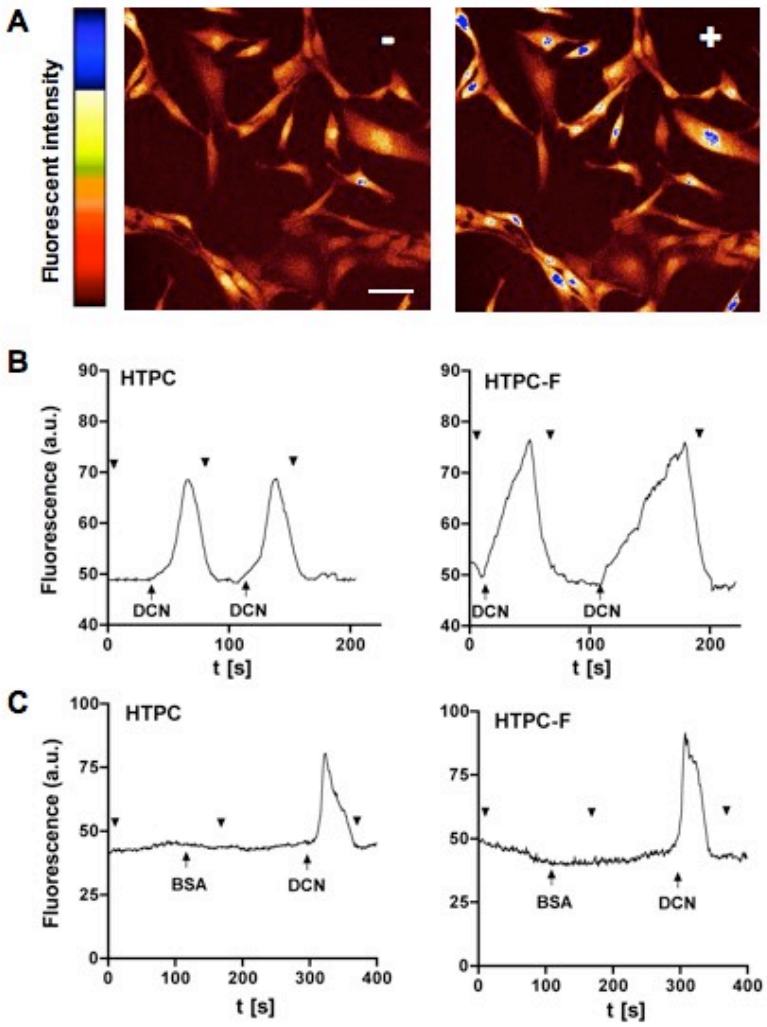

Figure 4-20: HTPC/HTPC-Fs respond to DCN with transient intracellular Ca^{2+} signals.
A, Microphotograph of HTPCs prior to (-; DMEM) and immediately after DCN addition (+; 10 µg/ml). **B,** Representative results of measurements of intracellular Ca^{2+} levels in a single HTPC (left) and HTPC-F (right): DCN (10 µg/ml) leads to acute and repeatable increases in intracellular Ca^{2+} in HTPC/-Fs. Arrows indicate the addition of DCN and arrowheads indicate the addition of buffer (DMEM). **C,** BSA addition (arrows) did not induce increased intracellular Ca^{2+} levels neither in HTPC (left), nor HTPC-Fs (right). Arrowheads indicate the addition of DMEM.

Furthermore, Ca^{2+}-measurement experiments testing different concentrations of EGF (50 ng/ml, 250 ng/ml and 1 µg/ml) or PDGF-BB (5 ng/ml and 10 ng/ml) showed that these growth factors can increase intracellular Ca^{2+} in HTPCs and HTPC-Fs in a similar manner as DCN (Figure 4-21). Concentrations of 50 ng/ml EGF and of 5 ng/ml PDGF-BB were already sufficient to induce transient and reversible calcium signals in the cells, thus proving the functionality of EGFRs and PDGFRs in cultured HTPC/-Fs. When cells were pre-treated with 10 µg/ml DCN for 24 h, intracellular Ca^{2+} levels did not change when challenged with EGF or PDGF-BB, but cells still responded to a challenge by histamine (data not shown).

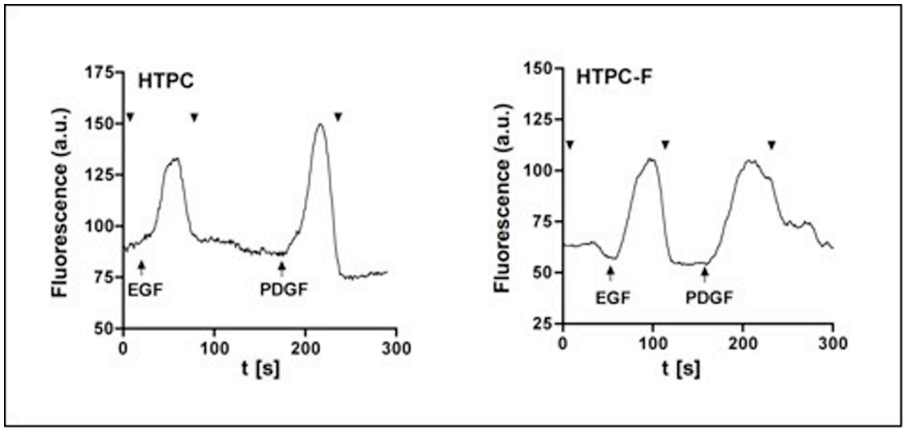

Figure 4-21: EGF and PDGF-BB induce intracellular Ca^{2+} signals in HTPC/-Fs. Representative results of measurements of changes of intracellular Ca^{2+} levels in a single HTPC (left) and HTPC-F (right) show that EGF (50 ng/ml) and PDGF-BB (5 ng/ml) lead to acute increases in intracellular Ca^{2+} in HTPC/-Fs. Arrowheads indicate the addition of DMEM.

4.6.2 Acute actions of DCN leads to phosphorylation of growth factor receptors in HTPC and HTPC-Fs

To examine whether exogenously added DCN may be able to activate RTKs expressed by HTPC/-Fs (Figure 4-10) a phosphorylation assay (Proteome Profiler) to determine the relative level of tyrosine phosphorylation of human RTKs was performed. Results of this dot blot screening indicated a phosphorylation of several RTKs by DCN (10 µg/ml), added to HTPCs for 5 min. Phosphorylation of the EGFR family (EGFR, ErbB2, ErbB3 and ErbB4) and HGFR, but not in cases of VEGFR or IGF-1R when evaluated in comparison to control cells only treated with PBS, was found (Figure 4-22). Differences between results for phosphorylated and non-phosphorylated PDGFR-α/β were small and therefore phosphorylation of this growth factor receptor was examined in further experiments using Western blotting. Protein array results of all 42 different human RTKs are listened in table 10-11 (see APPENDIX 10.11).

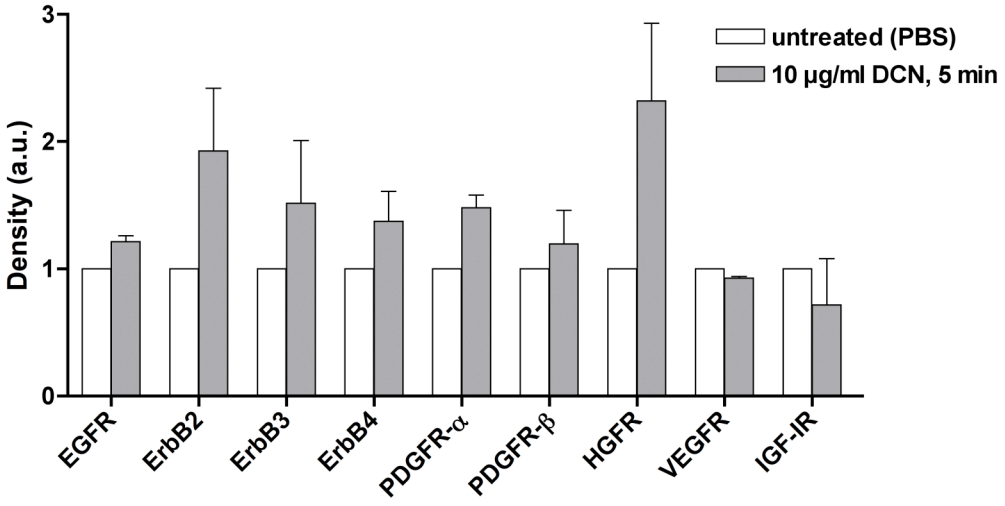

Figure 4-22: Evidence for DCN acting as a ligand for growth factor receptors in HTPCs.
Results of protein array experiment indicate that DCN (10 µg/ml) causes phosphorylation of the EGFR family (EGFR, ErbB2, ErbB3 and ErbB4) and HGFR in HTPCs within 5 min. A potential, but very low, phosphorylation was found in case of PDGFR-α/β. VEGFR and IGF-1R were not phosphorylated by DCN. Data for control cells (white columns) and treated cells (dark columns) are given. The values stem from densitometric evaluation of two experiments. Results (mean + SEM) shown were normalized to control values and expressed as a.u.

Since EGF and PDGF-BB were found to induce mitosis and proliferation in HTPCs, as well as in HTPC-Fs (see below points 4.6.4 and 4.6.5), possible DCN interactions with EGFR and PDGFR were examined further. Subsequent Western blot experiments, using anti-phospho-EGFR and anti-phospho-PDGFR-β antibodies, revealed that DCN (10 µg/ml) added to HTPCs or HTPC-Fs for 10 min, phosphorylates EGFR, but not PDGFR-β (Figure 4-23). As expected, phosphorylation of EGFR and PDGFR-β occurred in response to 50 ng/ml EGF or 5 ng/ml PDGF-BB added respectively for 10 min to the cells. The experiment was repeated with cells of three men with functional spermatogenesis and from two patients with impaired spermatogenesis and testicular fibrosis. Importantly, the addition of BSA (10 µg/ml) did not cause signals and therefore a non-specific protein effect can be excluded (Figure 4-23).

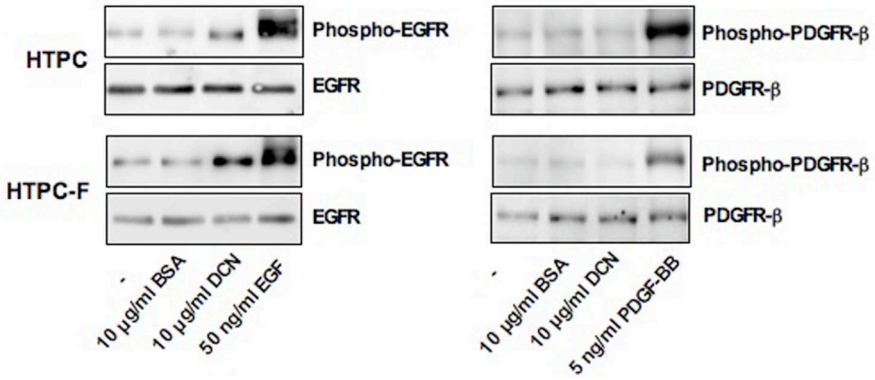

Figure 4-23: DCN phosphorylates EGFR, but not PDGFR-β, in HTPC and HTPC-Fs.
Representative Western blots showing that DCN (10 µg/ml) causes phosphorylation of EGFR within 10 min, while PDGFR-β is not phosphorylated. Negative control (-; addition of PBS) and BSA (10 µg/ml) treated samples are not phosphorylated as well. Control Western blots using non-phosphorylated EGFR and PDGFR-β antisera are shown below.

4.6.3 Chronic actions of DCN on viability of HTPC and HTPC-Fs.

To investigate actions of DCN when added exogenously to HTPCs and HTPC-Fs for longer time periods (24 h), experiments to assess cell apoptosis and viability were performed. Caspase assays, performed 24 h after cell stimulation with DCN (10 µg/ml), revealed that DCN does not induce apoptosis in both cell types (Figure 4-24).

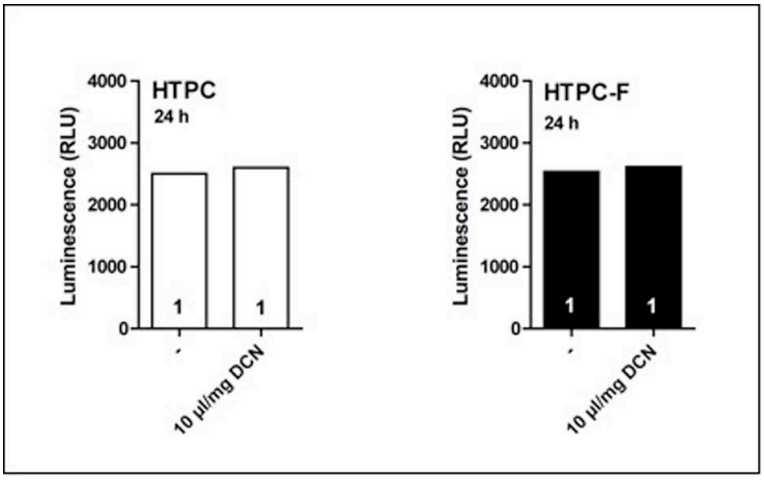

Figure 4-24: Effect of exogenous DCN on apoptosis in HTPCs and HTPC-Fs.
Results of measurements of caspase 3/7 levels in testicular peritubular cells of one patient displaying normal spermatogenesis (left) and cells of one patient with impaired spermatogenesis and testicular fibrosis (right) show that DCN (10 µg/ml) does not induce apoptosis in both cell types. Results are given in relative luminescence units (RLU).

Caspase assay results could be confirmed in experiments measuring ATP levels in HTPCs and HTPC-Fs after different concentrations of DCN (5, 10 and 50 µg/ml) were added for 24 h. ATP assay results show that DCN does not alter cellular viability of both cells types (Figure 4-25).

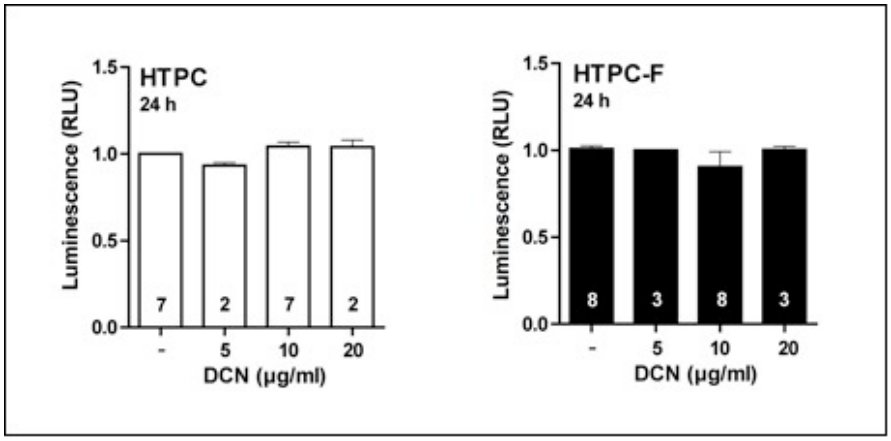

Figure 4-25: Effects of different concentrations of DCN on viability of HTPC/-Fs.
Measurements of ATP levels in HTPCs (left) and HTPC-Fs (right) revealed that different DCN concentrations (5, 10 and 50 µg/ml) for 24 h did not cause any significant alterations in cellular viability. Results (mean + SEM) were normalized to untreated controls. The numbers of patients are shown inside the columns. Results are given in relative luminescence units (RLU).

4.6.4 Chronic actions of DCN include inhibition of EGF- or PDGF-mediated viability and proliferation in HTPCs and HTPC-Fs

The roles of EGF and PDGF-BB signaling in human peritubular cells was investigated by measuring cellular ATP levels. Results revealed that EGF (250 ng/ml) and PDGF (5 ng/ml) increased viability of HTPCs and HTPC-Fs after 24 h. Interestingly, these growth factor actions were blocked in the presence of DCN (10 µg/ml). The data imply that DCN, if present for longer periods, can inhibit growth factor signaling (Figure 4-26). Viability experiments were performed with cells of five individual men with normal testis and five patients with testicular fibrosis and impaired spermatogenesis.

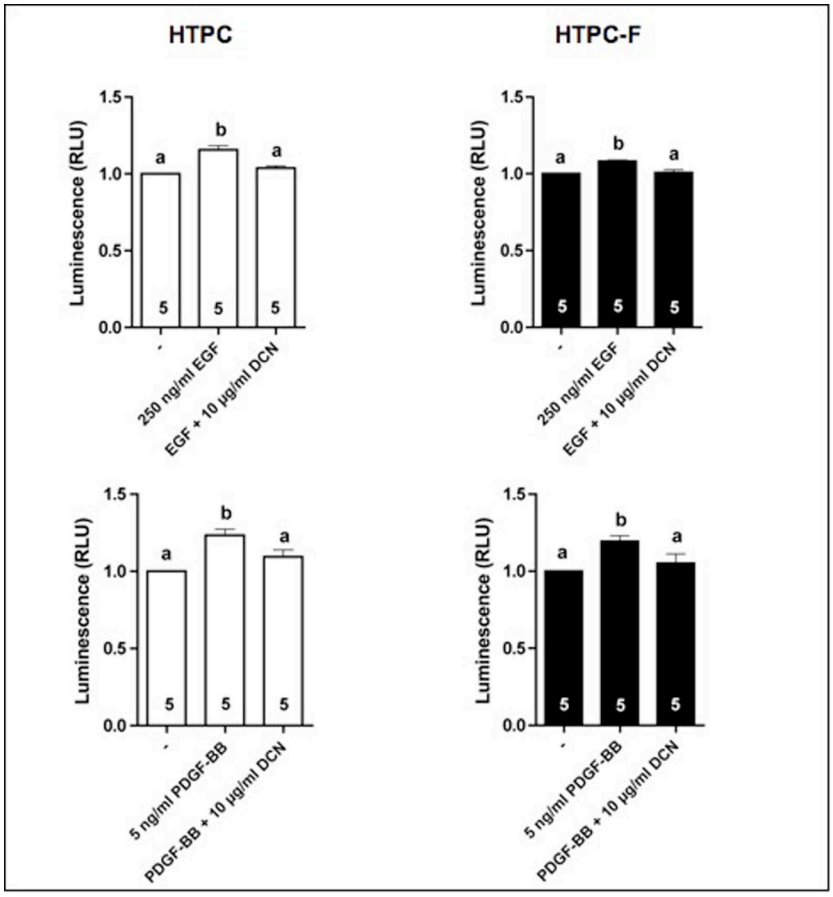

Figure 4-26: DCN blocks actions of EGF and PDGF on viability of HTPC/-Fs.
Results of ATP measurements show that EGF (250 ng/ml; top) and PDGF-BB (5 ng/ml; bottom) are effective stimulators of cellular ATP in HTPCs (left) and HTPC-Fs (right) after 24 h. Actions that were significantly blocked in the presence of 10 µg/ml DCN ($P < 0.05$). All results are mean + SEM and are expressed in RLU. Results were normalized to values of untreated control cells. Numbers of cells from different patients are indicated within the columns. Different letters over columns indicate statistically significant differences at $P < 0.05$ between the groups.

The role of EGF/EGFR and PDGF/PDGFR and the influence of DCN on these signaling systems in HTPC/HTPC-Fs were further examined performing DAPI staining experiments. Evaluating of mitotic events revealed that EGF (50 ng/ml) and PDGF-BB (5 ng/ml) significantly stimulate mitosis in HTPCs and HTPC-Fs, an effect only observed after 24 h, but not at earlier time points, i.e. 6 h or 18 h after treatment (data not shown). DCN (10 µg/ml) did not affect mitosis at any of these time points (6 h, 18 h, 24 h), but when it was added in combination with EGF or PDGF-BB to the cells, it significantly blocked the mitosis-stimulating actions of both growth factors (Figure 4-27).

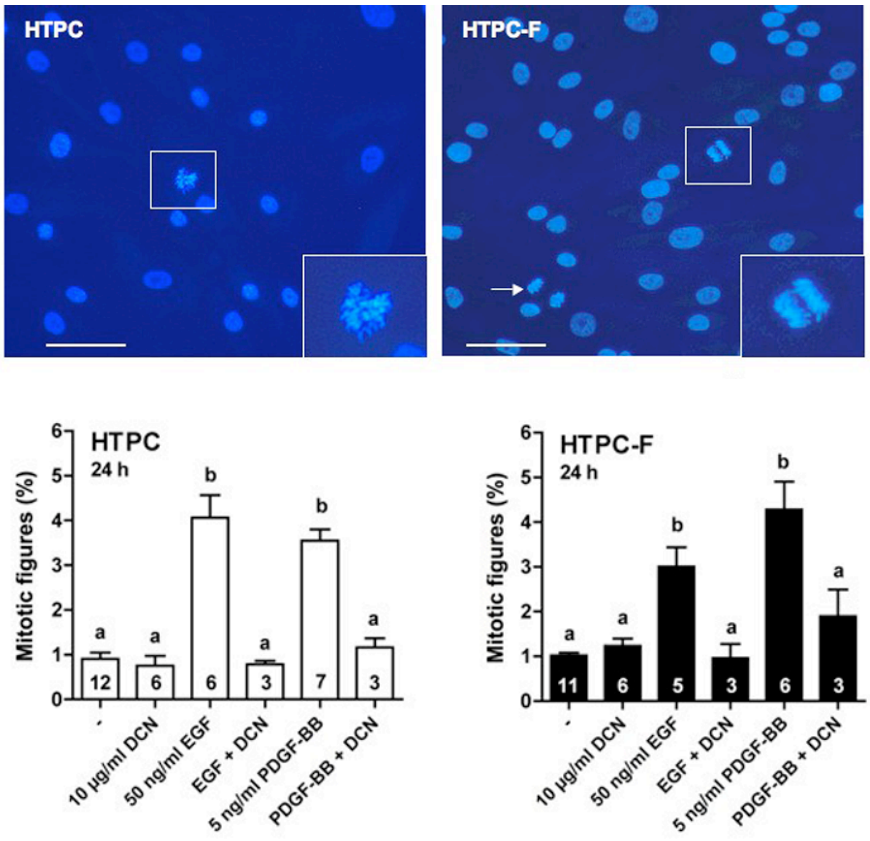

Figure 4-27: Mitosis induced by EGF and PDGF in HTPC/-Fs is blocked by DCN.
Microphotographs (top) of DAPI stainined nuclei in HTPCs (left) and HTPC-Fs (right) represent nuclei in different mitotic states. The length of the scale bar is approximately 10 µm. Higher magnification of the boxed area in the left panel shows a metaphase nucleus. In HTPC-Fs an anaphase (boxed area in higher magnification) and a telophase (arrow) are shown.
Results of evaluation of mitotic figures (bottom) after 24 h of exposure to EGF (50 ng/ml), PDGF-BB (5 ng/ml) and DCN (10 µg/ml) revealed that DCN can significantly block EGF/PDGF actions ($P < 0.05$). The letters above the columns indicate statistical differences. Results (mean + SEM) are expressed in percentage. The numbers in the columns give numbers of different patients.

The ability of PDGF-AA and PDGF-BB to stimulate cellular proliferation was demonstrated in CASY experiments. Results of automated cell counts indicated that PDGF-BB (5 ng/ml) added to the culture medium for 4 days can significantly increase proliferation of HTPC/-Fs, an action which was blocked in the presence of DCN (10 µg/ml; Figure 4-28 A). Similar results were observed in experiments with PDGF-AA in combination with DCN and were only performed with cells of one patient displaying normal spermatogenesis (data not shown).

Although expected, PDGF-AA (data not shown) and PDGF-BB did not alter cell sizes of HTPCs or HTPC-Fs within 4 days (Figure 4-28 B) as known from studies in rodents (151). Hence actions of DCN could not be tested on this aspect.

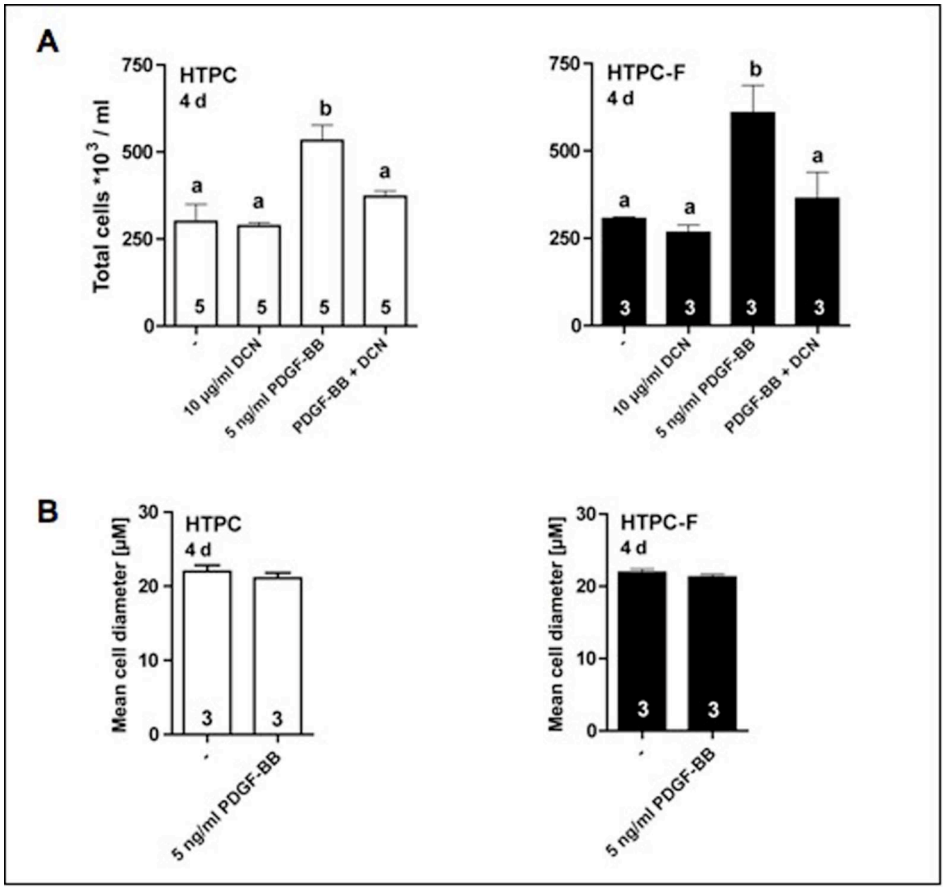

Figure 4-28: DCN blocks proliferation induced by PDGF in HTPC and HTPC-Fs. **A,** Results of automated cell counting after 4 days of exposure to PDGF-BB (5 ng/ml) and/or DCN (10 µg/ml). A significant increase in cell number was confirmed in cells treated with PDGF-BB ($P < 0.05$). While DCN alone has no effect, in combination with PDGF it significantly blocked the proliferative effect of PDGF in HTPCs and HTPC-Fs ($P < 0.05$). Cells of three different patients/group were used as indicated within the columns. Different letters above the columns indicate statistically significant differences. **B,** Measuring of cellular diameter upon stimulation with PDGF-BB (5 ng/ml) for 4 days revealed no hypertrophy of HTPCs and HTPC-Fs. Results (mean + SEM) of three individuals/group are shown.

4.6.5 DCN blocks PDGF-BB mediated SMA expression in HTPC/HTPC-Fs

Semi-quantitative RT-PCR experiments indicated increased mRNA levels of SMA in PDGF-BB treated HTPCs and HTPC-Fs after 4 days, indicating differentiation promoting actions of PDGF-BB. DCN (10 µg/ml) was able to inhibit this PDGF-BB action on SMA mRNA expression in both cell types (Figure 4-29).

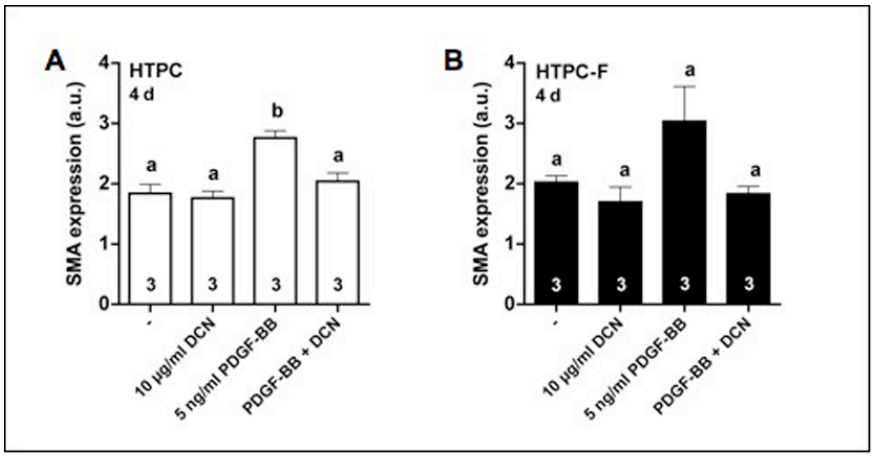

Figure 4-29: Activation of PDGFR increases SMA expression in HTPC/-Fs, an action blocked by DCN.
Summary of results of semi-quantitative RT-PCR experiments evaluating SMA, using cells of three different patients/group (number inside columns). Cells were exposed to DCN (10 µg/ml and/or PDGF-BB (5 ng/ml) for 4 days. Densitometric evaluation of the bands revealed a significant increase of SMA mRNA levels, which was blocked by DCN ($P < 0.05$). In HTPC-Fs PDGF showed the same tendencies, but changes are not significant. Levels of cyclophilin were used to normalize the results which represent a.u.

4.7 Imatinib – a further inhibitor of PDGF actions in HTPCs

4.7.1 Imatinib decreases viability in HTPCs in a dose-dependent manner

Effects of increasing imatinib concentrations on viability of human peritubular cells *in vitro* were investigated by challenging HTPCs with 10, 20, 50 or 100 µM for 24h. Viability of cells, judged by ATP measurements, was unaffected by concentrations ≤ 10 µM, but was reduced in a dose-dependent manner by higher concentrations (Figure 4-30). Therefore an imatinib concentration of 10 µM was used for further analysis.

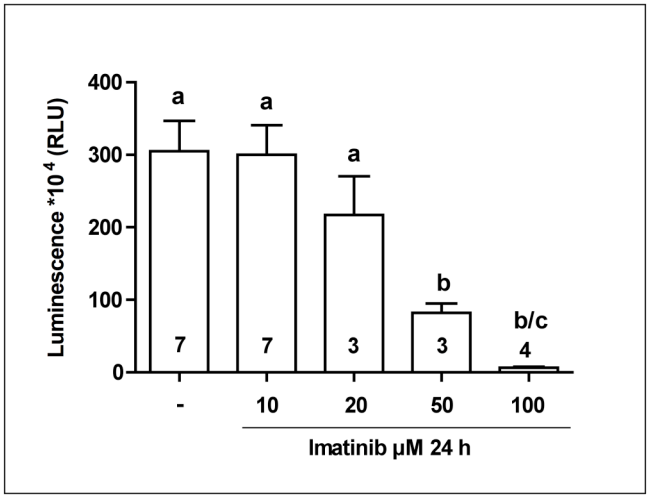

Figure 4-30: Effect of imatinib on viability of HTPCs.
Treatment of HTPCs with imatinib for 24 h resulted in significantly decreased ATP levels in a dose-dependent manner (mean + SEM). Results are expressed in RLU. Different letters over columns indicate statistically significant differences at levels of $P < 0.05$. Numbers within the columns represent the number of patients.

4.7.2 Imatinib inhibits PDGF-BB induced proliferation of HTPCs

Exposure of HTPCs to 10 µM imatinib had no effect on their viability and proliferation, as shown by CASY experiments after 4 days and ATP/DAPI experiments after 24 h (Figure 4-31). However, when HTPCs were stimulated with the mitogen PDGF-BB (5 ng/ml), a significant increase in viability and cell proliferation was detected compared to untreated control cells as mentioned before. PDGF-induced effects in HTPCs were blocked in the presence of 10 µM imatinib after 24 h respectively 4 days (Figure 4-31).

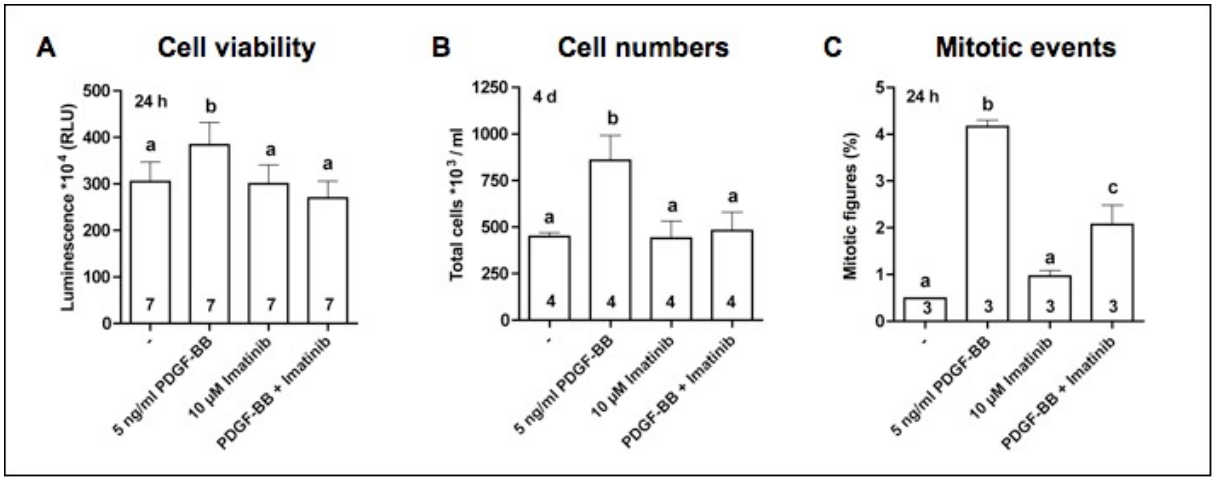

Figure 4-31: Effect of imatinib on PDGF-BB induced proliferation of HTPCs.
A, Results of ATP measurements after 24 h show that imatinib (10 µM) can significantly block PDGF-BB (5 ng/ml) induced increased viability of HTPCs ($P < 0.05$). **B,** Total cell counts: 5 ng/ml PDGF-BB stimulation of HTPCs for 4 days resulted in significant increase of proliferation ($P < 0.05$). **C,** DAPI results: Proportion of proliferating cells showing a mitotic figure (%). Imatinib blocks mitogenic actions of PDGF-BB. All results are mean + SEM. Different letters indicate significant differences. Numbers in columns indicate the number of patients used for cell harvesting.

5. DISCUSSION

5.1 Decorin expression in the testis in health and disease

In general, reports about proteoglycans in the human testis are rare. Years ago, Ungefroren *et al*. (1995) (89) identified two leucine-rich proteoglycans, biglycan and DCN, in the testis of healthy men. DCN was characterized as a product of barely explored, smooth muscle-like cells of the walls of the seminiferous tubules and of fibroblasts in the interstitial compartment. Testes of infertile men were not examined at that time. In the present study, cellular sites of DCN expression in the adult human testis could be confirmed in immunohistochemical studies using biopsies from normal and infertile men suffering from MA, GA and SCO syndrome. In addition, a striking accumulation of DCN in the ECM of the fibrotically remodeled tubular walls in the testes of men suffering from in- or subfertility was found. Since DCN is closely associated with collagens, it s not surprisingly, that it is increased under fibrotic conditions where connective tissue is increased.

As immunohistochemistry indicated, peritubular cells surrounding the seminiferous tubules are the source of DCN at this peritubular sites. In infertile men an increased production by these cells, possibly along with a reduced ability to degrade DCN, must therefore be responsible for the observed deposits in the peritubular compartment. Using a cellular model, namely cultured human testicular peritubular cells (HTPCs), it could be shown that peritubular cells synthesize DCN. That indeed peritubular cells from infertile men have a greater ability to produce and secrete DCN in a constitutive manner, was proven when mRNA and protein levels of HTPCs were compared to those of cells derived from infertile men with fibrotically altered testis (HTPC-Fs). This observation leads to the assumption that these primary cells mirror the *in vivo* situation.

Proteoglycans represent a main component of the ECM. Their ability to interact with several other ECM molecules suggest a central role in the assembly and tissue remodeling of the ECM, occurring i.e. under fibrotic conditions. The finding of increased testicular DCN during fibrotic conditions is in accordance with studies of several human fibrotic diseases of tissues such as kidney (50), lung (152), and muscles (153). For instance, in the rat liver, an upregulation of DCN goes in parallel with the first signs of fibrotic changes (154), suggesting an important role of the proteoglycan in the early events of this pathological process. In patients suffering from chronic pancreatitis, DCN overexpression in the growing ECM is associated with desmoplasia and stimulates the expression of mononuclear cell recruiting chemokine MCP-1. Other inflammatory cytokines, such as IL-1β and TNF-α, were not affected by DCN (155). In fibrotic human testis a similar DCN action might be responsible for fibrotic remodeling of the seminiferous tubules walls, a process that remains to be studied in future experiments. However, some studies describe DCN as an antifibrotic agent (156, 157). The reduction of muscle fibrosis after injury has been shown. Possible antifibrotic functions of DCN in the human testis were not studied within the present investigations and remain to be examined.

Within the present study, DCN expression in mouse testes was investigated. It was known that in normal mice, testicular DCN is undetectable throughout postnatal development and may not be of importance in the adult mouse (158, 159). These results are in line with immunohistochemical experiments in the present study, which show that it is barely detectable in gonads of young (3 - 5 moths of age) and old adult (9 - 10 months of age) males. By means of qRT-PCRs, DCN mRNA was however detected in mouse testes of both age groups. Thus, DCN in mouse testis may be only present at mRNA level or may be only marginally expressed at protein level. Indeed, connective tissue is not abundant in mouse testes and therefore DCN is barely present. Another possibility might be, that anti-human DCN antibody might not work well in mouse. However, in the testis of adult transgenic AROM+ mice, which represent a recently found model for male infertility with testicular fibrosis and more connective tissue (135-137), DCN expression was readily detected by immunohistochemistry and qRT-PCR. These results led to the assumption that the DCN antibody employed is not sensitive enough to detect small amounts of DCN.

Adult AROM+ males above the age of 2 - 3 months develop progressive age-dependent testicular fibrosis, inflammatory reactions and impaired spermatogenesis (135). This study revealed that these changes are correlated with high levels of testicular DCN. Accordingly, immunohistochemistry indicated strong DCN accumulation in the interstitial areas and to some degree also in the peritubular areas of AROM+ mice, a result in line with the general changes in infertile men. The peritubular region in human consists of several layers of peritubular cells whereas mice only possess one cell layer. Therefore fibrosis in the mouse testis occurs mainly in the interstitium and less in the peritubular region. Younger AROM+ mice, below the age of three months, were not included within this study because they are sexually immature and their testis resembles age-matched normal mouse testis.

DCN expression during gonadal development is not explored, and in mice it may not play a role (158, 159). In contrast, human and monkey testes show robust DCN expression. Since studies on DCN expression during ontogeny of human testis are not possible, it was investigated in postnatal testicular development of rhesus monkeys. The rhesus monkey, as a non-human primate possesses several layers of testicular peritubular cells, similar to men. Thus it appears to be an appropriate model for studies on the peritubular region. Immunohistochemistry using samples of monkeys of different ages, indicated that DCN expression in rhesus monkey testis decreases with sexual maturity. The degree of DCN staining of testicular connective tissue in the prepubertal monkey gonad is more pronounced than in the adult. What causes this physiological reduction of DCN during maturation remains to be shown. However, DCN is clearly inversely related to the degree of the activity of the testis, namely spermatogenesis, during testicular development.

To summarize this point, the ECM proteoglycan DCN was found in the normal human and the non-human primate testis. In mice DCN appears of low abundance, however in infertile AROM+ mice it becomes strongly expressed. Thus in infertile men and mice, the observed elevated DCN levels

correlate well with physiological or pathological states of infertility, irrespective of their cause. Furthermore, the present results of immunohistochemistry studies using testicular samples of rhesus monkeys of different ages indicated high DCN levels in the prepubertal, quiescent testes which are markedly decreased during sexual maturation and subsequently remained low even in the testes of old healthy animals. High levels of testicular DCN are inversely related to testicular functionality spermatogenesis, in health and disease.

5.2 Steroid hormones do not influence DCN expression in HTPCs and HTPC-Fs

Changes of testicular DCN expression during puberty may be related to the actions of steroid hormones, such as testosterone and estradiol, which are essential for normal testicular development as well as for spermatogenesis and thus male reproductive health. For instance, receptors for testosterone, ARs, are expressed in several testicular cell types, including peritubular cells, but which cell type mediates the specific androgen control of spermatogenesis remains contentious (19). Within the present study testosterone action on DCN levels was examined in normal peritubular cells and cells stemming from fibrotic testis. However, testosterone addition was not able to alter DCN mRNA levels in HTPCs and HTPC-Fs, at least under the experimental conditions used. This result leads to the assumption, that increased DCN levels in fibrotic testis and male sub- or infertility are not linked via testosterone. Further, this result goes in parallel with an other study, in which androgen action on proteoglycan biosynthesis in human vascular smooth muscle cells was tested (160). Treatment of vascular smooth muscle cells with testosterone at a concentration of 100 nM, the same concentration that was used on HTPC/HTPC-Fs, did not alter total DCN levels, but lead to increased [^{35}S]sulfate incorporation into proteoglycans and increased GAG chain length, a process that results to a higher binding capacity to low density lipoproteins. By forming lipoprotein-proteoglycan complexes atherogenic low density lipoprotein accumulates and leads to cellular chemotaxis, including smooth muscle cell migration and monocyte adhesion. This possibility remains to be studied in HTPC/-Fs.

Estradiol plays an important role in various physiological events, which are mediated via its nuclear estrogen receptors, ER-α and ER-β. 17β -estradiol, which was used in the present study, can interact with both receptors (203). The regulation of estradiol/testosterone ratio is important for male reproductive health. For instance, estradiol/testosterone levels are strongly elevated in male AROM+ mice which suffer from deranged spermatogenesis and infertility. Both human cellular models, employed in this study, express ER-α (unpublished data), but with regard to DCN 17β-estradiol, used at two concentrations, showed no influence on DCN regulation in HTPCs as well as in HTPC-Fs after 6 h and 24 h. It is known from the literature that estrogens are able to regulate DCN synthesis in several tissues. Reports of the ovariectomized mouse uterus indicated a DCN downregulation by

estradiol after 6 h and 12 h (161). In addition, in human endometrium, where DCN is strongly expressed in the stromal areas, it is upregulated by estrogen (162). In sheep studies, estradiol was found to significantly upregulate DCN mRNA expression and in this manner, may act as a potential stimulator responsible for the increased DCN in the myometrium during parturition, whereas progesterone treatment had no effect on DCN mRNA abundance (163).

To conclude this point, DCN mRNA expression was not altered by testosterone and estradiol, at least under the experimental conditions used within this study, but additional experiments employing different concentrations and time periods are required to fully exclude steroid hormone actions on DCN expression in HTPCs and HTPC-Fs. In case of androgens, the more potent androgen dihydrotestosterone, which has a three timer higher affinity for AR than testosterone, should be investigated with regard to DCN expression.

5.3 DCN expression in HTPCs and HTPC-Fs is not affected by forskolin and prostaglandin 15dPGJ2

Forskolin is a known stimulator of intracellular cAMP signaling in many tissues. The ability of cAMP to regulate ECM gene expression in cultured rat chondrocytes has been shown previously (164). In the present study this possibility was tested with regard to DCN expression in HTPCs and HTPC-Fs. QRT-PCR results indicated that forskolin after a stimulation period of 4 h does not change DCN synthesis in HTPCs and in HTPC-Fs. This result is in line with reported data of bovine chondrocytes in which forskolin significantly increased aggrecan proteoglycan synthesis after 1 h and 5 h, but had no influence on DCN and collagen type I mRNA levels (165).

Previous studies using HTPCs reported that metabolic activity was not affected by prostaglandins PGE_2, $PGF_2\alpha$, PGD_2 or PGJ_2, but was stimulated by 15dPGJ2 after two days (134). Furthermore, the study showed that HTPC treatment with 15dPGJ2 for seven days reduced smooth muscle cell markers, but not fibroblast markers. 15dPGJ2 influences the smooth muscle cell phenotype and the contractility of human peritubular cells via reactive oxygen species. For this reason, in the present study was examined whether 15dPGJ2 is able to alter DCN expression in HTPCs or HTPC-Fs, thus changing them from a contractile to a secretory phenotype. The same culture conditions, stimulation periods and concentrations, as have been reported by Schell *et al*. (2010), were used to treat HTPCs and HTPC-Fs (134). Results indicated that, under the experimental conditions used, 15dPGJ2 did not influence DCN mRNA expression in both cell types, thus 15dPGJ2 via reactive oxygen species are not linked to DCN expression in peritubular cells. This result correlates with results of a previously reported study, in which a prostaglandin, namely PGE_2, in equine tendon fibroblasts leads to increased gene expression of collagen type I, but not of DCN levels (166).

5.4 Immune cell products stimulate DCN expression in fibrotic testis

The present study indicated that DCN production and secretion differs quantitatively in HTPCs and HTPC-Fs. The second distinct difference between both cell types, which was found in the present study, is their response to immune cell products. The major mast cell product, the protease tryptase, and a peptide agonist to the tryptase receptor (PAR-2), SLIGKV, increased DCN mRNA and protein levels in HTPC-Fs, but not in HTPCs. However, both cell types possess functional PAR-2 (132) and were shown within this study to responde in a similar manner to tryptase and SLIGKV with transient elevations of intracellular Ca^{2+}. Regulation of DCN via PAR-2 activation, as observed in HTPC-Fs has not been reported yet, but the activation of a related receptor, PAR-1, by thrombin, has recently been revealed to result in increased DCN expression in vascular smooth muscle cells and to contribute to the development of atherosclerosis (167).

The cytokine TNF-α is a product of macrophages and mast cells in mouse and human testes and is significantly increased in AROM+ mice and in infertile men (58, 137). In the present study the involvement of TNF-α in the regulation of DCN using HTPCs and HTPC-Fs was investigated. TNF-α was able to further stimulate the already increased DCN mRNA and secreted protein levels in HTPC-Fs. Interestingly, in a recent study using a mouse model it was reported that DCN in turn enhances the release of cytokines like TNF-α by macrophages (168). Whether DCN produced by HTPC/HTPC-Fs can stimulate TNF-α production in macrophages in the human testis can only be speculated at that time and remains to be studied.

The regulation of *DCN* gene expression has been shown to occur commonly via different cytokines, including TNF-α, expressed by inflammatory cells. For instance, IL-1 and IL-4 can induce DCN transcription in human fibroblasts (112) and TGF-β has been described as a potent regulator of DCN expression in several tissues (169, 170). In general, the regulation of DCN synthesis by cytokines is not well understood. For instance, TGF-β can stimulate or inhibit DCN expression, depending on the cell type and culture conditions (170, 171). With regard to TNF-α, the results of the present investigations indicating stimulation of DCN expression in HTPC-Fs upon stimulation with TNF-α, are in line with reported effects of TNF-α on DCN in isolated human chondrocytes (172). In contrast, in human dermal fibroblast cultures DCN expression decreased after TNF-α addition (110). Additionally, investigations in human lung fibroblasts showed an increase in total proteoglycan production upon stimulation with TNF-α, but especially DCN was downregulated (173). These different findings show that TNF-α influence on DCN expression varies from cell type to cell type and may be dependent on culture conditions, as well.

Previous studies have dealt with regulatory actions of tryptase and the pro-inflammatory cytokine TNF-α in human peritubular cells. For instance, nerve growth factor (NGF), a secretory product of HTPCs, is upregulated by TNF-α in a dose- and time-dependent manner ((133) and Spinnler,

unpublished). Furthermore, the ability of TNF-α to induce the expression inflammatory markers, such as MCP-1, IL-6 and cyclooxygenase-2, has been shown in HTPCs (133). HTPC-Fs have not been investigated at that time. The response of HTPCs and HTPC-Fs to TNF-α, respectively tryptase, has been investigated with regard to GDNF expression (132). It has been found that neither HTPCs nor HTPC-Fs responded to one of the substances by altered production of GDNF. Therefore the increased sensitivity of DCN production in HTPC-Fs to tryptase and TNF-α is a distinct signature of these cells derived from patients with existing fertility problems.

The reason for these differences in tryptase, respectively TNF-α, responses of HTPC and HTPC-Fs may be related to the altered microenvironment during testicular fibrosis, which includes the increased occurrence of tryptase and TNF-α producing mast cell and macrophages in the fibrotically remodeled peritubular walls (54, 58). Such a link is supported by a recently observed loss of smooth muscle cell markers in peritubular cells of sub- and infertile men (134). Cultured HTPCs and HTPC-Fs respond in different ways to immune cell products and thus appear to mimic the *in vivo* situations, indicating that these cells are excellent models for the study of the properties of peritubular cells from testes of normal and infertility patients.

It has been reported that TNF-α preferentially uses the core protein of DCN as specific binding site (174), but it also binds to a certain degree to dermatan sulphate chains of DCN molecules. The mobility of these chains depends on the content of iduronic acid. Different tissues possess different levels of iduronic acid and Tufvesson and Westergren-Thorsson (2002) (174) therefore hypothesize that this causes a stronger DCN affinity for TNF-α in some tissues. Whether iduronic acid levels in the testis of infertile men differ from those in normal testis is not known, but cannot be completely excluded and could be a reason for different reactions of HTPCs and HTPC-Fs in DCN production and secretion upon TNF-α treatment.

In several pathological processes such as asthma (175) and systemic sclerosis (176), TNF-α is known to be upregulated during early stages of inflammation, while DCN is downregulated. However, in progressive inflammation, when fibrotic lesions are formed, an upregulation has been observed. These findings lead to the assumption that increased TNF-α levels may induce DCN production during later stages of inflammation when fibrotic remodeling occurs (176). This may also be the case in human testis, where a TNF-α-induced DCN production in HTPC-Fs correlates with fibrotically remodeled testis and impaired spermatogenesis, while DCN was not altered by TNF-α in peritubular cells of healthy human testis.

To summarize this point, tubular fibrosis is based on thickening of the peritubular region due to increased ECM production (57, 177). The present study shows that peritubular cells are involved in this process. Numbers of testicular mast cells and macrophages are increased in men suffering from infertility (54, 58, 150, 177). The present results therefore link immune cells, via their products

tryptase and TNF-α, to the increased production of the ECM component, DCN, during fibrotic conditions and impaired spermatogenesis.

5.5 Mouse testicular fibroblasts

A further aim of this study was to examine DCN expression and regulation in the testes of normal mice and infertile AROM+ males with fibrotically altered testes. Since TNF-α levels are elevated in AROM+ males, the regulation of DCN expression by TNF-α should be investigated in mouse fibroblasts.

It was attempted to isolate peritubular cells of the testes of normal and AROM+ mice, using the same explant method as described for human cells. In some cultured samples myofibroblast-like cells that were immunocytochemically stained positive for SMA, were observed. However, cell yields were not sufficient and cells could not be propagated using the same methods as for HTPCs and HTPC-Fs. This might be due to differences between the mouse and the human system. The number of cell layers surrounding the seminiferous tubule is highly species-specific and rodents, in contrast to humans who have several, possess only one layer of peritubular cells. This might be a reason why results of examinations performed on rodents could not be completely assigned to the human system and for investigating how the particular constituents of the peritubular region are involved in the fibrotic thickening in the testis, the mouse is not the best model (145, 178, 179).

In immunohistochemical experiments DCN deposits in AROM+ males were detected in fibrotically remodeled interstitial regions rather than in peritubular cells. Therefore in subsequent mouse testicular cell culture studies, interstitial fibroblasts were isolated. Although interstitial fibroblasts could be successfully isolated, cell numbers were not sufficient for additional studies. Cell culture conditions have to be optimized to successfully cultivate mouse testicular fibroblasts in a sufficient number in future experiments.

At least experiments with mouse fibroblasts of a standard cell line, namely NIH/3T3 cells, revealed that DCN mRNA expression and protein levels are upregulated by TNF-α after 24 h respectively 72 h. Because of these results it is worth to further investigate TNF-α action on DCN expression in the mouse testis.

5.6 Expression of growth factor receptors in the human testis, known to be partners of DCN

In the human testes DCN may be responsible for the assembly and/or protection of the ECM (121, 180, 181). DCN action via a distinct "DCN receptor" has not been reported. Previous studies demonstrated that DCN is catabolized by receptor-mediated uptake and subsequent intralysosomal degradation (182-184). Previously, two endosomal proteins of 51 kDa and 26 kDa have described to interact with DCN core protein and to mediate DCN endocytosis. Endocytosis of SLRPs may also be mediated by additional receptors, namely the endocytic mannose receptor, EGFR and IGF-1R (185). Since a own receptor for DCN downstream signaling, does not exist, the investigations of the present study concentrated on DCN interference with growth factor receptors, namely EGFR and PDGFR. Roles of DCN may include a storage function for growth factors and a role as a ligand for growth factor receptors.

As it is not possible to test any of these assumed functions of DCN in the human testis in health and disease *in vivo,* the examination of DCN interactions with growth factors/receptors expressed in primary cells (HTPC/HTPC-Fs) appear appropriate. In other cellular systems, DCN has been reported to interfere with signaling of several growth factors. One of the best-investigated growth factor receptor signaling systems that is affected by DCN is EGF and its receptos (121, 125, 126, 128). As previous studies in squamous carcinoma cells and tumor xenografts indicated, the proteoglycan inhibits EGFR by down-regulating its tyrosine kinase activity. DCN can act as a substrate, binding directly the EGFR kinase, subsequently inducing receptor dimerization, internalization and degradation (125, 126). In addition to EGF, PDGF signaling has been shown to be affected by DCN (117). In vascular smooth muscles cells, DCN binding to the ligand, namely PDGF, and the subsequent inhibition of PDGF-stimulated phosphorylation of PDGFR was demonstrated. Furthermore, in normal cells such as endothelial and renal cells, DCN affects different pathways via binding to IGF-1R, resulting in phosphorylation and activation, followed by receptor down-regulation (121-123, 186). In addition, it has been reported that VEGF (123) and HGF signaling (124) are further systems that were reported to be affected by DCN. The proteoglycan is a ligand to the respective RTK. In the present study receptors of the EGFR family (EGFR, ErbB2, ErbB3 and ErbB4), PDGFRs (PDGFR-α and PDGFR-β), IGF-1R, VEGFR and HGFR were examined and found to be present at mRNA level in HTPCs, as well as in HTPC-Fs. Nevertheless, studies performed concentrated especially on EGF/EGFRs and PDGF/PDGFRs as potential partners for DCN for several reasons. Firstly, EGFRs have been reported to be expressed in peritubular cells of the adult human testis (26). Expression of PDGFR in testicular peritubular cells has been shown in animal studies and the present study provides evidence for expression in the wall of seminiferous tubules in humans, as well. Secondly, a number of studies indicate that EGF and PDGF have distinct and important roles in the regulation of smooth muscle cells (117, 187-189), which may include testicular smooth muscle-like

peritubular cells (134). In fact several experiments performed within this study indicated a strong mitogenic role of EGF and PDGF in HTPCs, as well as in HTPC-Fs.

While previous reports describe EGFR expression in peritubular myoid cells (26), the expression of PDGFR-α and PDGFR-β at this site of adult human testis is contentious. In a previous study, employing immunohistochemistry using testes samples from healthy adult men, no expression of PDGFRs in the peritubular regions has been found (33). Yet during development the receptors are present and PDGF is considered as an important regulator for peritubular cells (29, 117, 189, 190). Interestingly, in rat studies, it was demonstrated that peritubular cells of the adult males cease to express PDGFRs (191, 192). This phenomenon has been attributed to the shift from a synthetic to a contractile phenotype of peritubular cells during morphological and functional maturation of the testis (193). With regard to the present results, the attempt to localize EGFR and PDGFR proteins in the human peritubular wall by immunohistochemistry using commercial anti-sera failed, but laser microdissection and subsequent RT-PCR studies identified PDGFRs in the peritubular region, at least in biopsies from MA patients. In infertile men peritubular myoid cells may change their phenotype from a contractile to a secreting cell type. Whether expression of PDGFRs in adult human peritubular cells *in vivo* may occur again during initiation and progression of sub- or infertility is a point that requires additional studies.

5.7 DCN can interact with EGF/EGFR and PDGF/PDGFR signaling in the human testis

The present study found that exogenous DCN acutely induces alterations of intracellular Ca^{2+} levels in HTPC/-Fs, which occurred within seconds and lasted only for seconds. This observation is in line with findings in human squamous carcinoma cells (120) and hints to activation of growth factor receptors expressed by these cells. Accordingly, in other cellular systems DCN can act as a ligand to growth factor receptors, especially EGFRs, and can acutely activate them (121, 123-125). Therefore this possibility was examined for human testis by using HTPCs and HTPC-Fs.

The concentration of DCN required for this action was higher than expected e.g. from the dissociation constant of DCN for EGFR (~ 87 nM) (98). However HTPCs and HTPC-Fs constantly secrete DCN in concentrations of approximately 0.1-1 µg/ml, which may thus constantly downregulate growth factor receptors. Therefore higher concentrations of at least 10 µg/ml are required in the experimental setting. With regard to the literature, even a lower DCN concentration was used to treat HTPCs and HTPC-Fs within the present investigations, than for studies in rabbit aortic smooth muscle cells where 30 µg/ml have been used (117). In addition, for measurements of intracellular Ca^{2+} levels, freshly trypsinized (12 h before) HTPCs and HTPC-Fs were used in each experiment to minimize a high DCN level caused by their own secretion. Interestingly, if cells were cultured for longer time periods (about

4 - 5 days), DCN induced Ca^{2+} signals were not observed. In support of the assumption that DCN downregulates growth factor signaling, pretreatment of freshly trypsinized HTPC/-Fs with exogenous DCN for 24 h abolished the ability of DCN, EGF and PDGF but not of histamine (55), to elevate intracellular Ca^{2+} levels. This result is in line with observations in carcinoma cells, in which DCN markedly attenuates the mobilization of intracellular Ca^{2+} stores, a key pathway in EGFR- and PDGFR-mediated signaling (32, 126).

Interactions of DCN with growth factors or activation of their RTKs have not been studied in HTPC/HTPC-Fs yet, but transient elevation of intracellular Ca^{2+} evoked by DCN, in a similar way as by EGF and PDGF, led to the suggestion that DCN interferes with testicular EGFR and PDGFR signaling. To study the mechanisms of DCN action and test this assumption an analysis of phosphorylation of growth factor receptor was performed. As expected (125), DCN directly interferes with EGFRs and causes phosphorylation of EGFR in HTPCs and HTPC-Fs, a result that was found in an initial screening for RTK phosphorylation using a commercial protein array. Western blot experiments confirmed these data. Furthermore a strong phosphorylation of EGFR became evident in a positive control, in which EGF was used for cell treatment. In contrast to EGFR, initial protein array suggested a very low phosphorylation of PDGFR-β by DCN. In subsequent Western blot experiments a DCN induced phosphorylation of PDGFR-β was not observed, but a strong phosphorylation of the receptor by PDGF-BB, which was used as a positive control because it is known to bind all PDGFR isoforms and dimerizes α- and β-receptors into different configurations (PDGFR-αα, -αβ,-ββ) (29), became evident. This result is in line with the apparent ability of DCN to interfere with the ligand rather than to affect phosphorylation of this receptor (117, 194). Screening for RTK phosphorylation in HTPCs indicates furthermore, that DCN may be a ligand for HGFR, while VEGR and IGF-1R, at least under the experimental conditions used, may not be affected by DCN. A final conclusion cannot be drawn however, because the binding of DCN occurs with different affinities to different receptors, and thus both expression patterns of growth factor receptors and the concentrations of available DCN are of importance (98).

Less is known about the function of HGF within the human testis, but evidence is emerging that it may regulate somatic cell function, including Leydig cell steroidogenesis. Changes in the cellular origin of HGF and c-met during testicular development suggest that HGF may contribute to regulate testicular morphogenesis and differentiation (195). HGF/HGFR signaling and DCN interference with this signaling system in HTPC and HTPC-Fs represents an interesting topic, that remains to be studied.

5.8 Consequences of DCN interference with growth factor signaling

In the present study special emphasis was put on the investigation of the consequences of the interference of DCN with EGF/EGFR and PDGF/PDGFR systems in HTPCs and HTPC-Fs. Results of several experiments measuring caspase-3/7 activity, ATP levels and cell proliferation indicated that in an experimental situation chronic actions of DCN might unfold only when growth factors are present. Results of DAPI, CASY, ATP and caspase-3/7 measurements indicated that DCN addition alone exerted no effect on mitosis and viability of the HTPCs and HTPC-Fs. These results are in line with e.g. studies in human airway smooth muscle cells, in which exogenous DCN affected neither cell proliferation, nor apoptosis (190). This observed lack of DCN action after 24 h also indicates that an initial activation, evidenced by increased Ca^{2+} or phosphorylation of growth factor receptors, is followed by a DCN induced down-regulation of growth factor receptor signaling (117, 125, 126, 194).

In previous studies, EGF and PDGF were shown to stimulate processes such as cell proliferation, differentiation and migration (29, 117, 151). In the present investigations EGF and PDGF evoked strong proliferative responses in HTPC and HTPC-Fs. These effects were observed in DAPI experiments after 24 h but not at earlier times (6 h or 18 h). Cellular ATP levels and mitotic events were significantly increased after 24 h EGF or PDGF-BB treatment. Increased cell numbers were found after four days of stimulation with EGF or PDGF. Importantly, the addition of DCN at the same time as the growth factor, significantly reduced these growth factor actions after 24 h or four days, results that clearly indicate that DCN is a factor that when present is able to interfere with growth factor signaling and actions. These finding are in accordance with previous reported animal study results. Pretreatment of rabbit aortic smooth muscle cells with DCN significantly inhibited PDGF-stimulated cell migration and proliferation (117).

It has been previously reported that testicular peritubular cells of the rat, when chronically stimulated with PDGF, undergo cellular hypertrophy and produce increased levels of smooth muscle cells markers, e.g. SMA (151, 191). Peritubular smooth muscle cells from the rat testis in primary serum-free cultures undergo contraction and subsequent hypertrophy in response to PDGF-BB (134, 151). In the human cellular model, investigated in the present study, PDGF-BB treatment did not alter the cell size of HTPCs or HTPC-Fs. This might be due to different culture conditions, but also the distinct differences between the human and the animal model may be responsible.

PDGF-BB treatment did not lead to hypertrophy, but resulted in elevations of SMA in HTPCs and HTPC-Fs, a well-known differentiation marker of myofibroblasts (196). In both cell types SMA mRNA levels and cell proliferation were found to be increased, indicating the important role of PDGF for differential processes in human peritubular cells. Interestingly, the PDGF induced elevation of SMA level could be blocked by DCN. DCN alone did not affect SMA levels in HTPCs and HTPC-Fs after four days. A recent report about human myofibroblast cell lines indicated that increased DCN levels were accompanied by suppression of SMA expression after six days, whereas knock down of

DCN expression lead to increased expression of SMA (196). These findings are in contrast to results in the present study and may be due to differences in the cellular systems, but possibly DCN has the same effect on SMA expression in HTPC/HTPC-Fs after six days, a fact that remains to be studied.

The inhibitory effect of the proteoglycan on EGF and PDGF-stimulated HTPC/-Fs functions was not due to cell apoptosis. These observations are in line with a study performed by Nili *et al.* (2003) (117), which demonstrated also no evidence of active caspase-3 in DCN-treated rabbit aortic smooth muscle cells. In contrast, in carcinoma cells studies DCN was reported to inhibit cancer growth and metabolism by enhancing apoptosis via caspase-3 activation and reducing the mitotic index, two events that have been associated with the suppression of EGFR signaling (197). These differences may be due to the distinct microenvironment in which carcinoma and HTPC/-Fs occur.

In view of the mechanism how DCN mediates its inhibitory effects on EGFR and PDGFR signaling in HTPCs and HTPC-Fs, the phosphorylation experiments of the present study revealed that in case of EGFR, DCN directly interacts with this RTK and thus may block EGF binding to its receptor. With regard to PDGFR signaling in human peritubular cells, DCN does not interact with the RTK, but may bind directly its ligand and thus regulate its availability to the receptor.

In addition, it is worth mentioning that the present investigation revealed DCN staining also in the interstitial compartment of the human testis and that several growth factor receptors have been described in Leydig cells (33, 192). Thus, the ability of DCN to interfere with growth factor actions in the human testis may extend to Leydig cells and others, as a well.

The possible regulation and signaling pathways of testicular DCN, investigated in the present study, are summarized in Figure 5-1.

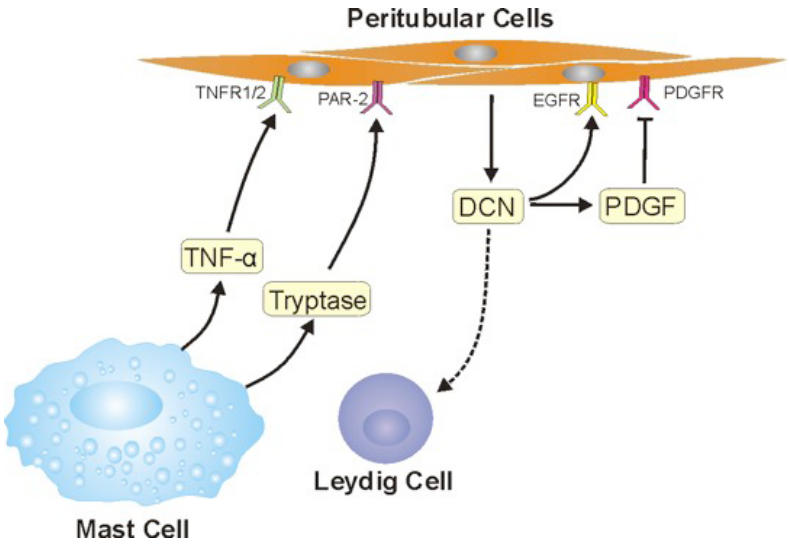

Figure 5-1: Overview of DCN regulation and signaling in the human testis. Human peritubular cells express receptors for TNF-α (TNFR-1/2) and tryptase (PAR-2). Both immune cell products lead to increased DCN production and secretion in HTPC-Fs, but not in HTPCs. DCN can interfere with EGF and PDGF signaling in HTPC/-Fs. Increased DCN levels in infertile men, which are a consequence of actions of immune cell derived TNF-α and tryptase, may imbalance paracrine signaling in the human testis.

5.9 Actions of imatinib mesylate in HTPCs

The present study revealed that DCN is emerging as an endogenous ligand/antagonist for growth factor signaling in peritubular cells of the human testis. In addition the effect of an exogenous ligand for growth factor receptors, namely the drug imatinib mesylate, in the normal human testis was investigated using HTPCs. Imatinib is a small molecular analog of ATP that inhibits the Abelson kinase, PDGFR-α, PDGFR-β and c-kit tyrosine kinases. This drug is used to treat patients with chronic myeloid leukemia (142, 144, 198, 199).

Previous studies demonstrated that imatinib, through its ability to inhibit PDGFR signaling, interferes with development of Leydig and peritubular cells during postnatal testicular ontogeny in the rat (145). Within the present investigations stimulations of HTPCs with different concentrations of imatinib for 24 h indicated a dose-dependent decrease of cellular viability of adult peritubular cells in the human testis. However, concentrations of 10 µM or lower did not disturb viability of HTPCs, but were able to block PDGF induced proliferative and mitogenic actions, when both substances were added at the same time.

Interestingly, first clinical case studies in patients suffering from systemic sclerosis demonstrated that imatinib, by its ability to block the pro-fibrotic Abelson kinase and PDGFR, reduces synthesis and accumulation of ECM in lesional skin (200, 201). The same work group found the reduction of established skin fibrosis in an animal model (202). The ability of imatinib to possibly reduce fibrosis in the testis remains to be examined.

6. SUMMARY

Testicular peritubular cells and the ECM of the walls of the seminiferous tubules were barely investigated. The aim of the present study was to characterize the wall of the tubules with regard to the ECM proteoglycan DCN. In addition the regulation and function of DCN were studied.

The expression of this proteoglycan during states of infertility and development was examined in human, rhesus monkey and rodent testes. While DCN mRNA was readily found in the testis of all examined species, DCN protein was only detected in peritubular and interstitial areas of adult human and monkey testes. In human, immunohistochemistry indicated that this proteoglycan, which is normally produced in low levels by testicular peritubular cells, is strongly increased in testicular biopsies of MA, GA and SCO syndrome patients. Furthermore DCN was almost undetectable in adult rodents, but was highly expressed in the testes of infertile, aromatase-overexpressing transgenic mice (AROM+). Immunohistochemical staining of testicular samples of rhesus monkeys of different ages indicated that levels and sites of expression of testicular DCN change also during postnatal maturation. In the non-human primate DCN is associated with the abundant connective tissue of the interstitial areas in the postnatal through prepubertal phases. In adult and old monkeys the DCN pattern was similar to the one in normal human testes. Thus levels of DCN inversely correlate with testicular functionality.

Impaired spermatogenesis in men is frequently accompanied by accumulation of tryptase-positive mast cells in the testis. One aim of this study was the investigation of testicular DCN expression, regulation and actions using cultured primary human testicular peritubular cells (HTPCs), which stem from testes with normal spermatogenesis and corresponding cells isolated from men suffering from impaired spermatogenesis and existing testicular fibrosis (HTPC-Fs). QRT-PCRs, Western blotting and ELISA measurements revealed that HTPC-Fs synthesize and secrete higher quantities of DCN than HTPCs, a finding, mirroring the situation *in vivo*. In contrast to HTPCs, HTPC-Fs also responded to immune cell products, namely mast cell tryptase and TNF-α, by further increased DCN production and secretion. The data indicate that the increased amount of DCN, found in human male infertility is a consequence of actions of immune cell-derived tryptase and TNF-α.

As DCN is known from other tissues to interfere with growth factor signaling, this possibility was investigated in HTPCs and HTPC-Fs. RT-PCR studies revealed that both cell types express receptor tyrosine kinases, namely the EGFR family (EGFR, ErbB2, ErbB3, ErbB4), PDGFRs (PDGFR-α and PDGFR-β), VEGFR, IGF-1R and HGFR which are known targets for DCN action. The acute abilities of DCN to transiently increase intracellular Ca^{2+} levels in both cell types, lead to the assumption that DCN might act via one or more of these growth factor receptors. Measurements of ATP levels, cell numbers and mitotic events after DAPI staining revealed strong mitogenic reponses in HTPC/-Fs upon stimulation with human recombinant EGF or PDGF. These actions could be blocked in the presence of DCN. Importantly, DCN alone did not influence viability and mitosis in both cell types.

Phosphorylation studies revealed a DCN caused phosphorylation of EGFR, but not of PDGFR-β. Thus, DCN is a factor able to influence growth factor signaling in human testicular peritubular cells. The general or focal deposits of DCN may imbalance paracrine signaling of the testis in health and disease.

In conclusion, the results of this study using human testicular cells from normal and sub/-infertile men, provide insights into the regulation and the roles of DCN as a factor involved in the paracrine signaling in the testis. In the testis of men suffering from infertility immune cell numbers are increased and via their products TNF-α and tryptase can act as regulators of DCN production by peritubular cells. Hence, the results indicate that the functions of testicular MCs may be intrinsically linked to changes of the testis of men with impaired spermatogenesis.

Furthermore, the data indicate that in testes of men with deranged spermatogenesis, the typical fibrotic changes include increased amounts of DCN, which may consequently imbalance testicular growth factor signaling via direct actions or by serving as a reservoir of growth factors. Although increased levels of DCN in HTPC-Fs were observed, no difference between HTPCs and HTPC-Fs with regard to Ca^{2+} increase, mitotic activity and phosphorylation of EGFR and PDGFR-β could be detected. Despite this, the possibility that increased DCN amounts upset the balance of normal testicular function, including growth factor actions, cannot be excluded.

7. ZUSAMMENFASSUNG

Testikuläre peritubuläre Zellen und die ECM in der Wand der Tubuli seminiferi wurden bisher wenig untersucht. Aus diesem Grund war das Ziel der vorliegenden Studie die Charakterisierung der Tubuliwand in Bezug auf DCN, ein Proteoglykan der ECM. Des Weiteren wurden die Regulation und Funktion von DCN untersucht.

Die Expression dieses Proteoglykans bei Infertilität und während der Entwicklung wurde im humanen Hoden und im Hoden von Rhesusaffen und Nagetieren untersucht. Obwohl DCN mRNA im Hoden aller untersuchten Spezies gefunden wurde, konnte das DCN Protein nur in pertitubulären und interstitiellen Bereichen im Hoden erwachsener Menschen und Affen detektiert werden. Beim Menschen ließen immunhistochemische Methoden erkennen, dass dieses Proteoglykan, das normalerweise in kleinen Mengen von testikulären, peritubulären Zellen produziert wird, in testikulären Biopsien von Patienten mit gemischter Atrophie, Keimzellarrest und Sertoli-cell-only-Syndrom vermehrt vorkommt. Darüber hinaus war DCN in adulten Nagetieren fast undetektierbar, aber im Hoden infertiler, Aromatase-überexprimierender, transgener Mäuse (AROM+) war es stark exprimiert. Immunhistochemische Färbung von testikulären Proben von Rhesusaffen verschiedenen Alters zeigte, dass die Mengen und Orte testikulärer DCN Expression auch während der postnatalen Entwicklung variieren. Im nicht-humanen Primaten ist DCN, in der postnatalen und durch die präpubertäre Phase hindurch, mit dem mächtigen Bindegewebe der interstitiellen Regionen assoziiert. Das DCN Muster im Hoden erwachsener und älterer Affen war dem im normalen humanen Hoden ähnlich. Demzufolge korrelieren die DCN Mengen invers mit der Funktionalität des Hodens.

Die beeinträchtigte Spermatogenese bei Männern geht oft mit der Anhäufung von Tryptase-positiven Mastzellen im Hoden einher. Ein Ziel dieser Studie war die Untersuchung der testikulären DCN-Expression, -Regulation und -Wirkung, an kultivierten primären humanen testikulären peritubulären Zellen (HTPCs), die von Hoden mit normaler Spermatogenese stammen und entsprechenden Zellen, die von Männern, die unter gestörter Spermatogenese und testikulärer Fibrose leiden, isoliert wurden (HTPC-Fs).

QRT-PCRs, Western blots und ELISA Messungen zeigten, dass HTPC-Fs mehr DCN synthetisieren und sezernieren als HTPCs, eine Entdeckung, die die Situation *in vivo* widerspiegelt. Im Gegensatz zu HTPCs, antworten HTPC-Fs auf die Produkte von Immunzellen, nämlich Mastzell-Tryptase und TNF-α, durch weitere DCN Produktion und Sekretion. Die Daten zeigen, dass die erhöhte DCN Menge, die bei humaner Infertilität gefunden wird, eine Konsequenz der Tryptase- und TNF-α-Wirkung ist.

Da aus Untersuchungen an anderen Geweben bekannt wurde, dass DCN mit Wachstumsfaktor-Signalwegen interagieren kann, wurde dies in HTPCs und HTPC-Fs untersucht. RT-PCR Studien zeigten, dass beide Zelltypen RTKs, nämlich EGFRs (EGFR, ErbB2, ErbB3, ErbB4), PDGFRs (PDGFR-α und PDGFR-β), VEGFR, IGF-1R und HGFR, die bekannte Ziele der DCN Wirkung sind,

besitzen. Die Fähigkeit von DCN kurzzeitig die Ca^{2+}-Spiegel in beiden Zelltypen zu erhöhen führte zu der Annahme, dass DCN möglicherweise über einen oder mehrere dieser Wachstumsfaktorrezeptoren wirkt. Durch Messungen des ATP Gehalts, der Zellzahl und der Mitosen nach DAPI Färbung wurden nach Stimulation mit humanen, rekombinanten EGF oder PDGF starke mitogene Antworten in HTPC/-Fs aufgedeckt. Diese Wirkungen konnten durch die Anwesenheit von DCN inhibiert werden. Von besonderer Wichtigkeit ist hierbei, dass DCN allein keinen Einfluss auf die Viabilität und die Mitose in beiden Zelltypen hatte. Phosphorylierungsstudien zeigten, dass DCN den EGFR, aber nicht den PDGFR-β, phosphoryliert. Demzufolge, ist DCN ein Faktor, der Wachstumsfaktor Signalwege in humanen testikulären Zellen beeinflussen kann. Die generellen oder fokalen DCN-Anhäufungen bringen möglicherweise die parakrine Signalübermittlung des Hodens aus dem Gleichgewicht.

Zusammenfassend geben die Ergbnisse dieser Untersuchungen an humanen testikulären Zellen von normalen und sub-/infertilen Männern Einblick in die Regulation und die Rolle von DCN als ein Faktor, der in parakrine Signalwege im Hoden involviert ist. Im Hoden von Männern die unter Infertilität leiden ist die Anzahl der Immunzellen erhöht, die über ihre Produkte, TNF-α and Tryptase, als Regulatoren der DCN Synthese in peritubulären Zellen dienen. Demzufolge zeigen die Ergebnisse, dass die Funktionen von testikulären Mastzellen tatsächlich mit Veränderungen im Hoden von Männern mit beeinträchtigter Spermatogenese in Verbindung stehen.

Ferner weisen die Daten darauf hin, dass im Hoden von Männern mit gestörter Spermatogenese, die typischen fibrotischen Veränderungen erhöhte Mengen an DCN enthalten. Dieses bringt möglicherweise direkt oder indem es als Speicher für Wachstumsfaktoren dient, das testikuläre Wachstumsfaktor-Signaling aus dem Gleichgewicht. Obwohl erhöhte DCN Mengen in HTPC-Fs beobachtet wurden, konnten keine Unterschiede zwischen HTPCs und HTPC-Fs im Hinblick auf die Erhöhung des intrazellulären Ca^{2+}-Spiegel, der Wirkung auf die Mitose und in der Phosphorylierung von EGFR und PDGFR-β aufgedeckt werden. Trotzdem kann die Möglichkeit, dass erhöhte DCN Mengen das Gleichgewicht normaler Hodenfunktion, einschließlich der Wachstumsfaktor-Signal-übertragung stören, nicht ausgeschlossen werden.

8. REFERENCES

1. **Brant WO, Myers JB, Carrell DT, Smith JF** 2011 Male athletic activities and their effects on semen and hormonal parameters. Phys Sportsmed 38:114-120

2. **Patel ZP, Niederberger CS** 2010 Male factor assessment in infertility. Med Clin North Am 95:223-234

3. **De Kretser D, Baker H** 1996 Human infertility: the male factor. In: Adashi EY, Rock JA, Rosenwaks Z eds. Reproductive endocrinology, surgery, and technology. Philadelphia: Lippincott-Raven; 2031-2062

4. **Feichtinger W** 1991 Environmental factors and fertility. Hum Reprod 6:1170-1175

5. **Agarwal A, Allamaneni SS** 2005 Sperm DNA damage assessment: a test whose time has come. Fertil Steril 84:850-853

6. **Baker H, Burger H, De Kretser DM, Hudson B** 1986 Relative incidence of etiologic disorders in male infertility. In: RJ S, RS S eds. Male reproductive dysfunction: diagnosis and management of hypogonadism, infertility and impotence. New York: Dekker; 341-372

7. **Malaga Correa YR, Ortiz Nunez DA, Hernandez Marin I, Tovar JM, Ayala Ruiz A** 2005 [Spermatogenesis arrest]. Ginecol Obstet Mex 73:500-508

8. **Sigg C, Hedinger C** 1981 Quantitative and ultrastructural study of germinal epithelium in testicular biopsies with "mixed atrophy". Andrologia 13:412-424

9. **Matsumoto AM** 1991 The testis and male sexual function. In: Wyngaarden JB, Smith LH, Bennett JC eds. Cecil textbook of medicine. 19th ed. Philadelphia: Saunders; 1333-1350

10. **Junqueira LCU, Caneiro J** 2005 Männliche Geschlechtsorgane. In: Gratzl M ed. Histologie. 6. Edition ed. Heidelberg: Springer Medizin Verlag Heidelberg

11. **Matsumoto AM** 1996 Spermatogenesis. In: Adashi EY, Rock JA, Rosenwaks Z eds. Reproductive endocrinology, surgery, and technology. Philadelphia: Lippincott-Raven; 359

12. **Kerr JB** 1992 Functional cytology of the human testis. Baillieres Clin Endocrinol Metab 6:235-250

13. **De Kretser DM, Kerr JB** 1988 The cytology of the testis. In: Knobil E, Neil J eds. The Physiology of Reproduction. New York: Raven Press; 837-932

14. **Maekawa M, Kamimura K, Nagano T** 1996 Peritubular myoid cells in the testis: their structure and function. Arch Histol Cytol 59:1-13

15. **Dufau ML, Khanum A, Winters CA, Tsai-Morris CH** 1987 Multistep regulation of Leydig cell function. J Steroid Biochem 27:343-350

16. **McLachlan RI, O'Donnell L, Meachem SJ, Stanton PG, de Kretser DM, Pratis K, Robertson DM** 2002 Identification of specific sites of hormonal regulation in spermatogenesis in rats, monkeys, and man. Recent Prog Horm Res 57:149-179

17. **Sharpe RM** 1994 Regulation of spermatogenesis. In: Knobil E, Neil J eds. The physiology of reproduction. 2nd ed. New York: Raven Press; 1363-1436

18. **Johnston DS, Russell LD, Friel PJ, Griswold MD** 2001 Murine germ cells do not require functional androgen receptors to complete spermatogenesis following spermatogonial stem cell transplantation. Endocrinology 142:2405-2408

19. **Welsh M, Saunders PT, Atanassova N, Sharpe RM, Smith LB** 2009 Androgen action via testicular peritubular myoid cells is essential for male fertility. FASEB J 23:4218-4230

20. **Jones ME, Boon WC, McInnes K, Maffei L, Carani C, Simpson ER** 2007 Recognizing rare disorders: aromatase deficiency. Nat Clin Pract Endocrinol Metab 3:414-421

21. **Lardone MC, Castillo P, Valdevenito R, Ebensperger M, Ronco AM, Pommer R, Piottante A, Castro A** 2009 P450-aromatase activity and expression in human testicular tissues with severe spermatogenic failure. Int J Androl 33:650-660

22. **Smith EP, Boyd J, Frank GR, Takahashi H, Cohen RM, Specker B, Williams TC, Lubahn DB, Korach KS** 1994 Estrogen resistance caused by a mutation in the estrogen-receptor gene in a man. N Engl J Med 331:1056-1061

23. **Huhtaniemi I, Toppari J** 1995 Endocrine, paracrine and autocrine regulation of testicular steroidogenesis. Adv Exp Med Biol 377:33-54

24. **Jegou B, Pineau C** 1995 Current aspects of autocrine and paracrine regulation of spermatogenesis. Adv Exp Med Biol 377:67-86

25. **Mather JP** 1984 Intratesticular Regulation: Evidence for autocrine and paracrine control of testicular function. In: Mather JP ed. Mammalian cell culture: The use of serum-free and hormone supplemented media. New York: Plenum Press; 164-197

26. **Nakazumi H, Sasano H, Maehara I, Orikasa S** 1996 Transforming growth factor-alpha, epidermal growth factor, and epidermal growth factor receptor in human testis obtained from biopsy and castration: immunohistochemical study. Tohoku J Exp Med 178:381-388

27. **Gill GN, Bertics PJ, Santon JB** 1987 Epidermal growth factor and its receptor. Mol Cell Endocrinol 51:169-186

28. **Yan YC, Sun YP, Zhang ML** 1998 Testis epidermal growth factor and spermatogenesis. Arch Androl 40:133-146

29. **Mariani S, Basciani S, Arizzi M, Spera G, Gnessi L** 2002 PDGF and the testis. Trends Endocrinol Metab 13:11-17

30. **Puglianiello A, Campagnolo L, Farini D, Cipollone D, Russo MA, Siracusa G** 2004 Expression and role of PDGF-BB and PDGFR-beta during testis morphogenesis in the mouse embryo. J Cell Sci 117:1151-1160

31. **Loveland KL, Hedger MP, Risbridger G, Herszfeld D, De Kretser DM** 1993 Identification of receptor tyrosine kinases in the rat testis. Mol Reprod Dev 36:440-447

32. **Gnessi L, Emidi A, Scarpa S, Palleschi S, Ragano-Caracciolo M, Silvestroni L, Modesti A, Spera G** 1993 Platelet-derived growth factor effects on purified testicular peritubular myoid cells: binding, cytosolic Ca2+ increase, mitogenic activity, and extracellular matrix production enhancement. Endocrinology 133:1880-1890

33. **Basciani S, Mariani S, Arizzi M, Ulisse S, Rucci N, Jannini EA, Della Rocca C, Manicone A, Carani C, Spera G, Gnessi L** 2002 Expression of platelet-derived growth factor-A (PDGF-A), PDGF-B, and PDGF receptor-alpha and -beta during human testicular development and disease. J Clin Endocrinol Metab 87:2310-2319

34. **Regaud C** 1901 Études sur la structure des tubes séminifères et sur la spermatogénèse chez les mammifères. Arch Anat Microsc 4:101-155

35. **Ross MH, Long IR** 1966 Contractile cells in human seminiferous tubules. Science 153:1271-1273

36. **Fawcett DW, Heidger PM, Leak LV** 1969 Lymph vascular system of the interstitial tissue of the testis as revealed by electron microscopy. J Reprod Fertil 19:109-119

37. **Cigorraga SB, Chemes H, Pellizzari E** 1994 Steroidogenic and morphogenic characteristics of human peritubular cells in culture. Biol Reprod 51:1193-1205

38. **Tung PS, Fritz IB** 1990 Characterization of rat testicular peritubular myoid cells in culture: alpha-smooth muscle isoactin is a specific differentiation marker. Biol Reprod 42:351-365

39. **Schlatt S, Weinbauer GF, Arslan M, Nieschlag E** 1993 Appearance of alpha-smooth muscle actin in peritubular cells of monkey testes is induced by androgens, modulated by follicle-stimulating hormone, and maintained after hormonal withdrawal. J Androl 14:340-350

40. **Virtanen I, Kallajoki M, Narvanen O, Paranko J, Thornell LE, Miettinen M, Lehto VP** 1986 Peritubular myoid cells of human and rat testis are smooth muscle cells that contain desmin-type intermediate filaments. Anat Rec 215:10-20

41. **Bustos-Obregon E** 1976 Ultrastructure and function of the lamina propria of mammalian seminiferous tubules. Andrologia 8:179-185

42. **Davidoff MS, Breucker H, Holstein AF, Seidl K** 1990 Cellular architecture of the lamina propria of human seminiferous tubules. Cell Tissue Res 262:253-261

43. **Skinner MK, Tung PS, Fritz IB** 1985 Cooperativity between Sertoli cells and testicular peritubular cells in the production and deposition of extracellular matrix components. J Cell Biol 100:1941-1947

44. **Skinner MK, Fritz IB** 1985 Testicular peritubular cells secrete a protein under androgen control that modulates Sertoli cell functions. Proc Natl Acad Sci U S A 82:114-118

45. **Skinner MK, Takacs K, Coffey RJ** 1989 Transforming growth factor-alpha gene expression and action in the seminiferous tubule: peritubular cell-Sertoli cell interactions. Endocrinology 124:845-854

46. **Skinner MK, Moses HL** 1989 Transforming growth factor beta gene expression and action in the seminiferous tubule: peritubular cell-Sertoli cell interactions. Mol Endocrinol 3:625-634

47. **Cailleau J, Vermeire S, Verhoeven G** 1990 Independent control of the production of insulin-like growth factor I and its binding protein by cultured testicular cells. Mol Cell Endocrinol 69:79-89

48. **de Winter JP, Vanderstichele HM, Verhoeven G, Timmerman MA, Wesseling JG, de Jong FH** 1994 Peritubular myoid cells from immature rat testes secrete activin-A and express activin receptor type II in vitro. Endocrinology 135:759-767

49. **Holstein AF, Maekawa M, Nagano T, Davidoff MS** 1996 Myofibroblasts in the lamina propria of human semi-niferous tubules are dynamic structures of heterogeneous phenotype. Arch Histol Cytol 59:109-125

50. **Gambichler T, Kreuter A, Skrygan M, Burkert B, Altmeyer P, Schieren G** 2009 Decorin is significantly overexpressed in nephrogenic systemic fibrosis. Am J Clin Pathol 132:139-143

51. **Kolb M, Margetts PJ, Sime PJ, Gauldie J** 2001 Proteoglycans decorin and biglycan differentially modulate TGF-beta-mediated fibrotic responses in the lung. Am J Physiol Lung Cell Mol Physiol 280:L1327-1334

52. **Kovalszky I, Nagy P, Szende B, Lapis K, Szalay F, Jeney A, Schaff Z** 1998 Experimental and human liver fibrogenesis. Scand J Gastroenterol Suppl 228:51-55

53. **Holstein AF, Roosen-Runge EC, Schirren C** 1988 Illustrated pathology of human spermatogenesis.: Grosse Verlag Berlin

54. **Meineke V, Frungieri MB, Jessberger B, Vogt H, Mayerhofer A** 2000 Human testicular mast cells contain tryptase: increased mast cell number and altered distribution in the testes of infertile men. Fertil Steril 74:239-244

55. **Albrecht M, Ramsch R, Kohn FM, Schwarzer JU, Mayerhofer A** 2006 Isolation and cultivation of human testicular peritubular cells: a new model for the investigation of fibrotic processes in the human testis and male infertility. J Clin Endocrinol Metab 91:1956-1960

56. **Agarwal S, Choudhury M, Banerjee A** 1987 Mast cells and idiopathic male infertility. Int J Fertil 32:283-286

57. **Apa DD, Cayan S, Polat A, Akbay E** 2002 Mast cells and fibrosis on testicular biopsies in male infertility. Arch Androl 48:337-344

58. **Frungieri MB, Calandra RS, Lustig L, Meineke V, Kohn FM, Vogt HJ, Mayerhofer A** 2002 Number, distribution pattern, and identification of macrophages in the testes of infertile men. Fertil Steril 78:298-306

59. **Gruber BL, Kew RR, Jelaska A, Marchese MJ, Garlick J, Ren S, Schwartz LB, Korn JH** 1997 Human mast cells activate fibroblasts: tryptase is a fibrogenic factor stimulating collagen messenger ribonucleic acid synthesis and fibroblast chemotaxis. J Immunol 158:2310-2317

60. **Maseki Y, Miyake K, Mitsuya H, Kitamura H, Yamada K** 1981 Mastocytosis occurring in the testes from patients with idiopathic male infertility. Fertil Steril 36:814-817

61. **Nagai T, Takaba H, Miyake K, Hirabayashi Y, Yamada K** 1992 Testicular mast cell heterogeneity in idiopathic male infertility. Fertil Steril 57:1331-1336

62. **Welter H, Kohn FM, Mayerhofer A** Mast cells in human testicular biopsies from patients with mixed atrophy: increased numbers, heterogeneity, and expression of cyclooxygenase 2 and prostaglandin D2 synthase. Fertil Steril 96:309-313

63. **Nistal M, Santamaria L, Paniagua R, Regadera J** 1986 Changes in the connective tissue and decrease in the number of mast cells in the testes of men with alcoholic and non-alcoholic cirrhosis. Acta Morphol Hung 34:107-115

64. **Pollanen P, Niemi M** 1987 Immunohistochemical identification of macrophages, lymphoid cells and HLA antigens in the human testis. Int J Androl 10:37-42

65. **Galli SJ** 1990 New insights into "the riddle of the mast cells": microenvironmental regulation of mast cell development and phenotypic heterogeneity. Lab Invest 62:5-33

66. **Ruoss SJ, Hartmann T, Caughey GH** 1991 Mast cell tryptase is a mitogen for cultured fibroblasts. J Clin Invest 88:493-499

67. **Woodbury RG, Everitt MT, Neurath H** 1981 Mast cell proteases. Methods Enzymol 80 Pt C:588-609

68. **Aguilar R, Anton F, Bellido C, Aguilar E, Gaytan F** 1995 Testicular serotonin is related to mast cells but not to Leydig cells in the rat. J Endocrinol 146:15-21

69. **Mayerhofer A, Bartke A, Amador AG, Began T** 1989 Histamine affects testicular steroid production in the golden hamster. Endocrinology 125:560-562

70. **Albrecht M, Frungieri MB, Kunz L, Ramsch R, Meineke V, Kohn FM, Mayerhofer A** 2005 Divergent effects of the major mast cell products histamine, tryptase and TNF-alpha on human fibroblast behaviour. Cell Mol Life Sci 62:2867-2876

71. **Akers IA, Parsons M, Hill MR, Hollenberg MD, Sanjar S, Laurent GJ, McAnulty RJ** 2000 Mast cell tryptase stimulates human lung fibroblast proliferation via protease-activated receptor-2. Am J Physiol Lung Cell Mol Physiol 278:L193-201

72. **Frungieri MB, Weidinger S, Meineke V, Kohn FM, Mayerhofer A** 2002 Proliferative action of mast-cell tryptase is mediated by PAR2, COX2, prostaglandins, and PPARgamma : Possible relevance to human fibrotic disorders. Proc Natl Acad Sci U S A 99:15072-15077

73. **Hartmann T, Ruoss SJ, Raymond WW, Seuwen K, Caughey GH** 1992 Human tryptase as a potent, cell-specific mitogen: role of signaling pathways in synergistic responses. Am J Physiol 262:L528-534

74. **Abe M, Kurosawa M, Ishikawa O, Miyachi Y, Kido H** 1998 Mast cell tryptase stimulates both human dermal fibroblast proliferation and type I collagen production. Clin Exp Allergy 28:1509-1517

75. **Cairns JA, Walls AF** 1997 Mast cell tryptase stimulates the synthesis of type I collagen in human lung fibroblasts. J Clin Invest 99:1313-1321

76. **Hermo L, Lalli M** 1978 Monocytes and mast cells in the limiting membrane of human seminiferous tubules. Biol Reprod 19:92-100

77. **Auger MJ, Ross JA** 1992 The biology of the macrophage. In: Lewis CE, McGlee JO eds. The macrophage. New York: Oxford University Press; 1-74

78. **Kern S, Robertson SA, Mau VJ, Maddocks S** 1995 Cytokine secretion by macrophages in the rat testis. Biol Reprod 53:1407-1416

79. **Cohen PE, Nishimura K, Zhu L, Pollard JW** 1999 Macrophages: important accessory cells for reproductive function. J Leukoc Biol 66:765-772

80. **Tuder RM** 1996 A pathologist's approach to interstitial lung disease. Curr Opin Pulm Med 2:357-363

81. **Ziangirova GG, Antonova OV, Kasparov AA** 1998 [The role of the mast cells of the conjunctiva in the intercellular interactions in keratoconus and epithelial-endothelial corneal dystrophy]. Vestn Oftalmol 114:48-51

82. **Gulkesen KH, Erdogru T, Sargin CF, Karpuzoglu G** 2002 Expression of extracellular matrix proteins and vimentin in testes of azoospermic man: an immunohistochemical and morphometric study. Asian J Androl 4:55-60

83. **Haider SG, Talati J, Servos G** 1999 Ultrastructure of peritubular tissue in association with tubular hyalinization in human testis. Tissue Cell 31:90-98

84. **Siu MK, Cheng CY** 2008 Extracellular matrix and its role in spermatogenesis. Adv Exp Med Biol 636:74-91

85. **Takaba H** 1990 [A morphological study of the testes in patients with idiopathic male infertility--immunohistochemical analysis of collagens and laminin in human testes]. Hinyokika Kiyo 36:1173-1180

86. **Dobashi M, Fujisawa M, Naito I, Yamazaki T, Okada H, Kamidono S** 2003 Distribution of type IV collagen subtypes in human testes and their association with spermatogenesis. Fertil Steril 80 Suppl 2:755-760

87. **Pollanen PP, Kallajoki M, Risteli L, Risteli J, Suominen JJ** 1985 Laminin and type IV collagen in the human testis. Int J Androl 8:337-347

88. **Santamaria L, Martinez-Onsurbe P, Paniagua R, Nistal M** 1990 Laminin, type IV collagen, and fibronectin in normal and cryptorchid human testes. An immunohistochemical study. Int J Androl 13:135-146

89. **Ungefroren H, Ergun S, Krull NB, Holstein AF** 1995 Expression of the small proteoglycans biglycan and decorin in the adult human testis. Biol Reprod 52:1095-1105

90. **Krusius T, Ruoslahti E** 1986 Primary structure of an extracellular matrix proteoglycan core protein deduced from cloned cDNA. Proc Natl Acad Sci U S A 83:7683-7687

91. **Ruoslahti E** 1988 Structure and biology of proteoglycans. Annu Rev Cell Biol 4:229-255

92. **Gallagher JT** 1989 The extended family of proteoglycans: social residents of the pericellular zone. Curr Opin Cell Biol 1:1201-1218

93. **Iozzo RV, Cohen I** 1993 Altered proteoglycan gene expression and the tumor stroma. Experientia 49:447-455

94. **Kresse H, Hausser H, Schonherr E** 1993 Small proteoglycans. Experientia 49:403-416

95. **Iozzo RV** 1997 The family of the small leucine-rich proteoglycans: key regulators of matrix assembly and cellular growth. Crit Rev Biochem Mol Biol 32:141-174

96. **Iozzo RV** 1998 Matrix proteoglycans: from molecular design to cellular function. Annu Rev Biochem 67:609-652

97. **Iozzo RV, Murdoch AD** 1996 Proteoglycans of the extracellular environment: clues from the gene and protein side offer novel perspectives in molecular diversity and function. FASEB J 10:598-614

98. **Iozzo RV, Schaefer L** 2010 Proteoglycans in health and disease: novel regulatory signaling mechanisms evoked by the small leucine-rich proteoglycans. FEBS J 277:3864-3875

99. **Jarvelainen H, Puolakkainen P, Pakkanen S, Brown EL, Hook M, Iozzo RV, Sage EH, Wight TN** 2006 A role for decorin in cutaneous wound healing and angiogenesis. Wound Repair Regen 14:443-452

100. **Bianco P, Fisher LW, Young MF, Termine JD, Robey PG** 1990 Expression and localization of the two small proteoglycans biglycan and decorin in developing human skeletal and non-skeletal tissues. J Histochem Cytochem 38:1549-1563

101. **Sawhney RS, Hering TM, Sandell LJ** 1991 Biosynthesis of small proteoglycan II (decorin) by chondrocytes and evidence for a procore protein. J Biol Chem 266:9231-9240

102. **Schonherr E, Hausser H, Beavan L, Kresse H** 1995 Decorin-type I collagen interaction. Presence of separate core protein-binding domains. J Biol Chem 270:8877-8883

103. **Svensson L, Heinegard D, Oldberg A** 1995 Decorin-binding sites for collagen type I are mainly located in leucine-rich repeats 4-5. J Biol Chem 270:20712-20716

104. **Vogel KG, Paulsson M, Heinegard D** 1984 Specific inhibition of type I and type II collagen fibrillogenesis by the small proteoglycan of tendon. Biochem J 223:587-597

105. **Thieszen SL, Rosenquist TH** 1995 Expression of collagens and decorin during aortic arch artery development: implications for matrix pattern formation. Matrix Biol 14:573-582

106. **Bidanset DJ, Guidry C, Rosenberg LC, Choi HU, Timpl R, Hook M** 1992 Binding of the proteoglycan decorin to collagen type VI. J Biol Chem 267:5250-5256

107. **Danielson KG, Fazzio A, Cohen I, Cannizzaro LA, Eichstetter I, Iozzo RV** 1993 The human decorin gene: intron-exon organization, discovery of two alternatively spliced exons in the 5' untranslated region, and mapping of the gene to chromosome 12q23. Genomics 15:146-160

108. **Scholzen T, Solursh M, Suzuki S, Reiter R, Morgan JL, Buchberg AM, Siracusa LD, Iozzo RV** 1994 The murine decorin. Complete cDNA cloning, genomic organization, chromosomal assignment, and expression during organogenesis and tissue differentiation. J Biol Chem 269:28270-28281

109. **Iozzo RV, Danielson KG** 1999 Transcriptional and posttranscriptional regulation of proteoglycan gene expression. Prog Nucleic Acid Res Mol Biol 62:19-53

110. **Mauviel A, Santra M, Chen YQ, Uitto J, Iozzo RV** 1995 Transcriptional regulation of decorin gene expression. Induction by quiescence and repression by tumor necrosis factor-alpha. J Biol Chem 270:11692-11700

111. **Heino J, Kahari VM, Mauviel A, Krusius T** 1988 Human recombinant interleukin-1 regulates cellular mRNA levels of dermatan sulphate proteoglycan core protein. Biochem J 252:309-312

112. **Wegrowski Y, Paltot V, Gillery P, Kalis B, Randoux A, Maquart FX** 1995 Stimulation of sulphated glycosaminoglycan and decorin production in adult dermal fibroblasts by recombinant human interleukin-4. Biochem J 307 (Pt 3):673-678

113. **Weber IT, Harrison RW, Iozzo RV** 1996 Model structure of decorin and implications for collagen fibrillogenesis. J Biol Chem 271:31767-31770

114. **Orgel JP, Eid A, Antipova O, Bella J, Scott JE** 2009 Decorin core protein (decoron) shape complements collagen fibril surface structure and mediates its binding. PLoS One 4:e7028

115. **Danielson KG, Baribault H, Holmes DF, Graham H, Kadler KE, Iozzo RV** 1997 Targeted disruption of decorin leads to abnormal collagen fibril morphology and skin fragility. J Cell Biol 136:729-743

116. **Ferdous Z, Peterson SB, Tseng H, Anderson DK, Iozzo RV, Grande-Allen KJ** 2010 A role for decorin in controlling proliferation, adhesion, and migration of murine embryonic fibroblasts. J Biomed Mater Res A 93:419-428

117. **Nili N, Cheema AN, Giordano FJ, Barolet AW, Babaei S, Hickey R, Eskandarian MR, Smeets M, Butany J, Pasterkamp G, Strauss BH** 2003 Decorin inhibition of PDGF-stimulated vascular smooth muscle cell function: potential mechanism for inhibition of intimal hyperplasia after balloon angioplasty. Am J Pathol 163:869-878

118. **Macri L, Silverstein D, Clark RA** 2007 Growth factor binding to the pericellular matrix and its importance in tissue engineering. Adv Drug Deliv Rev 59:1366-1381

119. **Ruoslahti E, Yamaguchi Y** 1991 Proteoglycans as modulators of growth factor activities. Cell 64:867-869

120. **Patel S, Santra M, McQuillan DJ, Iozzo RV, Thomas AP** 1998 Decorin activates the epidermal growth factor receptor and elevates cytosolic Ca2+ in A431 carcinoma cells. J Biol Chem 273:3121-3124

121. **Schaefer L, Iozzo RV** 2008 Biological functions of the small leucine-rich proteoglycans: from genetics to signal transduction. J Biol Chem 283:21305-21309

122. **Schonherr E, Sunderkotter C, Iozzo RV, Schaefer L** 2005 Decorin, a novel player in the insulin-like growth factor system. J Biol Chem 280:15767-15772

123. **Iacob D, Cai J, Tsonis M, Babwah A, Chakraborty C, Bhattacharjee RN, Lala PK** 2008 Decorin-mediated inhibition of proliferation and migration of the human trophoblast via different tyrosine kinase receptors. Endocrinology 149:6187-6197

124. **Goldoni S, Humphries A, Nystrom A, Sattar S, Owens RT, McQuillan DJ, Ireton K, Iozzo RV** 2009 Decorin is a novel antagonistic ligand of the Met receptor. J Cell Biol 185:743-754

125. **Zhu JX, Goldoni S, Bix G, Owens RT, McQuillan DJ, Reed CC, Iozzo RV** 2005 Decorin evokes protracted internalization and degradation of the epidermal growth factor receptor via caveolar endocytosis. J Biol Chem 280:32468-32479

126. **Csordas G, Santra M, Reed CC, Eichstetter I, McQuillan DJ, Gross D, Nugent MA, Hajnoczky G, Iozzo RV** 2000 Sustained down-regulation of the epidermal growth factor receptor by decorin. A mechanism for controlling tumor growth in vivo. J Biol Chem 275:32879-32887

127. **De Luca A, Santra M, Baldi A, Giordano A, Iozzo RV** 1996 Decorin-induced growth suppression is associated with up-regulation of p21, an inhibitor of cyclin-dependent kinases. J Biol Chem 271:18961-18965

128. **Iozzo RV, Moscatello DK, McQuillan DJ, Eichstetter I** 1999 Decorin is a biological ligand for the epidermal growth factor receptor. J Biol Chem 274:4489-4492

129. **Moscatello DK, Santra M, Mann DM, McQuillan DJ, Wong AJ, Iozzo RV** 1998 Decorin suppresses tumor cell growth by activating the epidermal growth factor receptor. J Clin Invest 101:406-412

130. **Santra M, Reed CC, Iozzo RV** 2002 Decorin binds to a narrow region of the epidermal growth factor (EGF) receptor, partially overlapping but distinct from the EGF-binding epitope. J Biol Chem 277:35671-35681

131. **Magnanti M, Gismondi A, Gandini O, Rossi FM, Michetti PM, Santiemma V, Morrone S** 2001 Integrin pattern and effect on contraction in cultured testicular peritubular myoid cells. Am J Reprod Immunol 45:21-27

132. **Spinnler K, Kohn FM, Schwarzer U, Mayerhofer A** 2010 Glial cell line-derived neurotrophic factor is constitutively produced by human testicular peritubular cells and may contribute to the spermatogonial stem cell niche in man. Hum Reprod 25:2181-2187

133. **Schell C, Albrecht M, Mayer C, Schwarzer JU, Frungieri MB, Mayerhofer A** 2008 Exploring human testicular peritubular cells: identification of secretory products and regulation by tumor necrosis factor-alpha. Endocrinology 149:1678-1686

134. **Schell C, Albrecht M, Spillner S, Mayer C, Kunz L, Kohn FM, Schwarzer U, Mayerhofer A** 2010 15-Deoxy-delta 12-14-prostaglandin-J2 induces hypertrophy and loss of contractility in human testicular peritubular cells: implications for human male fertility. Endocrinology 151:1257-1268

135. **Li X, Nokkala E, Yan W, Streng T, Saarinen N, Warri A, Huhtaniemi I, Santti R, Makela S, Poutanen M** 2001 Altered structure and function of reproductive organs in transgenic male mice overexpressing human aromatase. Endocrinology 142:2435-2442

136. **Li X, Makela S, Streng T, Santti R, Poutanen M** 2003 Phenotype characteristics of transgenic male mice expressing human aromatase under ubiquitin C promoter. J Steroid Biochem Mol Biol 86:469-476

137. **Li X, Strauss L, Kaatrasalo A, Mayerhofer A, Huhtaniemi I, Santti R, Makela S, Poutanen M** 2006 Transgenic mice expressing p450 aromatase as a model for male infertility associated with chronic inflammation in the testis. Endocrinology 147:1271-1277

138. **Frungieri MB, Urbanski HF, Hohne-Zell B, Mayerhofer A** 2000 Neuronal elements in the testis of the rhesus monkey: ontogeny, characterization and relationship to testicular cells. Neuroendocrinology 71:43-50

139. **Todaro GJ, Green H** 1963 Quantitative studies of the growth of mouse embryo cells in culture and their development into established lines. J Cell Biol 17:299-313

140. **Schell C, Frungieri MB, Albrecht M, Gonzalez-Calvar SI, Kohn FM, Calandra RS, Mayerhofer A** 2007 A prostaglandin D2 system in the human testis. Fertil Steril 88:233-236

141. **Druker BJ, Sawyers CL, Kantarjian H, Resta DJ, Reese SF, Ford JM, Capdeville R, Talpaz M** 2001 Activity of a specific inhibitor of the BCR-ABL tyrosine kinase in the blast crisis of chronic myeloid leukemia and acute lymphoblastic leukemia with the Philadelphia chromosome. N Engl J Med 344:1038-1042

142. **Buchdunger E** 2002 [Bcr-Abl inhibition as molecular therapy approach in chronic myeloid leukemia]. Med Klin (Munich) 97 Suppl 1:2-6

143. **Buchdunger E, O'Reilly T, Wood J** 2002 Pharmacology of imatinib (STI571). Eur J Cancer 38 Suppl 5:S28-36

144. **Nishimura N, Furukawa Y, Sutheesophon K, Nakamura M, Kishi K, Okuda K, Sato Y, Kano Y** 2003 Suppression of ARG kinase activity by STI571 induces cell cycle arrest through up-regulation of CDK inhibitor p18/INK4c. Oncogene 22:4074-4082

145. **Nurmio M, Toppari J, Zaman F, Andersson AM, Paranko J, Soder O, Jahnukainen K** 2007 Inhibition of tyrosine kinases PDGFR and C-Kit by imatinib mesylate interferes with postnatal testicular development in the rat. Int J Androl 30:366-376; discussion 376

146. **Saiki RK, Scharf S, Faloona F, Mullis KB, Horn GT, Erlich HA, Arnheim N** 1985 Enzymatic amplification of beta-globin genomic sequences and restriction site analysis for diagnosis of sickle cell anemia. Science 230:1350-1354

147. **Lowry OH, Rosebrough NJ, Farr AL, Randall RJ** 1951 Protein measurement with the Folin phenol reagent. J Biol Chem 193:265-275

148. **Hsu SM, Raine L, Fanger H** 1981 The use of antiavidin antibody and avidin-biotin-peroxidase complex in immunoperoxidase technics. Am J Clin Pathol 75:816-821

149. **Theiss AL, Simmons JG, Jobin C, Lund PK** 2005 Tumor necrosis factor (TNF) alpha increases collagen accumulation and proliferation in intestinal myofibroblasts via TNF receptor 2. J Biol Chem 280:36099-36109

150. **Spiess AN, Feig C, Schulze W, Chalmel F, Cappallo-Obermann H, Primig M, Kirchhoff C** 2007 Cross-platform gene expression signature of human spermatogenic failure reveals inflammatory-like response. Hum Reprod 22:2936-2946

151. **Romano F, Chiarenza C, Palombi F, Filippini A, Padula F, Ziparo E, De Cesaris P** 2006 Platelet-derived growth factor-BB-induced hypertrophy of peritubular smooth muscle cells is mediated by activation of p38 MAP-kinase and of Rho-kinase. J Cell Physiol 207:123-131

152. **van Straaten JF, Coers W, Noordhoek JA, Huitema S, Flipsen JT, Kauffman HF, Timens W, Postma DS** 1999 Proteoglycan changes in the extracellular matrix of lung tissue from patients with pulmonary emphysema. Mod Pathol 12:697-705

153. **Fadic R, Mezzano V, Alvarez K, Cabrera D, Holmgren J, Brandan E** 2006 Increase in decorin and biglycan in Duchenne Muscular Dystrophy: role of fibroblasts as cell source of these proteoglycans in the disease. J Cell Mol Med 10:758-769

154. **Krull NB, Zimmermann T, Gressner AM** 1993 Spatial and temporal patterns of gene expression for the proteoglycans biglycan and decorin and for transforming growth factor-beta 1 revealed by in situ hybridization during experimentally induced liver fibrosis in the rat. Hepatology 18:581-589

155. **Koninger J, Giese NA, Bartel M, di Mola FF, Berberat PO, di Sebastiano P, Giese T, Buchler MW, Friess H** 2006 The ECM proteoglycan decorin links desmoplasia and inflammation in chronic pancreatitis. J Clin Pathol 59:21-27

156. **Sato K, Li Y, Foster W, Fukushima K, Badlani N, Adachi N, Usas A, Fu FH, Huard J** 2003 Improvement of muscle healing through enhancement of muscle regeneration and prevention of fibrosis. Muscle Nerve 28:365-372

157. **Yamaguchi Y, Mann DM, Ruoslahti E** 1990 Negative regulation of transforming growth factor-beta by the proteoglycan decorin. Nature 346:281-284

158. **Miqueloto CA, Zorn TM** 2007 Characterization and distribution of hyaluronan and the proteoglycans decorin, biglycan and perlecan in the developing embryonic mouse gonad. J Anat 211:16-25

159. **Soto-Suazo M, San Martin S, Ferro ES, Zorn TM** 2002 Differential expression of glycosaminoglycans and proteoglycans in the migratory pathway of the primordial germ cells of the mouse. Histochem Cell Biol 118:69-78

160. **Hashimura K, Sudhir K, Nigro J, Ling S, Williams MR, Komesaroff PA, Little PJ** 2005 Androgens stimulate human vascular smooth muscle cell proteoglycan biosynthesis and increase lipoprotein binding. Endocrinology 146:2085-2090

161. **Hong SH, Nah HY, Lee JY, Gye MC, Kim CH, Kim MK** 2004 Analysis of estrogen-regulated genes in mouse uterus using cDNA microarray and laser capture microdissection. J Endocrinol 181:157-167

162. **Yanaihara A, Otsuka Y, Iwasaki S, Aida T, Tachikawa T, Irie T, Okai T** 2005 Differences in gene expression in the proliferative human endometrium. Fertil Steril 83 Suppl 1:1206-1215

163. **Wu WX, Zhang Q, Unno N, Derks JB, Nathanielsz PW** 2000 Characterization of decorin mRNA in pregnant intrauterine tissues of the ewe and regulation by steroids. Am J Physiol Cell Physiol 278:C199-206

164. **Rockel JS, Grol M, Bernier SM, Leask A** 2009 Cyclic AMP regulates extracellular matrix gene expression and metabolism in cultured primary rat chondrocytes. Matrix Biol 28:354-364

165. **Malemud CJ, Papay RS, Hering TM** 1996 Forskolin Stimulates Aggrecan Gene Expression in Cultured Bovine Chondrocytes. Am J Ther 3:120-128

166. **Cissell JM, Milton SC, Dahlgren LA** 2010 Investigation of the effects of prostaglandin E on equine superficial digital flexor tendon fibroblasts in vitro. Vet Comp Orthop Traumatol 23:417-423

167. **Ivey ME, Little PJ** 2008 Thrombin regulates vascular smooth muscle cell proteoglycan synthesis via PAR-1 and multiple downstream signalling pathways. Thromb Res 123:288-297

168. **Comalada M, Cardo M, Xaus J, Valledor AF, Lloberas J, Ventura F, Celada A** 2003 Decorin reverses the repressive effect of autocrine-produced TGF-beta on mouse macrophage activation. J Immunol 170:4450-4456

169. **Pulkkinen L, Alitalo T, Krusius T, Peltonen L** 1992 Expression of decorin in human tissues and cell lines and defined chromosomal assignment of the gene locus (DCN). Cytogenet Cell Genet 60:107-111

170. **Westergren-Thorsson G, Antonsson P, Malmstrom A, Heinegard D, Oldberg A** 1991 The synthesis of a family of structurally related proteoglycans in fibroblasts is differently regulated by TFG-beta. Matrix 11:177-183

171. **Bassols A, Massague J** 1988 Transforming growth factor beta regulates the expression and structure of extracellular matrix chondroitin/dermatan sulfate proteoglycans. J Biol Chem 263:3039-3045

172. **Dodge GR, Diaz A, Sanz-Rodriguez C, Reginato AM, Jimenez SA** 1998 Effects of interferon-gamma and tumor necrosis factor alpha on the expression of the genes encoding aggrecan, biglycan, and decorin core proteins in cultured human chondrocytes. Arthritis Rheum 41:274-283

173. **Tufvesson E, Westergren-Thorsson G** 2000 Alteration of proteoglycan synthesis in human lung fibroblasts induced by interleukin-1beta and tumor necrosis factor-alpha. J Cell Biochem 77:298-309

174. **Tufvesson E, Westergren-Thorsson G** 2002 Tumour necrosis factor-alpha interacts with biglycan and decorin. FEBS Lett 530:124-128

175. **Westergren-Thorsson G, Chakir J, Lafreniere-Allard MJ, Boulet LP, Tremblay GM** 2002 Correlation between airway responsiveness and proteoglycan production by bronchial fibroblasts from normal and asthmatic subjects. Int J Biochem Cell Biol 34:1256-1267

176. **Hesselstrand R, Westergren-Thorsson G, Scheja A, Wildt M, Akesson A** 2002 The association between changes in skin echogenicity and the fibroblast production of biglycan and versican in systemic sclerosis. Clin Exp Rheumatol 20:301-308

177. **Hussein MR, Abou-Deif ES, Bedaiwy MA, Said TM, Mustafa MG, Nada E, Ezat A, Agarwal A** 2005 Phenotypic characterization of the immune and mast cell infiltrates in the human testis shows normal and abnormal spermatogenesis. Fertil Steril 83:1447-1453

178. **Christl HW** 1990 The lamina propria of vertebrate seminiferous tubules: a comparative light and electron microscopic investigation. Andrologia 22:85-94

179. **Fawcett DW** 1973 Observations on the organization of the interstitial tissue of the testis and on the occluding cell junctions in the seminiferous epithelium. Adv Biosci 10:83-99

180. **Reed CC, Iozzo RV** 2002 The role of decorin in collagen fibrillogenesis and skin homeostasis. Glycoconj J 19:249-255

181. **Seidler DG, Dreier R** 2008 Decorin and its galactosaminoglycan chain: extracellular regulator of cellular function? IUBMB Life 60:729-733

182. **Hausser H, Kresse H** 1991 Binding of heparin and of the small proteoglycan decorin to the same endocytosis receptor proteins leads to different metabolic consequences. J Cell Biol 114:45-52

183. **Hausser H, Schonherr E, Muller M, Liszio C, Bin Z, Fisher LW, Kresse H** 1998 Receptor-mediated endocytosis of decorin: involvement of leucine-rich repeat structures. Arch Biochem Biophys 349:363-370

184. **Hausser H, Wedekind P, Sperber T, Peters R, Hasilik A, Kresse H** 1996 Isolation and cellular localization of the decorin endocytosis receptor. Eur J Cell Biol 71:325-331

185. **Sofeu Feugaing DD, Kresse H, Greb RR, Gotte M** 2006 A novel 110-kDa receptor protein is involved in endocytic uptake of decorin by human skin fibroblasts. ScientificWorldJournal 6:35-52

186. **Fiedler LR, Schonherr E, Waddington R, Niland S, Seidler DG, Aeschlimann D, Eble JA** 2008 Decorin regulates endothelial cell motility on collagen I through activation of insulin-like growth factor I receptor and modulation of alpha2beta1 integrin activity. J Biol Chem 283:17406-17415

187. **Dreux AC, Lamb DJ, Modjtahedi H, Ferns GA** 2006 The epidermal growth factor receptors and their family of ligands: their putative role in atherogenesis. Atherosclerosis 186:38-53

188. **Fohr KJ, Mayerhofer A, Sterzik K, Rudolf M, Rosenbusch B, Gratzl M** 1993 Concerted action of human chorionic gonadotropin and norepinephrine on intracellular-free calcium in human granulosa-lutein cells: evidence for the presence of a functional alpha-adrenergic receptor. J Clin Endocrinol Metab 76:367-373

189. **Romano F, Tripiciano A, Muciaccia B, De Cesaris P, Ziparo E, Palombi F, Filippini A** 2005 The contractile phenotype of peritubular smooth muscle cells is locally controlled: possible implications in male fertility. Contraception 72:294-297

190. **D'Antoni ML, Torregiani C, Ferraro P, Michoud MC, Mazer B, Martin JG, Ludwig MS** 2008 Effects of decorin and biglycan on human airway smooth muscle cell proliferation and apoptosis. Am J Physiol Lung Cell Mol Physiol 294:L764-771

191. **Chiarenza C, Filippini A, Tripiciano A, Beccari E, Palombi F** 2000 Platelet-derived growth factor-BB stimulates hypertrophy of peritubular smooth muscle cells from rat testis in primary cultures. Endocrinology 141:2971-2981

192. **Gnessi L, Emidi A, Jannini EA, Carosa E, Maroder M, Arizzi M, Ulisse S, Spera G** 1995 Testicular development involves the spatiotemporal control of PDGFs and PDGF receptors gene expression and action. J Cell Biol 131:1105-1121

193. **Kormano M, Hovatta O** 1972 Contractility and histochemistry of the myoid cell layer of the rat seminiferous tubules during postnatal development. Z Anat Entwicklungsgesch 137:239-248

194. **Kozma EM, Wisowski G, Olczyk K** 2009 Platelet derived growth factor BB is a ligand for dermatan sulfate chain(s) of small matrix proteoglycans from normal and fibrosis affected fascia. Biochimie 91:1394-1404

195. **Zachow R, Uzumcu M** 2007 The hepatocyte growth factor system as a regulator of female and male gonadal function. J Endocrinol 195:359-371

196. **Nakatani T, Honda E, Hayakawa S, Sato M, Satoh K, Kudo M, Munakata H** 2008 Effects of decorin on the expression of alpha-smooth muscle actin in a human myofibroblast cell line. Mol Cell Biochem 308:201-207

197. **Seidler DG, Goldoni S, Agnew C, Cardi C, Thakur ML, Owens RT, McQuillan DJ, Iozzo RV** 2006 Decorin protein core inhibits in vivo cancer growth and metabolism by hindering epidermal growth factor receptor function and triggering apoptosis via caspase-3 activation. J Biol Chem 281:26408-26418

198. **Dewar AL, Doherty KV, Hughes TP, Lyons AB** 2005 Imatinib inhibits the functional capacity of cultured human monocytes. Immunol Cell Biol 83:48-56

199. **Krause DS, Van Etten RA** 2005 Tyrosine kinases as targets for cancer therapy. N Engl J Med 353:172-187

200. **Beyer C, Distler JH, Distler O** 2010 Are tyrosine kinase inhibitors promising for the treatment of systemic sclerosis and other fibrotic diseases? Swiss Med Wkly 140:w13050

201. **Distler JH, Distler O** 2010 Tyrosine kinase inhibitors for the treatment of fibrotic diseases such as systemic sclerosis: towards molecular targeted therapies. Ann Rheum Dis 69 Suppl 1:i48-51

202. **Iwamoto N, Distler JH, Distler O** 2011 Tyrosine kinase inhibitors in the treatment of systemic sclerosis: from animal models to clinical trials. Curr Rheumatol Rep 13:21-27

203. **Dahlman-Wright K, Cavailles V, Fuqua SA, Jordan VC, Katzenellenbogen JA, Korach KS, Maggi A, Muramatsu M, Parker MG, Gustafsson JA** 2006 International Union of Pharmacology. LXIV. Estrogen receptors. Pharmacol Rev 58:773-781

204. World Health Organization 2003. WHO laboratory manual for the examination of human semen and semen-cervical mucus interaction. 4th edition. Cambridge, UK: Cambridge University Pres

9. ACKNOLEDGEMENTS

This study was carried out at the Institute for Anatomy and Cell biology, LMU Munich.
First I want to thank Professor Artur Mayerhofer for providing this interesting topic and for excellent and inspiring guidance during the whole dissertation.
My doctoral thesis supervisor PD Dr. Lars Kunz is acknowledged for careful and critical review of this thesis. Thank you for discussions and expertise in several laboratory methods.
All my co-authors are kindly acknowledged for their contribution to this work. I especially wish to thank Professor Matti Poutanen for giving me the opportunity to work in his lab and Dr. Leena Strauss for introducing me to the world of AROM+ mice. I also wish to thank both for fruitful discussion and productive collaboration. Many thanks to all the people at the Department of Physiology and Pediatrics at the University of Turku for the all their support and nice company during my visits. I want to thank especially Dr. Mirja Nurmio for fruitful discussions.
Professor Jorma Toppari and Professor Lauri J. Pelliniemi are thanked for nice discussions concerning male reproductive health and decorin.
I thank all the people at the Institute for Anatomy and Cell biology for creating a nice working environment. I thank PD Dr. Martin Albrecht for discussions and expertise in various laboratory methods. I want to express my thanks to Dr. Cornelia Kampfer, Dr. Harald Welter, Dr. Silvana Lauf and Dr. Sabine Saller for nice discussions, especially during literature seminar. Special thanks to Sandra Raffael for excellent and never-ending help in solving all kind of problems. I also wish to thank Sabine Ströbel, Julia Merz-Lange, Christina Jarrin-Franco, Christoph Merz, Catherina Lücke, Dr. Thomas Winkle, Simone Hebele, Daniel Einwang, Astrid Tiefenbacher, Gabriele Terfloth and Karin Metztrath for a nice working athmosphere. Especially, I wish to thank Dr. Katrin Spinnler for help with coreldraw and high-quality company along this journey.
My warmest gratitude to my friends for great company and joyful moments spent together. Words fail to express my gratitude to my dear family. Many thanks for all your encouragement and support.
This thesis work was financially supported by the Deutsche Forschungsgemeinschaft, by the Deutscher Akademischer Austauschdienst e.V. and the Academy of Finland.

10. APPENDIX

10.1 Primer

Table 10-1: Overview of primers, their GenBank accession numbers, product sizes and annealing temperatures.

Target	Sequence (5´-3´)	GenBank Accession no.	Amplicon (bp)	Annealing temperature (C°)/cycles
Calponin		NM_001299.4	183	50/30
forward	CGA AGA CGA AAG GAA ACA AGG			
reverse	GCT TGG GGT CGT AGA GGT G			
CD90		NM_006288.3	138	61/30
forward	AGC ATC GCT CTC CTG CTA ACA			
reverse	CTC GTA CTG GAT GGG TGA ACT			
Collagen IV		NM_001846.2	352	62/35
forward	CTC CGC ACT CAA GAG GCT C			
reverse	AGA CGC TCT GGG CGA GGA A			
Cyclophilin		NM_006347	325	56/25
forward	CTC CTT TGA GCT GTT TGC AG			
reverse	CAC CAC AGT CTT GCC ATC C			
DCN		NM_001920	221	59/35-39
forward	GGA ATT GAA AAT GGG GCT TT			
reverse	GCC ATT GTC AAC AGC AGA GA			
DCN nested		NM_001920	122	59/35
forward	CAC CAG CAT TCC TCA AGG TC			
reverse	TCA ATC CCA ACT TAG CCA AA			
EGFR		NM_005228.3	195	56/35-39
forward	CAG CGC TAC CTT GTC ATT CA			
reverse	TGC ACT CAG AGA GCT CAG GA			
EGFR nested		NM_005228.3	114	56/35
forward	CAT TCA GGG GGA TGA AAG AA			
reverse	ATG AGG TAC TCG TCG GCA TC			
ErbB2		NM_001005862	194	58/35
forward	AGT ACC TGG GTC TGG ACG TG			
reverse	CTG GGA ACT CAA GCA GGA AG			
ErbB3		NM_001982	243	54/35
forward	GCC AAT GAG TTC ACC AGG AT			
reverse	ACG TGG CCG ATT AAG TGT TC			
ErbB4		NM_001042599	183	54/35
forward	TTT CGG GAG TTT GAG AAT GG			
reverse	GAA ACT GTT TGC CCC CTG TA			
HGFR		NM_000245	201	56/35
forward	CAG GCA GTG CAG CAT GTA GT			
reverse	GAT GAT TCC CTC GGT CAG AA			
IGF-1R		NM_000875	172	57/35
forward	AAC CCC AAG ACT GAG GTG TG			
reverse	TGA CAT CTC TCC GCT TCC TT			
Mouse DCN		NM_001190451	181	60/35
forward	TGA GCT TCA ACA GCA TCA CC			
revese	AAG TCA TTT TGC CCA ACT GC			
MYH11		NM_002474.2	656	60/35
forward	GGA CGA CCT GGT TGT TGA TT			
reverse	GTA GCT GCT TGA TGG CTT CC			

PDGFR-α		NM_006206	391	56/35
forward	GGG GAG AGT GAA GTG AGCTG			
reverse	TCC CAT TAA AGC GCT GTC TG			
PDGFR-α nested		NM_006206	158	56/35
forward	AGA AAA CAA CAG CGG CCT TT			
reverse	CTA CAT CTG GGT CTG GCA CA			
PDGFR-β		NM_002609	155	58/35
forward	GTG ACG TAC TGG GAG GAG GA			
reverse	TTA AAG GGC AAG GAG TGT GG			
PDGFR-β semi-nested		NM_002609	136	58/35
forward	AGC AGG AGT TTG AGG TGG TG			
reverse	TTA AAG GGC AAG GAG TGT GG			
RPL19		NM_000981	199	58/39
forward	AGG CAC ATG GGC ATA GGT AA			
reverse	CCA TGA GAA TCC GCT TGT TT			
SMA		NM_006347	205	61/30
forward	GTG ACC TCA CGG TGT TGA TT			
reverse	CCA ATG GTG ATA ACC TGC CC			
VEGFR		NM_002253	218	57/35
forward	GTG ACC AAC ATG GAG TCG TG			
reverse	TGC TTC ACA GAA GAC CAT GC			

10.2 Chemicals

Table 10-2: List of used chemicals, manufacturers and cities.

Reagent	Manufacturer	City
Acrylamide solution 30 %	AppliChem	Darmstadt, Germany
Agarose Metaphor	Biozym	Oldendorf, Germany
Ammonium persulfate	Merck	Darmstadt, Germany
Aprotinin	Sigma Aldrich	Deisenhofen, Germany
Boric acid	Sigma Aldrich	Deisenhofen, Germany
Bromophenol blue	Serva	Heidelberg, Germany
Bovine serum albumin	PAA	Cölbe, Germany, Germany
CASYclean	InnovatisAG	Reutlingen, Germany
CASYton	InnovatisAG	Reutlingen, Germany
Chloroform	Merck	Darmstadt, Germany
Citric acid	Roth	Karlsruhe, Germany
Collagenase I	Sigma Aldrich	Deisenhofen, Germany
Decorin, human recombinant	Immundiagnostik	Bensheim, Germany
Decorin, from bovine articular cartilage	Sigma Aldrich	Deisenhofen, Germany
15-deoxy-Δ-PGJ2	Cayman Chemicals	Ann Arbor, MI, USA
DEPC-treated water	Invitrogen	Karlsruhe, Germany
Dimethylsulfidoxide	Sigma Aldrich	Deisenhofen, Germany
dNTPs	Promega GmbH	Mannheim, Germany
dNTPs (dATP, dCTP, dTTP, dGTP)	Peqlab	Erlangen, Germany
Dipotassium phosphate	Merck	Darmstadt, Germany
Disodium phosphate	Merck	Darmstadt, Germany

Dithiothreitol (DTT) 0.1 M	Invitrogen	Karlsruhe, Germany
DMEM high Glucose, w Phenol red w L-Glutamine	PAA	Cölbe, Germany
DMEM high Glucose, w/o Phenol red w L-Glutamine	PAA	Cölbe, Germany
DMEM/Ham`s F12,	PAA	Cölbe, Germany
EGF, human recombinant	New England Biolabs	Frankfurt, Germany
Entellan	Merck	Darmstadt, Germany
17β-Estradiol	Sigma Aldrich	Deisenhofen, Germany
Ethanol 100 % p. a.	Roth	Karlsruhe, Germany
Ethidium bromide	Sigma Aldrich	Deisenhofen, Germany
Ethylene diaminetetraacetic acid (EDTA)	Sigma Aldrich	Deisenhofen, Germany
Ethylene glycol tetraacetic acid (EGTA)	Sigma Aldrich	Deisenhofen, Germany
Fetal calf serum	PAA	Cölbe, Germany
5x First strand buffer	Invitrogen	Karlsruhe, Germany
Fluo-4, acetoxy-methylester	Molecular Probes	Eugene, OR, USA
Formaldehyde	Sigma Aldrich	Deisenhofen, Germany
Forskolin	Sigma Aldrich	Deisenhofen, Germany
Full Range Mol Weight Marker Rainbow	GE Healthcare Bio-Sciences	Munich, Germany
Glycerol	Merck	Darmstadt, Germany
Glycine	Applichem	Darmstadt, Germany
GoTaq DNA-Polymerase	Promega GmbH	Mannheim, Germany
5x Green GoTaq-Reaction-Buffer	Promega GmbH	Mannheim, Germany
Ham`s F12	PAA	Cölbe, Germany
Hydrogen peroxide 30 %	Sigma Aldrich	Deisenhofen, Germany
Imatinib mesylate	Glivec®, Novartis Pharma	Basel, Switzerland
Isopropyl alcohol	Apotheke, Klinikum Rechts der Isar	München, Germany
Leupeptin	Sigma Aldrich	Deisenhofen, Germany
Magnesium chloride	Sigma Aldrich	Deisenhofen, Germany
MassRuler Low Range DNA Ladder	Fermentas	St.-Leon-Rot, Germany
2-Mercaptoethanol	Sigma Aldrich	Deisenhofen, Germany
Methanol	Roth	Karlsruhe, Germany
M-Mul VRT Rnase	Finnzymes Oy	Espoo, Finland
Monosodium phosphate	Merck	Darmstadt, Germany
Monopotassium phosphate	Merck	Darmstadt, Germany
Normal serum donkey	Sigma Aldrich	Deisenhofen, Germany
Normal serum goat	Sigma Aldrich	Deisenhofen, Germany
Nuclease eliminator	MoBiTec	Göttingen, Germany
Paraformaldehyde	Merck	Darmstadt, Germany
PDGF-AA, human	New England Biolabs	Frankfurt, Germany
PDGF-BB, human	Sigma Aldrich	Deisenhofen, Germany
Penicillin	PAA	Cölbe, Germany
pH Calibration standard pH 4/7/10	Roth	Karlsruhe, Germany
Phenylmethanesulfonylfluoride (PMSF)	Invitrogen	Karlsruhe, Germany
Phosphate buffered saline	Biochrom	
Pipes	Sigma Aldrich	Deisenhofen, Germany
Ponceau S	Sigma Aldrich	Deisenhofen, Germany
Precission Plus Protein Kaleidoscope Standard	Bio-Rad	München, Germany
Random hexamer primer (300 ng/µl)	Finnzymes Oy	Espoo, Finland
RNAsin Plus Rnase Inhibitor 40 units/µl	Promega GmbH	Mannheim, Germany
RPMI medium 1640, ready mix	PAA	Cölbe, Germany
Saccharose	Merck	Darmstadt, Germany
Skin ß Tryptase, human recombinant	Promega GmbH	Mannheim, Germany
Smooth muscle cell growth medium 2	PromoCell	Heidelberg, Germany
Sodium chloride	Merck	Darmstadt, Germany
Sodiumdodecylsulfate (SDS)	Sigma Aldrich	Deisenhofen, Germany

Sodium orthovanadate	Sigma Aldrich	Deisenhofen, Germany
Super Script II	Invitrogen	Karlsruhe, Germany
Streptomycin	PAA	Cölbe, Germany
N,N,N',N'-Tetramethylendiamin (TMED) 100 %	Bio-Rad	München, Germany
TNF-α, human	Sigma Aldrich	Deisenhofen, Germany
TNF-α, mouse	New England Biolabs	Frankfurt, Germany
Trichloroacetic acid	Roth	Karlsruhe, Germany
Tris Base	Sigma Aldrich	Deisenhofen, Germany
Trisodium citrate	Roth	Karlsruhe, Germany
TRIsure	Bioline GmbH	Luckenwalde, Germany
Triton® X-100	Bio-Rad	München, Germany
Trypsin-EDTA	PAA	Cölbe, Germany
Tween 20	Sigma Aldrich	Deisenhofen, Germany
Xylene 99 %	Roth	Karlsruhe, Germany

10.3 Antibodies

Table 10-3: Summary of antibodies, manufacturers, order numbers and cities.

Antibody	Manufacturer	Order number	City
Biot. Goat anti rabbit	Dianova	111-065-144	Hamburg, Germany
Biot. Donkey anti goat	Dianova	705-066-147	Hamburg, Germany
Pox goat anti rabbit	Dianova	111-035-144	Hamburg, Germany
Pox goat anti mouse	Dianova	115-036-003	Hamburg, Germany
Pox rabbit anti goat	Dianova	305-036-003	Hamburg, Germany
β-Actin mouse monoclonal	Sigma Aldrich	A5441	Deisenhofen, Germany
Anti-Actin alpha smooth muscle monoclonal antibody, clone 1A4	Sigma Aldrich	A5228	Deisenhofen, Germany
CD90 mouse monoclonal, clone AS02	Dianova	DIA 100	Hamburg, Germany
Collagen type I, mouse monoclonal, clone I-8H5	Acris Antibodies	AF5610-1	Hiddenhausen, Germany
Collagen type IV, mouse monoclonal, clone IV-4H12	Acris Antibodies	AF5910	Hiddenhausen, Germany
DCN goat monoclonal antibody	R&D systems	AF143	Wiesbaden-Nordenstadt, Germany
p44/p42 MAPK (Erk1/1) monoclonal antibody, rabbit	Cell Signaling Technology, New England Biolabs	9102	Frankfurt am Main, Germany
Phospho-p44/p42 MAPK monoclonal antibody, mouse	Cell Signaling Technology, New England Biolabs	9106	Frankfurt am Main, Germany
PDGFR-α	Santa Cruz Biotechnology	sc-338	Santa Cruz, CA, USA
PDGFR-β	Santa Cruz Biotechnology	sc-339	Santa Cruz, CA, USA
Anti-Phospho-PDGFR-β (Y1021) antibody, rabbit	R&D systems	AF2316	Wiesbaden-Nordenstadt, Germany
Anti-Phospho-EGFR (Y1173) antibody, rabbit	R&D systems	AF1095	Wiesbaden-Nordenstadt, Germany

10.4 Kits and assays

Table 10-4: List of employed commercial kits and assays, their manufacturer and origin.

Kit/Assay	Manufacturer	City
Caspase-Glo 3/7 Assay	Promega GmbH	Mannheim, Germany
CellTiter-Glo® Luminescent Cell Viability Assay	Promega GmbH	Mannheim, Germany
DAB-Tablet Set	Sigma Aldrich	Deisenhofen, Germany
DC Protein Assay	Bio-Rad	München, Germany
Deoxyribonuclease I, Amplification Grade	Invitrogen	Espoo, Finland
DuoSet® ELISA Development System, human Decorin	R&D Systems	Wiesbaden-Nordenstadt, Germany
DyNAmo two-step SYBR Green qRT-PCR kit	Finnzymes Oy	Espoo, Finland
MinElute® PCR Purification Kit	QIAGEN GmbH	Hilden, Germany
Prolong Antifade Kit		
Proteome Profiler Array, Human Phospho-RTK	R&D Systems	Wiesbaden-Nordenstadt, Germany
RNeasy FFPE kit	QIAGEN GmbH	Hilden, Germany
RNeasy Plus Mini kit	QIAGEN GmbH	Hilden, Germany
Substrate Reagent Pack Color Reagent A (H_2O_2), Color Reagent B (Tetramethylbenzidine)	R&D Systems	Wiesbaden-Nordenstadt, Germany
SuperSignal® West Femto Maximum Sensitivity Substrate	Pierce, Thermo Fisher Scientific	Bonn, Germany
QIAquick Gel Extraction Kit	QIAGEN GmbH	Hilden, Germany
Vectashield Mounting medium with DAPI	Vector Laboratories	Burlingame, CA, USA
Vectastain ABC Kit	Vector Laboratories	Burlingame, CA, USA
Venor® GeM – Mycoplasma Detection Kit	Minerva Biolabs GmbH	Berlin, Germany

10.5 Tools and machines

Table 10-5: Overview of manufacturers and cities of employed tools and machines.

Tool/Machine	Manufacturer	City
Analytical balance XS 205	Mettler Toledo	Giessen, Germany
Biophotometer	Eppendorf AG	Hamburg, Germany
Camera ProRes CT3 (Axiovert 135)	Jenoptik	Jena, Germany
CASY-system	Schärfe Systems	Reutlingen, Germany
Centrifuge Biofuge fresco	Heraeus Holding GmbH	Hanau, Germany
Centrifuge Labofuge 400	Heraeus Holding GmbH	Hanau, Germany
CFX96 Real Time System and C1000 Thermal Cycler	Bio-Rad	Helsinki, Finland
ChemiSmart 5000	Peqlab	Erlangen, Germany
Confocal microscope TCS SP2 with laser and scanner	Leica Microsystems	Wetzlar, Germany
Count-Down Timer	Roth	Karlsruhe, Germany
ELISA-Reader	Dynex Technologies	Guernsey, Great Britain
Engine Opticon system	MJ Research, Inc.	Waltham, MA, USA
Fireboy plus	Integra Biosciences	Wallisellen, Switzerland
Fluorescence lamp HBO 100 W	Carl Zeiss AG	München, Germany
Fluorescence microscope Axioplan	Carl Zeiss AG	München, Germany
Fluostar Optima	BMG Labtech	Offenburg, Germany
Freezer -80 °C	Sanoy	München, Germany
IKA-Magnetic stirrer RCT	IKA®-Labortechnik	Staufen, Germany
IKA-Shaker MTS4	IKA®-Labortechnik	Staufen, Germany
Incubator BBD 6220	Heraeus Holding GmbH	Hanau, Germany
Laboratory pump	KNF Neuberger	Freiburg i. Br.; Germany
Laboratory pump	Chromaphor	Duisburg, Germany
Laminar airflow cabinet	Holten LaminAir	Allerød, Denmark
Laser microdissection	Carl Zeiss AG	München, Germany
Micro centrifuge	Neolab	Heidelberg, Germany
Microscope Axiovert 135	Carl Zeiss AG	München, Germany
Microwave M690	Miele	Gütersloh, Germany
Multichannel pipet 20 – 200 µl 100–1200 µl	Rainin	Giessen, Germany
NanoDrop ND-1000	Finnzymes Oy	Espoo, Finland
PH-Meter	Mettler Toledo	Giessen, Germany
Pipet 2µl/ 10µl/ 20µl/ 100µl/ 200µl/ 1000 µl/ 5000µl	Gilson	Limburg-Offenheim, Germany
Power Pac 300	Bio-Rad	München, Germany
SDS-PAGE Protean 3	Bio-Rad	München, Germany
Tender Cooker	Nordic Ware	Minneapolis, MN, USA
Thermocycler PTC 200	Bio-Rad	München, Germany
Thermomixer comfort	Eppendorf AG	Hamburg, Germany
Ultrasonic sound processor 50 H	Dr. Hielscher GmbH	Teltow, Germany
Ultraturax T25	Janke & Kunkel, IKA®-Labor-technik	Staufen, Germany
UV detection system	MWG Biotech	Ebersberg, Germany
Electronic stirrer Multipoint HP	Variomag	Daytona Beach, FL, USA
Vortex-Genie 2	Scientific Industries	Bohemia, NY, USA

10.6 Consumable supplies

Table 10-6: List of used laboratory material, manufacturers and cities.

Material	Manufacturer	City
Cell scraper 24 cm	TPP	Trasadingen, Switzerland
Centrifuge tubes, 15/50 ml	Sarstedt	Nümbrecht, Germany
Crypure tubes, 1.6 ml	Sarstedt	Nümbrecht, Germany
Culture flasks, 25/75 cm^2	Sarstedt	Nümbrecht, Germany
Eppendorf tubes, 0.5/1.5/2.0 ml	Sarstedt	Nümbrecht, Germany
Microplates, 96-well	Greiner Bio-One GmbH	Solingen, Germany
Microplates maxisorp, 96-well	Nunc	Wiesbaden, Germany
Multidish, 24-well	Nunc	Wiesbaden, Germany
Nitrocellulose membran	Whatman	Dassel, Germany
PAP pen	Kisker	Steinfurt, Germany
Parafilm	American National Can	Chicago, IL, USA
Pasteur pipettes, 150 mm	Neolab	Heidelberg, Germany
Petri dishes, 35/60 mm	Sarstedt	Nümbrecht, Germany
Pipette tips, 5000/1000/200/100/10 µl	Rainin	Giessen, Germany
Feather disposable scalpel	Pfm medical ag	Köln, Germany
Serological pipettes, 5/10/25/50 ml	Sarstedt	Nümbrecht, Germany
Syringe filter, 0.2/0.45	Sarstedt	Nümbrecht, Germany

10.7 Solutions

Table 10-7: Overview and composition of used buffers and solutions.

Solution	Components
APS for SDS-PAGE (10 %)	1 g APS in 10 ml ddH_2O
Separating gel buffer for SDS-PAGE	45.4 g Tris (1.5 M); total 250 ml, pH 8.8
Calcium chloride (1 mM)	0.20 g $MgCl_2$ (1 mM) 2.38 g HEPES (10 mM) 1.8 g glucose (10 mM) pH 7.4
10 x Laemmli buffer	30.28 g Tris (250 mM)
Loading gel buffer for SDS-PAGE	15.2 g Tris (0.5 M); total 250 ml, pH 6.8
1 x Buffer for proteinlysates	1.89 Tris (62.5 mM) 5 g SDS (2 %) 25 g Saccharose (10 %); total 250 ml, pH 6.8
Bromophenol blue	0.75 g Tris (62.5 mM) 2 g SDS (2 %) 10 g Saccharose (10 %); total 100 ml, pH 6.8
Ethidium bromide	10 mg/ml, use 1:10 dilution
HEPES (10 mM):	0.76 g EGTA (2 mM) 30.45 g Potassium gluconate (130 mM) 0.29 g NaCl (5 mM) pH 7.4
KPBS	1.47 g KH_2PO_4 8.59 g K_2HPO_4 27 g NaCl total 500 ml, pH 7.4
LKPBS	48.85 ml 0.02 M KPBS 1 ml Normal serum 0.15 ml Triton® X-100
NPE-Buffer	4.4 g NaCl (150 mM) 1.5 Pipes (10 mM) 0.15 g EDTA (1 mM); total 500 ml, pH 7.2
10 x Ponceau S	1 g Ponceau S in 500 ml 3 % trichloroacetic acid
Protease inhibitorcocktail	10 µl PMSF (10 mg/ml) 10 µl Aprotinin 10 µl Leupeptin 0.5 µl Sodium orthovanadate (1 M) 1 ml 1 x Buffer for proteinlysates
Sodium dodecyl sulfate (SDS)	1 g SDS in 10 ml ddH_2O
Solution A for immunohistochemistry (0.1 M)	21.01 g Citric acid 1 l ddH_2O
Solution B for immunohistochemistry (0.1 M)	29.41 g Trisodium citrate in 1 l ddH_2O
5 x TBE buffer	54 g Tris 27.5 Boric acid 20 ml EDTA; total 1 l, pH 8.0
20 x Tris-buffered saline (TBS) – Tween 20	116,8 g NaCl (2 M) 12.1 g Tris 10 ml Tween 20 (1 %); total 1 l, pH 7.5
10 x Tranfer buffer	144.1 g Glycin (1.92 M) 121.1 g Tris (250 mM) 100 ml Methanol (10 %) 1 ml SDS (0.01 %)

10.8 Proteome Profiler results

Table 10-8: Summary of RTKs phosphorylated by DCN in HTPCs.

Receptor family/Control	RTK/Control	Phosphorylation by DCN (+: yes; -: no)
EGFR	EGFR	+
EGFR	ErbB2	+
EGFR	ErbB3	+
EGFR	ErbB4	+
FGFR	FGFR1	-
FGFR	FGFR2α	-
FGFR	FGFR3	-
FGFR	FGFR4	-
Insulin R	Insulin R	-
Insulin R	IGF-1R	-
Axl	Axl	-
Axl	Dtk	-
Axl	Mer	-
HGFR	HGFR	+
HGFR	MSPR	+/-
PDGFR	PDGFR-α	+/-
PDGFR	PDGFR-β	+/-
PDGFR	SCFR	-
PDGFR	Flt-3	-
PDGFR	M-CSF-R	-
RET	c-Ret	-
ROR	ROR1	-
ROR	ROR2	-
Tie	Tie-1	-
Tie	Tie-2	+
NGFR	TrkA	+
NGFR	TrkB	+
NGFR	TrkC	+
VEGFR	VEGFR1	-
VEGFR	VEGFR2	-
VEGFR	VEGFR3	-
MuSK	MuSK	-
EphR	EphA1	-
EphR	EphA2	-
EphR	EphA3	-
EphR	EphA4	-
EphR	EphA6	+
EphR	EphA7	+
EphR	EphB1	+/-
EphR	EphB2	-
EphR	EphB4	-
EphR	EphB6	-
Control (-)	Mouse IgG_1	-
Control (-)	Mouse IgG_{2A}	-
Control (-)	Mouse IgG_{2B}	-
Control (-)	Goat IgG	-
Control (-)	PBS	-

10.9 Publications

Manuscripts:

Adam M, Schwarzer JU, Köhn FM, Strauss L, Poutanen M, Mayerhofer M 2011 Mast cells tryptase stimulates production of decorin by human testicular peritubular cells: possible role in male infertility by interfering with growth factor signaling Hum Reprod 26:2613-2625

Adam M, Urbanski HF, Garyfallou VT, Schwarzer JU, Welsch U, Köhn FM, Strauss L, Poutanen M, Mayerhofer M High levels of the extracellular matrix proteoglycan decorin are associated with inhibition of testicular function. Epub ahead of print doi:10.1111/j.1365-2605.2011.01225.x

Nurmio M, Kallio J, Adam M, Mayerhofer A, Toppari J, Jahnukainen K. Peritubular myoid cells regulate the postnatal testicular growth. In preparation.

Talk:

Adam M, Spinnler K, Schwarzer JU, Köhn FM, Strauss L, Poutanen M, Mayerhofer A. Mast cells and human testicular peritubular cells: Role in regulation of testicular decorin. International Workshop of Molecular Andrology, Giessen 2009.

Poster:

Spinnler K, Adam M, Schwarzer JU, Köhn FM, Mayerhofer A. Mast cells and human testicular peritubular cells: Role in production of NGF. International Workshop of Molecular Andrology, Giessen 2009.

Adam M, Schwarzer JU, Köhn FM, Strauss L, Poutanen M, Mayerhofer A. Decorin-expression by human peritubular cells and its role in paracrine regulation. 43. Jahrestagung Physiologie und Pathologie der Fortpflanzung, München 2010.

Adam M, Schwarzer JU, Köhn FM, Mayerhofer A. Growth factors and growth factor signaling in human testicular peritubular cells: PDGF. 22. Jahrestagung der deutschen Gesellschaft für Andrologie, Hamburg 2010.

Adam M, Schwarzer JU, Köhn FM, Strauss L, Poutanen M, Mayerhofer A. Mast cell tryptase stimulates production of decorin by human testicular peritubular cells: Possible role in male infertility by interfering with growth factor signaling. 90th Annual meeting of the German Physiological Society, Regensburg 2011.